UNIVERSITY OF CENTRAL FLORIDA

COLLEGE OF ENGINEERING
ENGINEERING AND INDUSTRIAL EXPERIMENT STATION

FINAL REPORT

LARGE REFLECTOR ANTENNA STUDY

PRINCIPAL INVESTIGATOR

Christos G. Christodoulou

August 1986

Sponsored by:

National Aeronautics and Space Administration

Langley Recearch Center

Hampton, Virginia

Grant Number 1-615

PART I

THE TWO DIMENSIONAL PROBLEM (GRID) USING

THE FFT-CONJUGATE GRADIENT METHOD

ABSTRACT

In some applications, the wires used to construct the grids are plated over with highly conducting materials such as gold or silver. In those cases, depending on the frequency of operation, the coating may not be thick enough to prevent currents from flowing in the substrate. The conjugate gradient method, in conjunction with the fast Fourier transform is employed to solve the problem of scattering from such rectangular grids. An internal impedance is utilized to account for the effects of the substrate conductivity on the induced current densities. Calculated values of the reflection coefficient and induced currents for different coating thicknesses, angles of incidence and polarizations are presented and discussed.

TABLE OF CONTENTS

INTRODUCTION

The subject of reflection and transmission of plane
electromagnetic waves from grids made of perfectly conducting
wires, or wires with finite conductivity has been studied by a
number of investigators [1-5]. In some applications, such as,
mesh deployable antennas, the mesh wires are made of molybdenum
substrate coated with a highly conductive material. Depending on
the frequency of operation, the depth of penetration for the
incident wave can be larger than the coating thickness. In these
cases, the electric field will penetrate in the substrate. The
effects of the resistivity of the substrate on the reflection
coefficient and induced currents are the aims of this study.

The FFT-conjugate gradient method [6-12] is used to solve for
the induced currents on the conducting strips of the grid. An
internal impedance is used to account for any losses due to the
finite conductivities of both the substrate material and the
coating material. This impedance is a function of a) coating
thickness, b) frequency of operation, c) conductivity of coating
material, and c) conductivity of substrate material.

In this work, results for single infinite grids are given as
a function of the substrate conductivity, coating thickness, and
polarization of the incident wave. The effects of the substrate
material on the reflection coefficient and induced currents are

also discussed for different angles of incidence. This study can easily be extented to the problem of any number of cascaded grids. In the case of cascaded grids, there is an interference action [13] which is usually extremely sensitive to the losses of the wires, which in this particular case it would primarily be due to the finite conductivity of the substrate conductivity.

2.CURRENT DENSITY FORMULATION

The magnetic field $\vec{H}$ due to an electric current density $\vec{J}$ is given by :

$$\vec{H}(x,y) = \frac{\nabla \times \vec{A}(x,y,z)}{\mu} \tag{2.1}$$

where $\vec{A}$ is the associated magnetic vector potential. $\vec{A}$ and $\vec{J}$ are related by the free space Creen's function

$$\overline{\overline{G}}(\vec{r}) = \frac{\exp(-j\hat{k} \cdot \hat{r})}{4 \pi r}$$

as follows:

$$\overline{A}(\vec{r}) = \mu \int \overline{\overline{G}}(\vec{r},\vec{r}') \cdot \overline{J}(\vec{r}') \tag{2.2}$$

From this the electric field intensity $\vec{E}$ can be derived from Maxwell's equations and expressed as:

$$\vec{E}^{s}(x,y,z) = -j \omega \vec{A}(x,y,z) + \frac{\nabla \nabla \cdot \vec{A}(x,y,z)}{j \omega \mu \epsilon} \tag{2.3}$$

For planar structures we set the z-component of the magnetic vector $\vec{A}$ equal to zero. Now upon expanding equation (2.3) in cartesian coordinates we obtain, for z=0:

$$\vec{E}^s(x,y) = \frac{1}{j\omega\epsilon} \begin{bmatrix} k_o^2 + \frac{\partial^2}{\partial x^2} & \frac{\partial^2}{\partial x \partial y} \\ \frac{\partial^2}{\partial x \partial y} & k_o^2 + \frac{\partial^2}{\partial y^2} \end{bmatrix} \begin{array}{c} \int G.J_x \\ \int G.J_y \end{array} \tag{2.4}$$

Considering the periodicity of the two dimensional strucuture shown in Figure (2.1) (planar structure), and taking the Fourier trasform of equation (2.4) lead to :

$$\vec{E}^s(\alpha_{mn}, \beta_{mn}) = \frac{1}{j\omega\epsilon} \begin{bmatrix} k_o^2 - \alpha_{mn}^2 & -\alpha_{mn}\beta_{mn} \\ -\alpha_{mn}\beta_{mn} & k_o^2 - \beta_{mn}^2 \end{bmatrix} \tilde{\tilde{G}}\ \tilde{\tilde{J}} \tag{2.5}$$

where the sign ($\sim$) denotes the Fourier trasformed quantity.

α_{mn} and β_{mn} represent the Floquet coefficients which are defined as:

$$\alpha_{mn} = 2\pi m/a - k_o \sin\theta \sin\phi \qquad \text{and}$$

$$\beta_{mn} = 2\pi n/c - 2\ m/a\ \cot\Omega - k_o \sin\theta \sin\phi$$

$$G(\alpha_{mn}, \beta_{mn}) = -j/2\ (k_o^2 - \alpha_{mn}^2 - \beta_{mn}^2)^{1/2}\ \overline{\overline{I}}$$

is the Fourier trasform of Green's function, and J_x , J_y are the unknown current densities. Notice that the spectrum of $\vec{E}^s$ is discrete, that is, it exists for discrete values of α_{mn} and β_{mn}. Note, also, that the convolution problem is avoided and instead of dealing with an integro differential equation we only

have to consider algebraic equations. Taking the inverse Fourier trasform of equation (2.5) yields:

$$\vec{E}^s(x,y) = \frac{1}{j\omega\epsilon} \sum_{mn} \begin{bmatrix} k_o^2 - \alpha_{mn}^2 & -\alpha_{mn}\beta_{mn} \\ -\alpha_{mn}\beta_{mn} & k_o^2 - \beta_{mn}^2 \end{bmatrix} \widetilde{\overline{\overline{G}}}.\widetilde{\vec{J}}$$

$$\cdot \exp[j(\alpha_{mn}x + \beta_{mn}y)] \qquad (2.6)$$

To enforce the boundary condition over the surface of all metallic regions we require that the total tangential electric field should satisfy the condition :

$$\vec{E}^i(x,y) + \vec{E}^s(x,y) = 0 \qquad (2.7)$$

where $\vec{E}^i$ is the incident electric field and $\vec{E}^s$ is the scattered electric field. Substituting for the value of $\vec{E}^s$ from equation (2.7) into equation (2.6) yields:

$$-\vec{E}^i = \frac{1}{j\omega\epsilon} \sum_{mn} \begin{bmatrix} k_o^2 - \alpha_{mn}^2 & -\alpha_{mn}\beta_{mn} \\ -\alpha_{mn}\beta_{mn} & k_o^2 - \beta_{mn}^2 \end{bmatrix} G(\alpha_{mn},\beta_{mn}) \; J(\alpha_{mn},\beta_{mn})$$

$$\cdot \exp[j(\alpha_{mn}x + \beta_{mn}y)] \qquad (2.8)$$

Equation (2.8) can be recognized as the inverse discrete Fourier transform which can be performed via the fast Fourier

transform (FFT). Equation (2.8) could now be written in an operator form as:

$$-\vec{E}^i = Z_{mn} \, \vec{J}_{mn} \tag{2.9}$$

where Z_{mn} is the product of $\widetilde{\widetilde{G}}$, the Floquet modes and the inverse Fourier transform.

A solution of the above equation will yield the unknown current densities J_x and J_y from which the reflected and transmitted fields can be obtained and hence the reflection and transmission coefficients could be calculated.

Now, one way to solve for J_x and J_y is to use the conjugate gradient method [12]. To guarantee a convergent scheme, equation (2.9) has to be properly modified. To do that, multiply both sides of equation (2.9) by Z^*_{mn} (i.e. the conjugate transpose of Z_{mn}) to obtain:

$$-Z^*_{mn} \, \vec{E}^i = Z^*_{mn} \, Z_{mn} \, \vec{J} \tag{2.10}$$

where the product $Z^*_{mn} \, Z_{mn}$ is a Hermitian matrix and therefore positive definite. Now the conjugate gradient method can be applied directly to equation (2.10).

3. FORMULATION OF THE FFT-CONJUGATE GRADIENT METHOD FOR COATED WIRES

3.1 EQUIVALENT RADIUS PRINCIPLE AND INTERNAL IMPEDANCE

The strip analysis can be used to determine the scattering characteristics from a mesh of cylindrical wires by employing the "equivalent radius principle" concept. This is accomplished by replacing the non-circular cross section of a metallic strip with a circular wire whose radius is the "equivalent radius" of the non-circular cross section as shown in Figure (3.1). Butler[14] has shown that the equivalent radius of a narrow conducting strip is one fourth of its width i.e

$$a_{eq} = a/4$$

where a_{eq} is the equivalent radius of a cylindrical wire, and a is the width of a thin metallic strip.
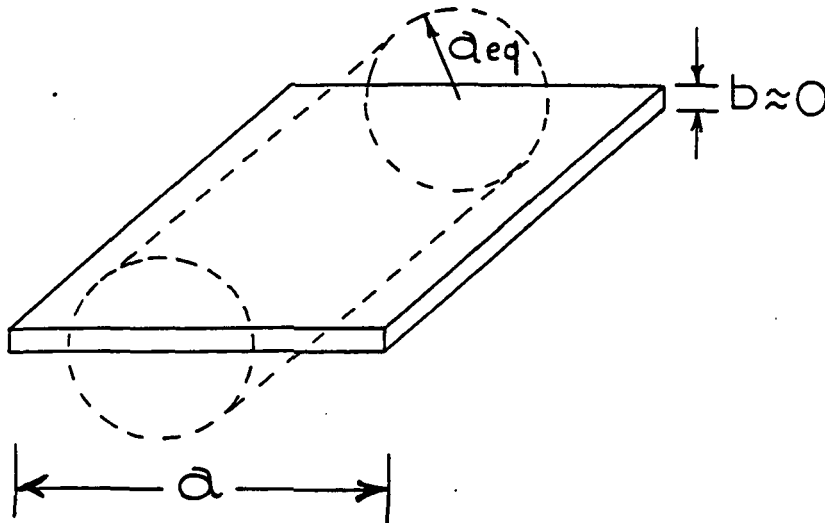

Fig. 3.1 Equivalent radius of a strip

For the case where the wires are coated (See Figure 3.2) the necessary boundary condition that must be satisfied is :

$$\vec{E}^i + \vec{E}^s = Z_{int} \, I \tag{3.1}$$

instead of $\vec{E}^s + \vec{E}^i = 0$, where I is the current in the wires and Z_{int} is the internal impedance of the wire. For coated wires Z_{int} is given by [15] :

$$Z_{int} = \frac{(1+j) \, [\sinh(t_1 d) + (R_{s2}/R_{s1}) \cosh(t_1 d)]}{b \quad [\cosh(t_1 d) + (R_{s2}/R_{s1}) \sinh(t_1 d)]} R_{s1} \tag{3.2}$$

where
$$t_1 = (1+j) \sqrt{\pi f \, \mu_1 \, \sigma_1} \qquad \text{and} \tag{3.3}$$

$$t_2 = (1+j) \sqrt{\pi f \, \mu_2 \, \sigma_2} \tag{3.4}$$

d=coating thickness

$$R_{s1} = \sqrt{\pi f \, \mu_1 / \, \sigma_1} \qquad \text{and} \quad R_{s2} = \sqrt{\pi f \, \mu_2 / \, \sigma_2} \tag{3.5}$$

μ_1 = permeability of coating

σ_1 = conductivity of. coating

μ_2 = permeability of substrate

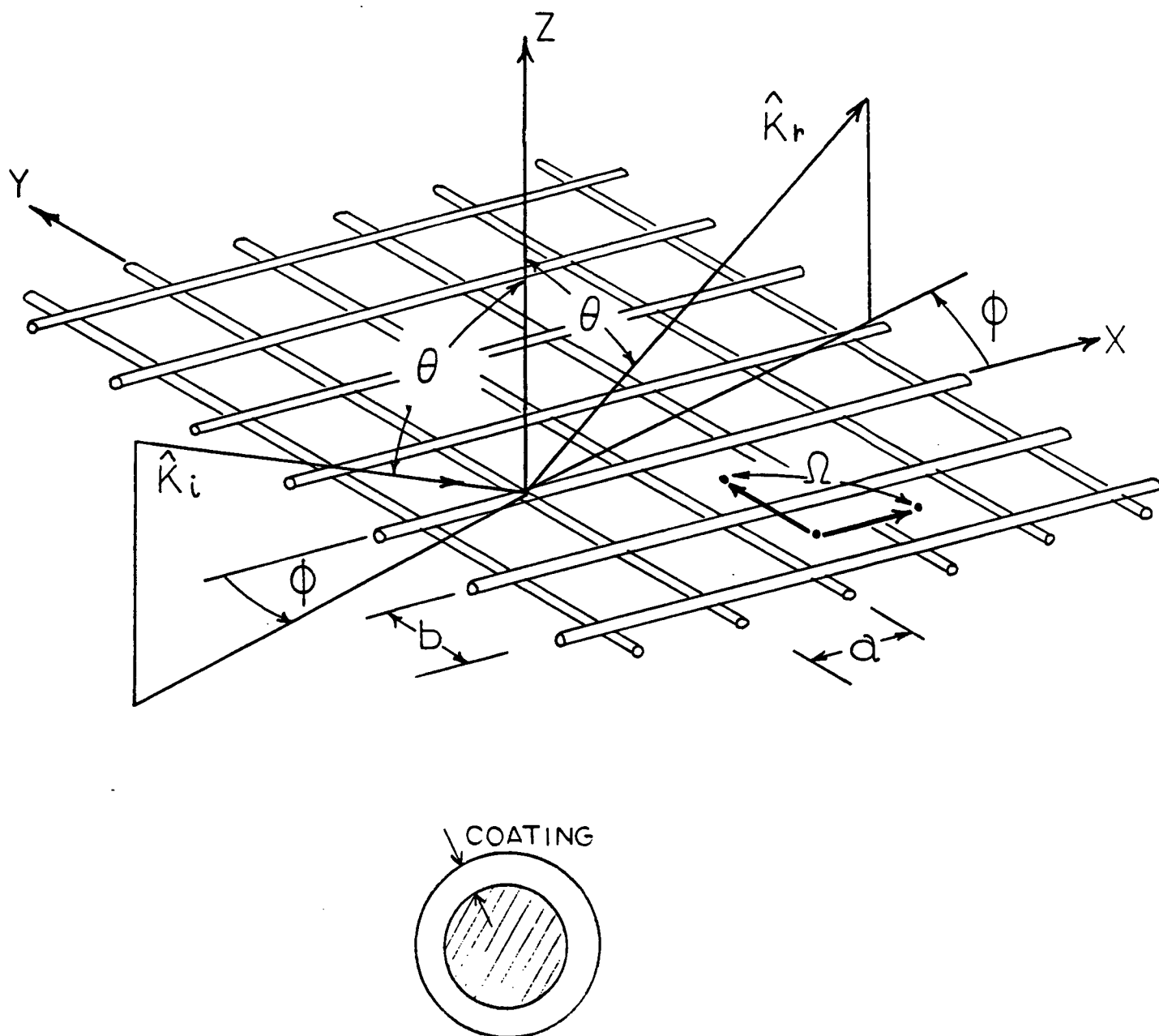σ_2 = conductivity of substrate

Fig. 3.2 Mesh geometry for coated wires

This expression for Z_{int} can now be used in equation (2.9)i.e.

$$\vec{E}^S + \vec{E}^i = Z_{int} \, I = (Z_{int} \, A) \, \vec{J} = \overline{\overline{Z}}_{int} \, \vec{J} \tag{3.6}$$

since $\vec{J} = I/A$ where A is the surface area of the wire. This leads to :

$$\vec{E}^S = -\vec{E}^i + \overline{\overline{Z}}_{int} \, \vec{J} \tag{3.7}$$

Replacing this expression for $\vec{E}_S$ in equation (2.6) yields :

$$-\vec{E}^i + \overline{\overline{Z}}_{int} \, \vec{J} = Z_{mn} \qquad\qquad \text{or}$$

$$-\vec{E}^i = (Z_{mn} - \overline{\overline{Z}}_{int}) \, \vec{J} = B \, \vec{J} \tag{3.8}$$

Now equation (3.8) can be solved for $\vec{J}$ using the conjugate gradient algorithm. Rather than form the matrix $(Z_{mn} - \overline{\overline{Z}}_{int})$ explicitly, one can apply the conjugate gradient method using the algorithm given on the next page.

In Figures 3.3 and 3.4, and internal impedance with a ratio of $R_{s2}/R_{s1} = 0.34$ and 1.6 are shown, respectively [15]. These figures are important, because they show that Z_{int} will not be that of the coating material alone, despite the fact that the ratio of the coating thickness to the skin depth is greater than one.

CONJUGATE GRADIENT ALGORITHM

$$\vec{r}^{(0)} = \vec{E}^i + Z_{mn} \vec{J}^{(0)} - \overline{\overline{Z}}_{int} \vec{J}^{(0)}$$

$$\vec{p}^{(0)} = Z^*_{mn} \vec{r}^{(0)} - \overline{\overline{Z}}^*_{int} \vec{r}^{(0)}$$

$$ERRF = \left\| \vec{r}^{(0)} \right\|^2$$

The equations for the nth iteration are :

$$\alpha_n = \frac{\left\| Z^*_{mn} \vec{r}^{(n)} - \overline{\overline{Z}}^*_{int} \vec{r}^{(n)} \right\|^2}{\left\| Z_{mn} \vec{p}^{(n)} - \overline{\overline{Z}}_{int} \vec{p}^{(n)} \right\|^2} \qquad (3.9)$$

$$\vec{J}^{(n+1)} = \vec{J}^{(n)} + \alpha_n \vec{p}^{(n)}$$

$$ERRF^{(n+1)} = ERRF^{(n)} - \left\{ \frac{\left\| Z^*_{mn} \vec{r}^{(n)} - \overline{\overline{Z}}^*_{int} \vec{r}^{(n)} \right\|^2}{\left\| Z_{mn} \vec{p}^{(n)} - \overline{\overline{Z}}_{int} \vec{p}^{(n)} \right\|^2} \right\}^2$$

$$\vec{r}^{(n+1)} = \vec{r}^{(n)} - \alpha_n Z^*_{mn} \vec{p}^{(n)} - \overline{\overline{Z}}^*_{int} \vec{p}^{(n)}$$

$$\beta_n = \frac{\left\| Z^*_{mn} \vec{r}^{(n+1)} - \overline{\overline{Z}}^*_{int} \vec{r}^{(n+1)} \right\|^2}{\left\| Z^*_{mn} \vec{r}^{(n)} - \overline{\overline{Z}}^*_{int} \vec{r}^{(n)} \right\|^2}$$

$$\vec{p}^{(n+1)} = Z^*_{mn} \vec{r}^{(n+1)} - \overline{\overline{Z}}^*_{int} \vec{r}^{(n+1)} + \beta_n \vec{p}^{(n)}$$
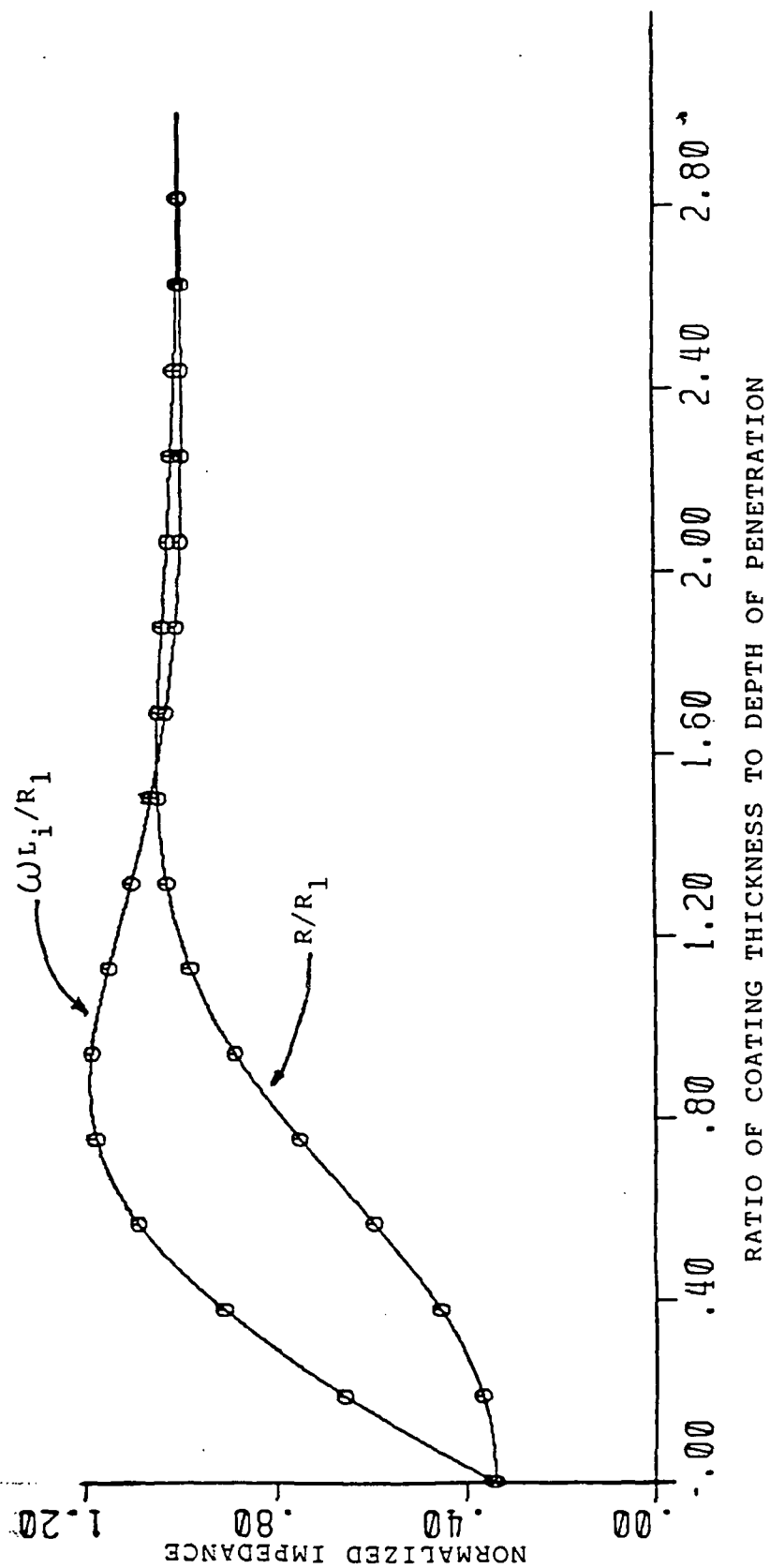
END OF DO LOOP

Fig. 3.3   Normalized Impedance. Solder coating on a copper substrate.
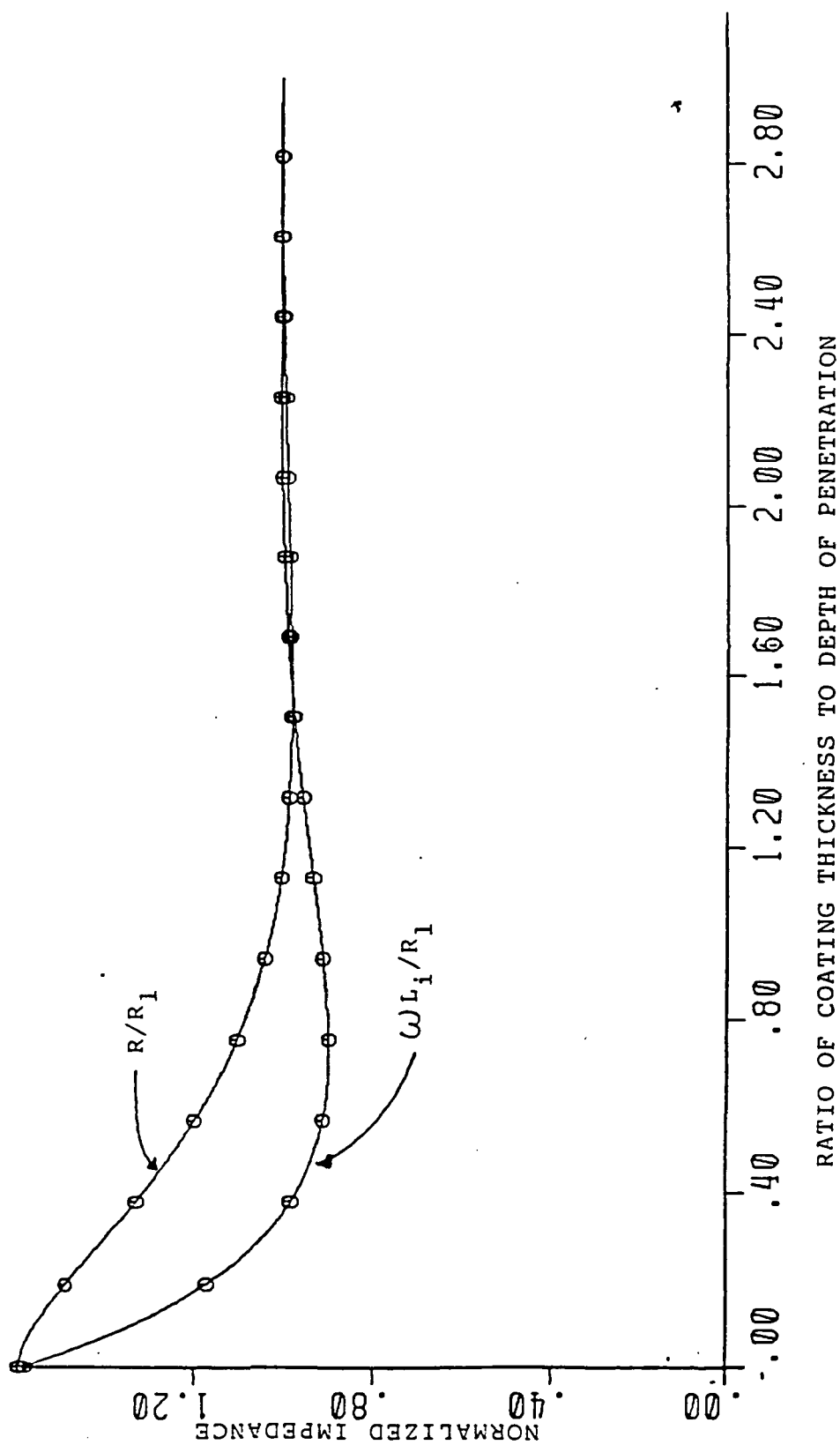Rs2/Rs1 = 0.34

RATIO OF COATING THICKNESS TO DEPTH OF PENETRATION

Fig 3.4   Normalized Impedance. Silver Coating on a Brass Substrate.
$Rs2/Rs1 = 1.6$

In the current algorithm, if this ratio is less than the number four, equation (3.2) is calculated. On the other hand, if the ratio is greater than the number four, Z_{int} is due to the coating material only, and it is given by [16] :

$$Z_{int} = \frac{Z_m}{2 \pi a_{eq}} \frac{I_0(\gamma a_{eq})}{I_1(\gamma a_{eq})} \qquad 3.10)$$

where

$$Z_m = \left(\frac{j\omega\mu}{\sigma_m + j\omega\epsilon_m}\right)^{1/2}$$

is the intrinsic impedance of the metal. γ is equal to $(j \mu_m \omega(\sigma_m + j\omega\epsilon_m))^{1/2}$ and I_0 and I_1 are the modified Bessel functions. At high frequencies the ratio I_0/I_1 is approximately equal to one. Thus, any uneccessary computations are avoided by evaluating equation (3.10) instead of equations (3.2),(3.3),(3.4), and (3.5).

3.2 SOLUTION OF APERTURE FIELDS

To solve for the aperture fields (See Figure 3.5), the incident H field is expressed in terms of the electric field E in the aperture region by :

$$\vec{H}^i = \frac{2j}{\omega \mu} \sum_{mn} \begin{bmatrix} \alpha_{mn} \, \beta_{mn} & k_o^2 - \alpha_{mn}^2 \\ -(\beta_{mn}^2 - k_o^2) & -\alpha_{mn} \, \beta_{mn} \end{bmatrix} \overset{\approx}{G}(\alpha_{mn}, \beta_{mn}) \, \tilde{E}^a$$
$$\cdot \exp[j(\alpha_{mn}x + \beta_{mn}y)]$$
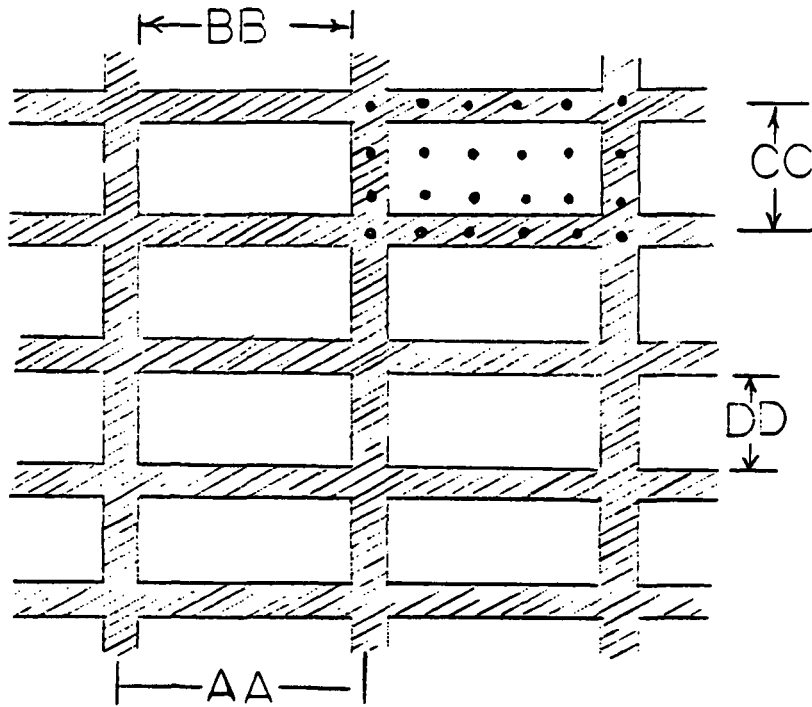
(3.11)

Fig. 3.5 Sampling for the Aperture fields.

For a complete derivation of equation (3.11) see [17].

4. REFLECTION COEFFICIENTS

The transmission and reflection coefficients are the quantities of most importance in characterizing the properties of a mesh. In order to define those coefficients for both polarizations, transverse electric (TE) and transverse magnetic (TM), it is necessary to first define the incident and scattered fields. For TE polarization, the incident fields are :

$$E_x = E_o \sin(-\phi) \quad ; \quad E_y = E_o \cos\phi$$

$$H_x = \frac{E_o \cos\theta \cos\phi}{\eta} \quad ; \quad H_y = \frac{E_o \sin\phi \cos\theta}{\eta}$$

where E_o is the amplitude of the incident electric field and $\eta = (\mu_o / \epsilon_o)^{1/2}$ is the free space wave impedance. For TM polarization, the incident fields are given by :

$$E_x = E_o \cos\theta \cos\phi \quad ; \quad E_y = E_o \cos\theta \sin\phi$$

$$H_x = \frac{E_o \sin(\phi - \pi/2)}{\eta} \quad H_y = \frac{E_o \cos(\phi - \pi/2)}{\eta}$$

According to Wait and Hill [4], when the spacing between adjacent wires of the mesh is less than $\lambda/2$, only the J_{oox} and J_{ooy} components contibute to the scattered field. J_{oox} and J_{ooy} are the zero-mode current density components. The rectangular components of the scattered field, can be obtained

from equation (2.6) as follows : Solve for J and substitute the solution in equation (2.6) to obtain the E_x and E_y components of the scattered field. Once these components are found the reflection (amplitude) coefficient becomes :

$$R_x = E_x^s / (E_x^2 + E_y^2)^{1/2} \qquad (4.1)$$

$$R_y = E_y^s / (E_x^2 + E_y^2)^{1/2} \qquad (4.2)$$

If the total power reflection coefficient R is desired then the following expression can be used :

$$|R| = \frac{\text{Real}\left\{ \int\limits_{\text{unit cell}} \vec{E}^s \times \vec{H}^s \cdot \hat{z} \; ds \right\}}{\text{REAL}\left\{ \int\limits_{\text{unit cell}} \vec{E}^i \times \vec{H}^i \cdot (-\hat{z}) \; ds \right\}} \qquad (4.3)$$

$\vec{H}^s$ is the scattered magnetic field derived from $\vec{E}^s$ by making use of Maxwell's equations.

Moreover, if the total power transmission coefficient, T, is to be computed, one can employ the formula below :

$$|T| = \frac{\text{Real}\left\{ \int\limits_{\text{aperture}} \vec{E}^a \times \vec{H}^a \cdot (-\hat{z}) \; dA \right\}}{\text{Real}\left\{ \int\limits_{\text{aperture}} \vec{E}^i \times \vec{H}^i \cdot (-\hat{z}) \; dA \right\}} \qquad (4.4)$$

where $\vec{E}^a$ is the aperture electric field and $\vec{H}^a$ is the aperture magnetic field.

5. RESULTS

A number of cases were examined to check the reflection coefficients and induced current densities as functions of wave polarization, angle of incidenece, wire spacing, coating thickness, and substrate conductivity. Since no other theoretical or experimental data currently exist, only results obtained via this new algorithm are presented herein.

Figure (5.1) depicts the change in the reflection coefficient (amplitude) as the thickness of the coating material changes. In this case, the substrate conductivity is 50 S/m and the coating conductivity is 10^8 S/m. As expected, the thinner the coating material is the deeper the fields will penetrate and hence more losses should be expected in the strips. That means that the amplitude of the reflection coefficient will decrease. This figure also shows that when the thickness of the coating material is large the losses are mainly due to the finite conductivity of this coating material. On the other hand, at small coating thicknesses the losses will be primarily due to the substrate conductivity. Figure (5.2) depicts the behavior of the reflection coefficient for two different angles of incidence as the substrate conductivity is varied. The thickness and conductivity of the coating material are kept constant. From this figure one can see that as the conductivity of the substrate gets larger the reflection coefficient increases. This is an
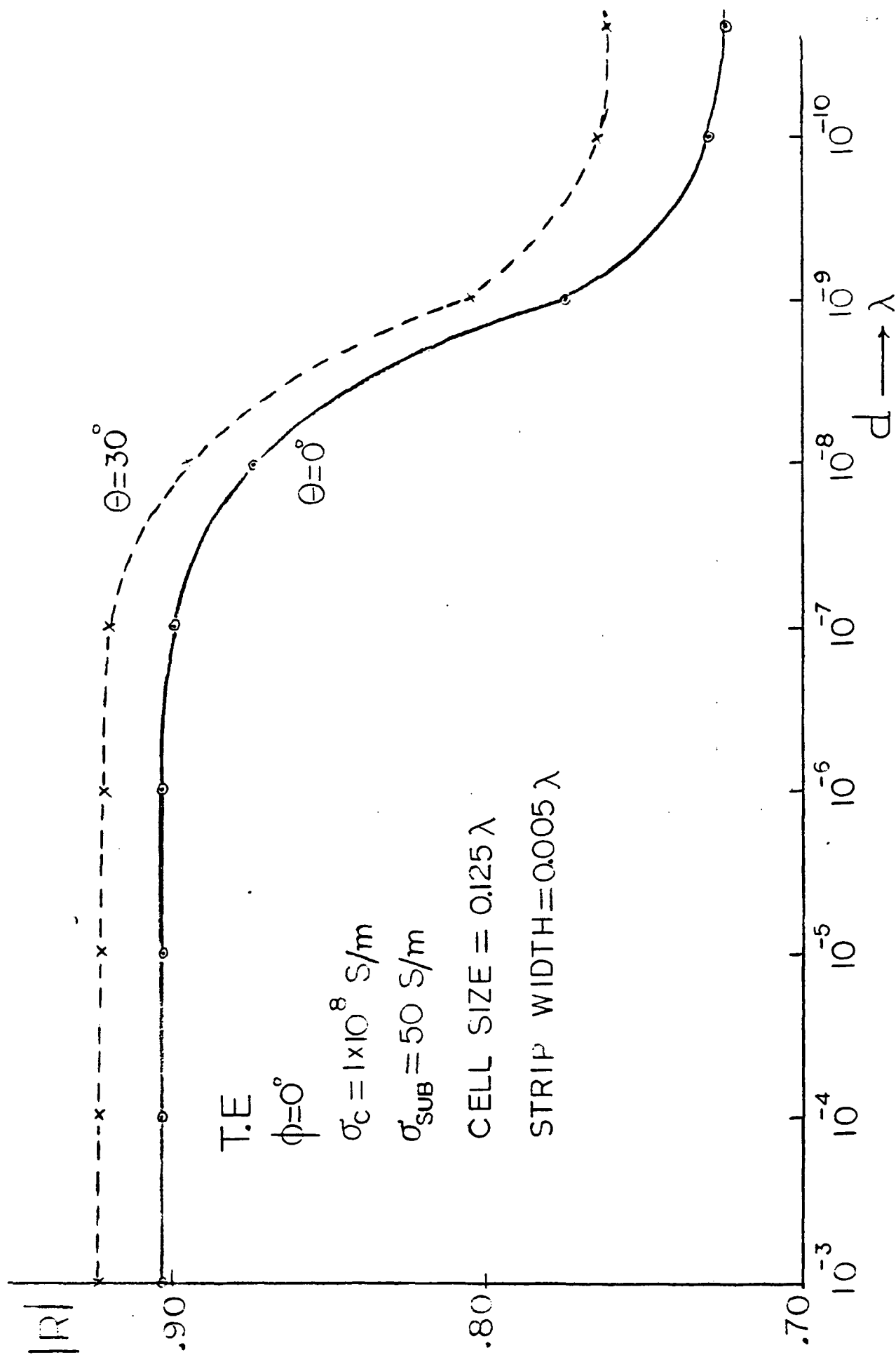
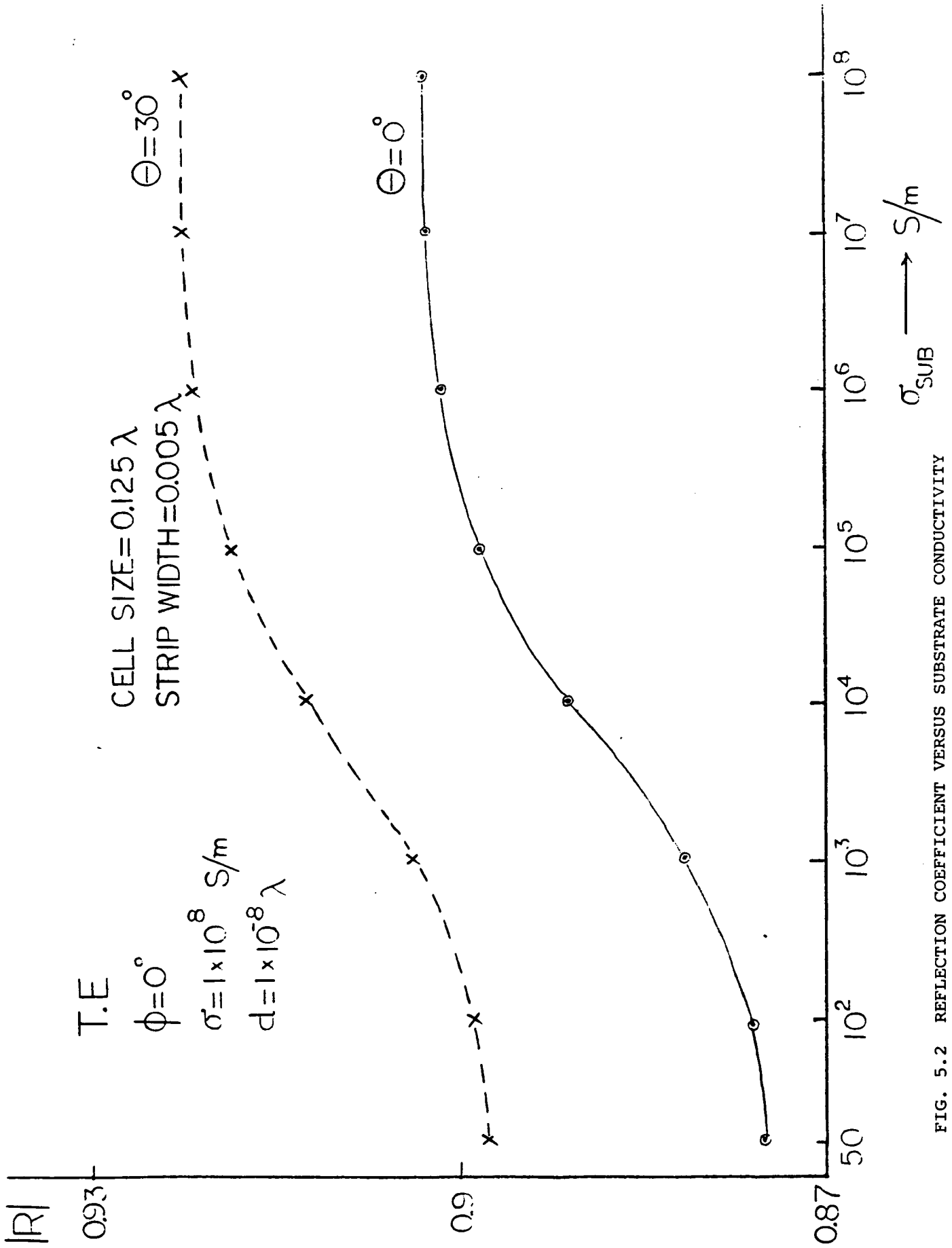FIG. 5.1 REFLECTION COEFFICIENT VERSUS COATING THICKNESS

FIG. 5.2 REFLECTION COEFFICIENT VERSUS SUBSTRATE CONDUCTIVITY

anticipated result since the losses in the strips decrease by increasing the conductivity of the substrate.

Figure (5.3) exhibits a similar behavior in the case of thansverse magnetic polarization for angles $\theta = 60^\circ$ and $\theta = 0^\circ$. By comparing Figures (5.2) and (5.3), one can make the additional observation that for TM polarization the reflection coefficient does not change as drastically as in the TE polarization case. Table (5.1) shows that if the substrate conductivity is 10^5 S/m and the coating conductivity 10^8 S/m , the change in the reflection coefficient is not very much. The fact that the reflection coefficient for $\theta = 0^\circ$ is larger than the reflection coefficient for $\theta = 70^\circ$ is due to the general behavior of conducting grids ($\sigma = \infty$, or finite) and not due to the coated material. In Table (5.2) the reflection coefficient is calculated for TM polarization at $\theta = 0^\circ$ and $\theta = 70^\circ$. Note that the substrate conductivity is much smaller than the conductivity of the the coating material.This difference is basically the reason for having a noticable change in the reflection coefficient at small coating thicknesses.

Next, the current densities were calculated to study their behavior as we vary the substrate conductivity and the angle of incidence   . Figures (5.4) and (5.5) depict the behavior of the copolar component of the current density J_y, for a grid with wide strips. The current densities do not really change very drastically when the substrate conductivity is changed. The
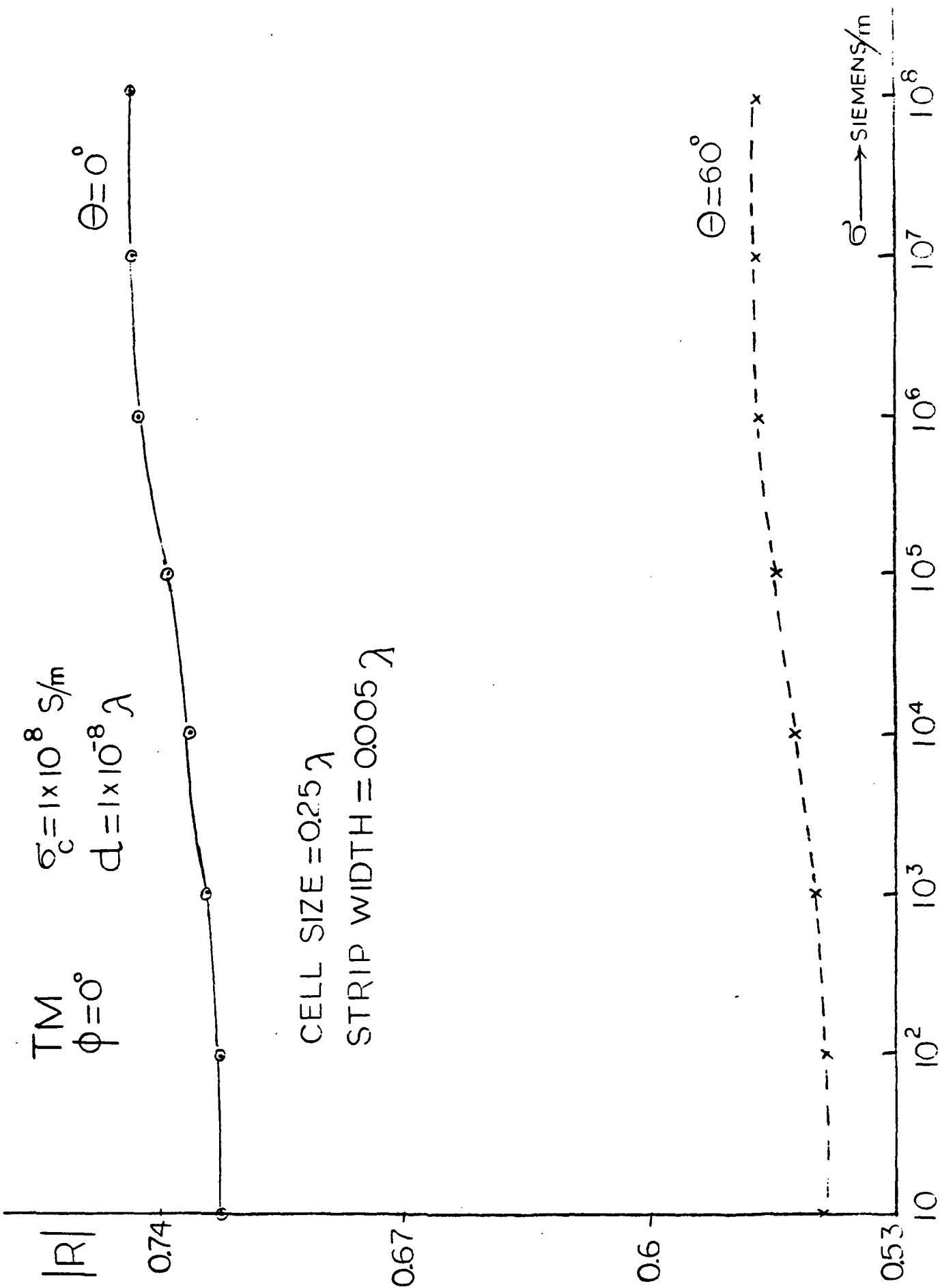
FIG. 5.3 REFLECTION COEFFICIENT VERSUS SUBSTRATE CONDUCTIVITY

TABLE 5.1. Reflection coefficients for a cell of a=0.25λ and a strip width of 0.005λ ,with θ=0° and θ=70°, respectively. σ_{coat}=10^8 S/m and σ_{sub}=10^5 S/m. TE polarization case with a sampling rate of 32x32 samples

Thickness of coating in λ	Reflection coefficient θ=0°	Reflection coefficient θ=70°
10^{-3}	0.6073501	0.9077239
10^{-4}	0.6073501	0.9077239
10^{-5}	0.6086803	0.9076653
10^{-6}	0.6066462	0.9077298
10^{-7}	0.6063545	0.9064933
10^{-8}	0.6060203	0.9045778
10^{-9}	0.6028293	0.9045168
10^{-10}	0.6022630	0.9045149

Table 5.2. Reflection coefficients for TM incidence and a

square cell of a=0.25λ.The strip width is 0.005λ

$\sigma_{coat}=10^8$ S/m and $\sigma_{sub}=10^2$ S/m. The

sampling rate is 16x16 samples.

Thickness of coating in λ	Reflection coefficient $\theta=0°$	Reflection coefficient $\theta=70°$
10^{-3}	0.7405149	0.4434715
10^{-4}	0.7405149	0.4434715
10^{-5}	0.7405282	0.4434533
10^{-6}	0.7405004	0.4434442
10^{-7}	0.7385695	0.4423161
10^{-8}	0.7225416	0.4307751
10^{-9}	0.6665412	0.3766584
10^{-10}	0.6449590	0.3511487

FIG. 5.3   CURRENT DENSITIES
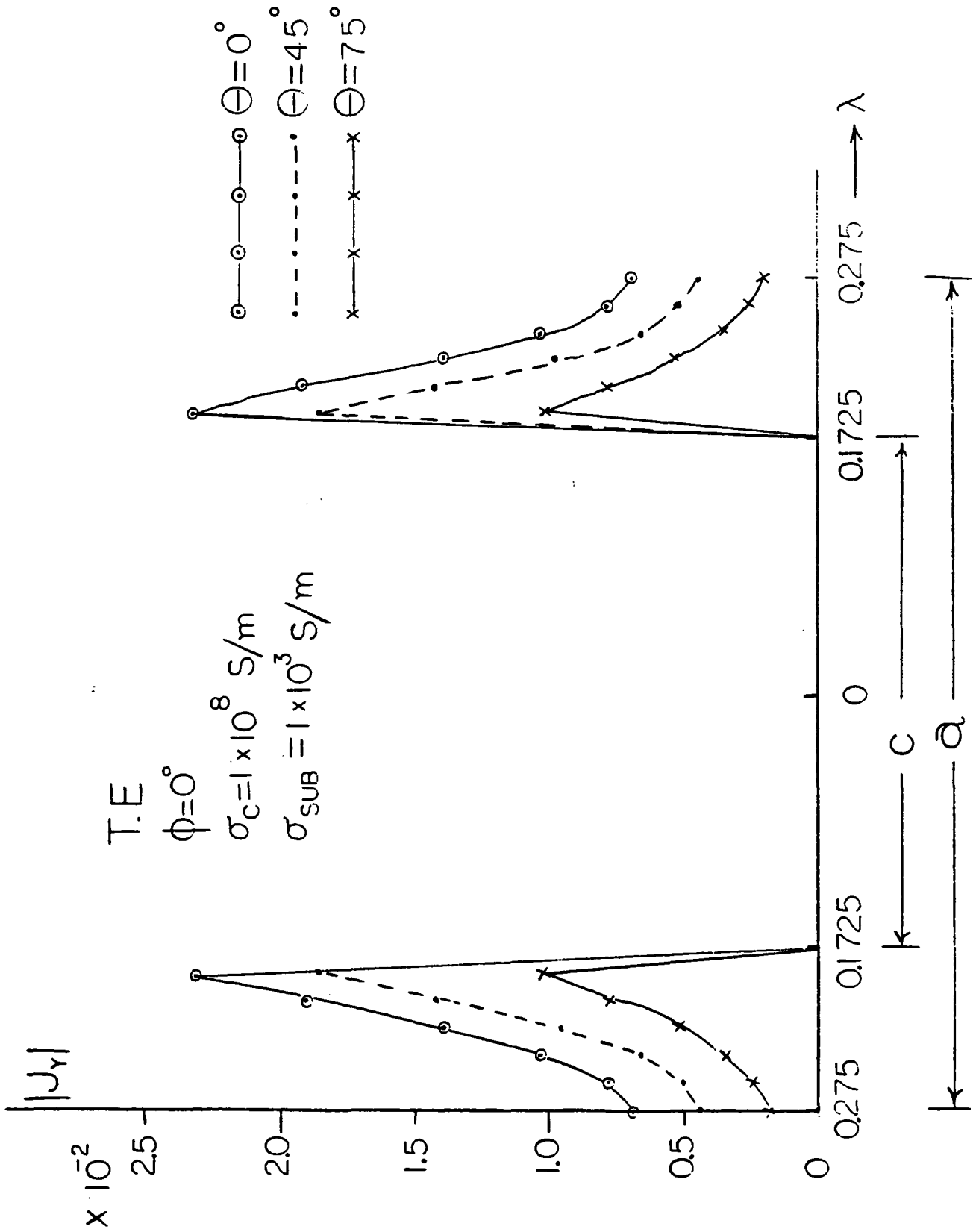
FIG. 5.5 CURRENT DENSITIES VERSUS ANGLE OF INCIDENCE

general behavior, though, of the current density on the strip,i.e. J is large at the edges and it dips at the center, is still maintained.

Finally, the reflection coefficients of the structure shown in Figure (5.6) were studied , since this structure generates a cross polarized component. Tables (5.3) and (5.4) show that for both polarizations, TM and TE, the changes in the thickness of the coating material do not correspond to any drastic changes in the amplitude of the reflection coefficient. This is an interesting observation since the actual weaved mesh used for deployable antennas resembles this last structure more than the rectangular periodic structure. In both of these tables the wave was normally incident on the periodic structure . The substrate conductivity was $\sigma = 10^3$ S/m and the conductivity of the coating material was $\sigma = 10^9$ S/m.
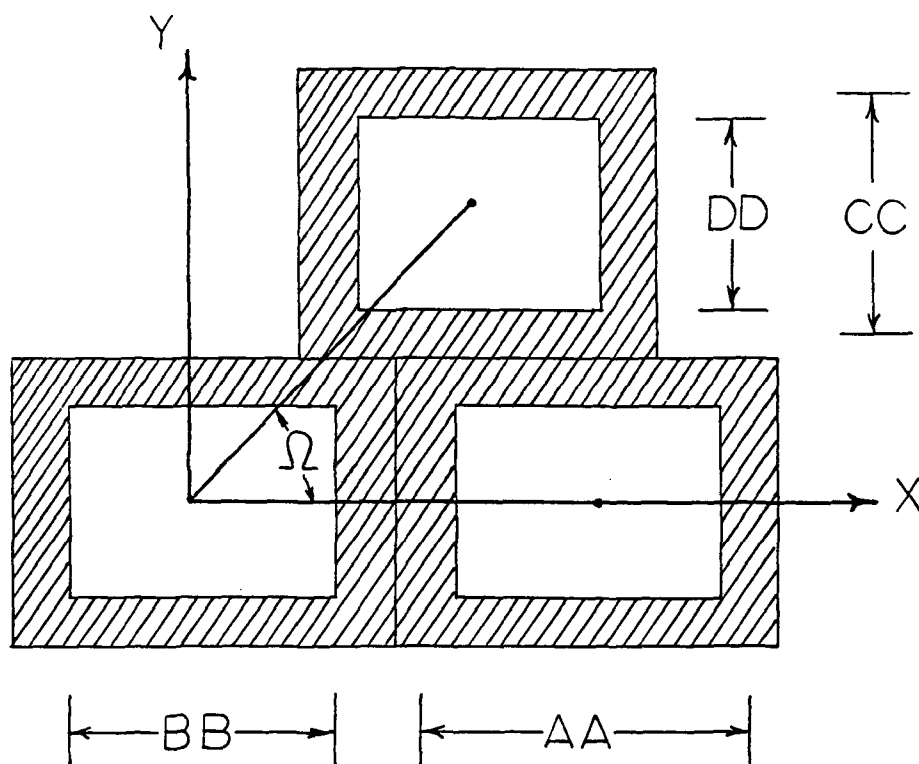
FIG. 5.6   DIFFERENT PERIODIC STRUCTURE

TABLE 5.3 Reflection coefficients for a cell of a=b=0.55 and a strip width of 0.005λ with θ =70° and θ =80°, respectively. σ_{coat}=10^9 S/m, and σ_{sub}=10^3 S/m. A TM polarization case with a sampling rate of 32x32 samples is used.

Thickness of coating in λ	Reflection coefficient θ =70°		Reflection coefficient θ =80°	
	copolar	crosspolar	copolar	crosspolar
10^{-5}	0.3372	0.1074	0.3169	0.0517
10^{-7}	0.3370	0.1074	0.3169	0.0517
10^{-8}	0.3368	0.1072	0.3166	0.0516
10^{-9}	0.3338	0.1051	0.3136	0.0508
10^{-10}	0.3273	0.1023	0.3073	0.0498

TABLE 5.4 Reflection coefficients for a cell of a=b=0.55 and a strip width of 0.005λ , with θ =70° and θ =80°, respectively. σ_{coat}=10^9 S/m and σ_{sub}=10^3 S/m. A TE polarization and a sampling rate of 32x32 samples is used.

Thickness of coating in λ	Reflection coefficient θ =70°		Reflection coefficient θ =80°	
	copolar	crosspolar	copolar	crosspolar
10^{-5}	0.28756	0.10101	0.30488	0.05212
10^{-7}	0.28755	0.10103	0.30493	0.05235
10^{-8}	0.28726	0.10083	0.30462	0.05210
10^{-9}	0.28441	0.09671	0.30171	0.05151
10^{-10}	0.27840	0.09805	0.29547	0.05064

6. CONCLUSIONS AND RECOMMENDATIONS

An algorithm was developed which can solve the problem of electromagnetic scattering from meshes made of coated wires. The algorithm solves for the reflection coefficients and the induced current densities. A variety of grids were checked as functions of polarization, angle of incidence , coating thickness coating conductivity, and substrate conductivity. Generally, it was found that when the difference in conductivity between the coating material and the substrate material is large the algorithm is very sensitive to the losses due to the finite substrate material. Also, when the thickness of the coating material becomes small compared to the depth of penetration the losses are primarily due to the substrate material. On the other hand, if this thickness is comparable or larger than the depth of penetration the losses are determined by the finite conductivity of the coating material. Moreover, it was observed that for non rectangular structures the amplitude of the reflection material does not change very much even at small coating thicknesses.

This algorithm could be extended to more complicated structures such as the skew-symmetric grids and cascaded grids.

7. REFERENCES

1) J.R. Wait,Theories of Scattering from Wire Grid and Mesh Structures in Electromagnetic scattering, P.L.E. Uslenghi, Ed. New York: Academic Press, 1978,pp. 253-287.

2) M.I.Kontorovich,"Averaged boundary conditions at the surface of a grating with a square mesh," Radio Eng.Electon.Phys., vol.8,no. 9,pp. 1446-1454,Sept. 1963.

3) M.I. Astrakham, "Reflecting and screening properties of plane wire grids," Telecommun. Radio Eng.,vol. 23,pt. 2, no. 1,pp. 76-83, Jan. 1968.

4) J.R.Wait, "Reflection at arbitrary incidence from a parallel wire grid," Appl. Sci. Res., sec. B, vol.4,pp. 393-400,1954.

5) D.A. Hill and J.R. Wait, "Electromagnetic scattering of an arbitrary plane wave by two non-intersecting perpendicular wire grids," Can. Jour. Phys., vol. 52, no. 3, pp. 227-237, 1974.

6) P.M. Van den Berg, "Iterative computational techniques in scattering based upon the integrated square error criterion,"IEEE Trans. Antennas Propagat., vol. AP-32, no. 10, pp. 1063-1071,Oct. 1984.

7) T.K. Sarkar and S.M. Rao, "The application of the conjugate gradient method for the solution of electromagnetic scattering from arbitrarily oriented wire antennas," IEEE Trans. Antennas Propagat., vol. AP-32, no. 4, pp. 398-403, Apr. 1984.

8) J.P. Montgomery and K.R. Davey, "Conjugate gradient solution of arbitrary planar frequency selective surfaces," in Proc. Int. URSI-Symp.,Boston, MA, 1984, p. 155.

9) T. Cwik and R. Mittra, "Spectral domain solution of scattering from periodic surfaces using the FFT, "in Proc. IEEE Antennas Propagat. Symp., Boston, MA, 1984, pp. 913-916.

10) T.K.Sarkar and S.M. Rao, "An iterative method for solving electrostatic problems," IEEE Trans. Antennas Propagat., vol. AP-30, pp. 611-617, July, 1982.

11) T.K. Sarkar , E. Arvas and S. Rao, " Application of the FFT and the Conjugate Gradient Method for the Solution of Electromagnetic Radiation from Electrically Large and Small Conducting Bodies," IEEE Trans. Antennas Propagat., vol. AP-34, pp. 635-640, May 1986.

12) C.G. Christodoulou and J.F. Kauffman,"On the Electromagnetic Scattering from Infinite Rectangular Grids with Finite Conductivity," IEEE Trans. Antennas Propagat.,vol. AP-34, pp. 144-154, Feb. 1986.

13) E.A. Lewis and J. P. Casey,Jr, " Electromagnetic Reflection and Transmission ", J. Appl. Phys. 23, 1952, pp. 605-608.

14) C.M. Butler, "The equivalent radius of a narrow conducting strip," IEEE Trans. Antennas Propagat., vol. AP-30, no. 4, pp. 755-757, July 1982.

15) S. Ramo, J.R. Whinnery and T. Van Duzer, Fields and Waves in Comuunications Electronics, 1st ed., John Wiley and Sons, Inc., New YOrk, 1944.

16) E.C. Jordan and K.D. Balmain, Electromagnetic Waves and Radiative Systems, 2nd ed. Englewood Cliffs, NJ: Prentice-Hall, 1966, pp. 557-568.

17) C.G. Christodoulou, " On the Electromagnetic Wave Scattering From Infinite Rectangular Conducting Grids",PhD Dissertation, North Carolina State University, Department of Electrical and Computer Engineering, 1985.

8. LISTING OF THE FFT-CG METHOD FOR THIN STRIPS

```fortran
C ****CONJUGATE GRADIENT METHOD *****
C **** SOLVES FOR THE CURRENT DENSITIES ***
C **** MINIMIZATION IN THE RANGE ****
      COMPLEX CONE, CZERO, CXMN, CREFX, CREFY, CRET, CREF, ZINT, GUESS, T1,
     .SINHH, COSHH, CTT, CTF
      COMPLEX Y(32, 32)/1024*(0. 0, 0. 0)/
      COMPLEX X(32, 32)/1024*(0. 0, 0. 0)/
      COMPLEX G(32, 32)/1024*(0. 0, 0. 0)/
      COMPLEX XU(32, 32)/1024*(0. 0, 0. 0)/
      COMPLEX YU(32, 32)/1024*(0. 0, 0. 0)/
      COMPLEX RX(32, 32)/1024*(0. 0, 0. 0)/
      COMPLEX RY(32, 32)/1024*(0. 0, 0. 0)/
      COMPLEX J, HXI, HYI, CWK(32), F10
      COMPLEX DY(32, 32)/1024*(0. 0, 0. 0)/
      COMPLEX DX(32, 32)/1024*(0. 0, 0. 0)/
      COMPLEX TX(32, 32)/1024*(0. 0, 0. 0)/
      COMPLEX .TY(32, 32)/1024*(0. 0, 0. 0)/
      REAL K, K2, RWK(342)
      DIMENSION  IWK(342), RR(250), CH(250), AMP(32), RINDEX(32),
     .CROS(32)
      REAL U(32)/32*0. 0/
      REAL V(32, 32)/1024*0. 0/
      OPEN (10, FILE='FASTDATA', STATUS='OLD')
      open (11, file='fastout', status='new')
      WRITE(*, *) 'INPUT AA, BB, CC, DD, F, ERR'
      READ(10, *) AA, BB, CC, DD
C22    FORMAT(8E10. 4)
      F=2. 998E+8
C **** IOPT=0 FOR A RECTANGULAR MESH *******
C **** IOPT=1 FOR A PARALLEL GRID   **********
C
      IX=32
      IOPT=0
      IF(IOPT. GT. 0) CC=1. 500E+15
      IF(IOPT. GT. 0) DD=1. 500E+15
      WRITE(11, *) AA, BB, CC, DD
C     . 'DD= ', F15. 8, 'ERR= ', F15. 8)
      WRITE(*, *)F
C44    FORMAT('0', ' FREQ = ', E10. 4)
      WRITE(11, *) 'INPUT PHI, THI, PSI'
      READ(10, *) PHI, THI, PSI
      WRITE(11, *) PHI, THI, PSI
C55    FORMAT('0', ' PHI= ', F10. 1, ' THETA= ', F10. 1, ' PSI= ', F10. 1)
C *** ITM=1 FOR TM POLARIZATION ******
      READ(10, *) ITM
      WRITE(11, *) 'INPUT ITM=0 FOR TE POLAR. OR ITM=1 FOR TM POL'
      WRITE(11, *) ITM
      WRITE(11, *) 'INPUT CONDUCTIVITY OF COATING'
      READ(10, *) SIGMA1
      WRITE(11, *) SIGMA1
      WRITE(11, *) 'INPUT CONDUCTIVITY OF SUBSTRATE'
      READ(10, *) SIGMA2
      WRITE(11, *) SIGMA2
      WRITE(11, *) 'THICKNESS OF COATING ?'
      READ(10, *) THICKNESS
      WRITE(11, *) THICKNESS
C *** READ THE NUMBER OF ITERATIONS ****
      READ(10, *) NOI
      WRITE(11, *) 'NUMBER OF ITERATIONS'
      WRITE(11, *) NOI
```

```
C66      FORMAT(I3)
         PI=3.141593
         PI2=PI/2.
         TPI=6.283185
         CV=2.997956E+8
         UU=4.E-7*PI
         RTD=57.29578
         EP=8.854E-12
         ETA=SQRT(UU/EP)
         J=CMPLX(0.0,1.0)
         ITER = 0
         CONE=CMPLX(1.0,0.0)
         CZERO=CMPLX(0.0,0.0)
         W=TPI*F
C *** COMPUTE INTERNAL IMPEDANCE OF STRIP ****
C
         T1=(1.0,1.0)*SQRT(PI*F*UU*SIGMA1)
         RS1=SQRT(PI*F*UU/SIGMA1)
         RS2=SQRT(PI*F*UU/SIGMA2)
         SKIND1=1./SQRT(PI*F*UU*SIGMA1)
         RATIO=THICKNESS/SKIND1
         IF(RATIO.GE.4.0) THEN
            ZINT=(1.0,1.0)*SQRT(PI*F*UU/SIGMA1)
         ELSE
         ZINT=(1.0,1.0)*(SINHH(T1*THICKNESS)+(RS2/RS1)*COSHH(T1*THICKNESS))
         ZINT=ZINT*RS1/(COSHH(T1*THICKNESS)+(RS2/RS1)*SINHH(T1*THICKNESS))
         END IF
         WRITE(*,*) RATIO,ZINT,RS1,RS2,T1,THICKNESS,SKIND1
         ALAMB=CV/F
         AA=AA/ALAMB
         BB=BB/ALAMB
         CC=CC/ALAMB
         DD=DD/ALAMB
C *** DETERMINE SAMPLING POINTS THAT CORRESPOND TO THE
C      CONDUCTING REGIONS AND THE APERATURE      *********
         NX=IFIX(BB/AA*FLOAT(IX)*2.)/4*2
         NY=IFIX(DD/CC*FLOAT(IX)*2.)/4*2
         NX1=(IX-NX)/2+1
         NX2=NX1+NX-1
         NY1=(IX-NY)/2 +1
         NY2=NY1+NY-1
         WRITE(11,*) NX,NX1,NX2,NY,NY1,NY2
         K=TPI/ALAMB
         K2=K**2
         STSPK=SIN(THI/RTD)*SIN(PHI/RTD)*K
         STCPK=SIN(THI/RTD)*COS(PHI/RTD)*K
         CPS=COS(PSI/RTD)/SIN(PSI/RTD)
70       CONTINUE
C *** CALCULATE FLOQUET MODES ******
         DO 100 M=1,IX
         IF (M.GT.IX/2+1) GOTO 75
         U(M)=TPI*(M-1)/AA-STCPK
         GOTO 80
75       U(M) = TPI*(M-IX-1)/AA-STCPK
80       CONTINUE
         DO 90 N=1,IX
         IF(M.GT.IX/2+1.AND.N.GT.IX/2+1) GOTO 84
         IF(M.GT.IX/2+1) GO TO 83
         IF(N.GT.IX/2+1) GOTO 81
         V(M,N)=TPI*(N-1)/CC-TPI*(M-1)/AA*CPS-STSPK
```

```
        GOTO 85
81      V(M,N)=TPI*(N-IX-1)/CC-TPI*(M-1)/AA*CPS-STSPK
        GOTO 85
83      V(M,N)=TPI*(N-1)/CC-TPI*(M-IX-1)/AA*CPS-STSPK
        GOTO 85
84      V(M,N)=TPI*(N-IX-1)/CC-TPI*(M-IX-1)/AA*CPS-STSPK
85      IF(K2.GE.U(M)**2+V(M,N)**2) G(M,N)=-J*SQRT(K2-(U(M)**2
                                             +V(M,N)**2))
        IF(K2.LT.U(M)**2+V(M,N)**2) G(M,N)=-SQRT(U(M)**2+V(M,N)**2-K2)
                                             *CONE
90      CONTINUE
100     CONTINUE
        IF(ITM.GT.0) GOTO 110
C *** INCIDENT FIELDS FOR TE POLARIZATION ****
        EXI = SIN(-PHI/RTD)
        EYI = COS(PHI/RTD)
        HXI=COS(PHI/RTD)*COS(THI/RTD)/ETA
        HYI=SIN(PHI/RTD)*COS(THI/RTD)/ETA
        EF=1.0
        GOTO 120
C *** INCIDENT FIELDS FOR TM POLORIZATION ****
110     EXI=COS(PHI/RTD)*COS(THI/RTD)
        EYI=SIN(-PHI/RTD)*COS(THI/RTD)
        HYI=SIN(PHI/RTD-PI2)/ETA
        HXI=COS(PHI/RTD-PI2)/ETA
        ET=1.0*COS(THI/RTD)
120     CONTINUE
C**** CALCULATE THE RESIDUAL VECTORS RX AND RY ****
C
333     DO 200 M=1,IX
        DO 190 N=1,IX
        RX(M,N)=EXI+X(M,N)
        RY(M,N)=EYI+Y(M,N)
        IF(M.GE.NX1.AND.M.LE.NX2.AND.N.GE.NY1.AND.N.LE.NY2)
     .  RX(M,N)=CZERO
        IF(M.GE.NX1.AND.M.LE.NX2.AND.N.GE.NY1.AND.N.LE.NY2)
     .  RY(M,N)=CZERO
        ERROR=ERROR+RX(M,N)*CONJG(RX(M,N))+RY(M,N)*CONJG(RY(M,N))
        IF(ITER.EQ.0) F5=F5+RX(M,N)*CONJG(RX(M,N))+RY(M,N)*CONJG(RY(M,N))
        DX(M,N)=RX(M,N)
        DY(M,N)=RY(M,N)
190     CONTINUE
200     CONTINUE
C
C***** MULTIPLY THE RESIDUALS BY THE CONJG. TRANS. OF  Z TO
C       FIND THE DIRECTION VECTORS DX AND DY         *******
C **** FIND THE FOURIER TRANSFORM OF THE RESIDUALS *****
C
        CALL FFT3D(DX,IX,IX,IX,IX,1,69,IWK,RWK,CWK)
        CALL FFT3D(DY,IX,IX,IX,IX,1,69,IWK,RWK,CWK)
        DO 220 M=1,IX
        DO 210 N=1,IX
        CXMN=DX(M,N)
        DX(M,N)=(CONJG(G(M,N)-V(M,N)**2/G(M,N))*DX(M,N)-
     .  CONJG(V(M,N)*U(M)/G(M,N))*DY(M,N))/CONJG(J*W*EP)/2.
        DY(M,N)=(CONJG(-V(M,N)*U(M)/G(M,N))*CXMN+
     .  CONJG(G(M,N)-U(M)**2/G(M,N))*DY(M,N))/CONJG(J*W*EP)/2.
210     CONTINUE
220     CONTINUE
C
```

```
        CALL FFT3D(DX, IX, IX, IX, IX, 1, -69, IWK, RWK, CWK)
        CALL FFT3D(DY, IX, IX, IX, IX, 1, -69, IWK, RWK, CWK)
C*** STORE DX AND  DY IN  TX   AND   TY ****
        DO 360 M=1, IX
        DO 350 N=1, IX
        DX(M, N)=DX(M, N)-RX(M, N)*CONJG(ZINT)
        DY(M, N)=DY(M, N)-RY(M, N)*CONJG(ZINT)
        IF(M. GE. NX1. AND. M. LE. NX2. AND. N. GE. NY1. AND. N. LE. NY2)
       . DX(M, N)=CZERO
        IF(M. GE. NX1. AND. M. LE. NX2. AND. N. GE. NY1. AND. N. LE. NY2)
       . DY(M, N)=CZERO
        TY(M, N)=DY(M, N)
        TX(M, N)=DX(M, N)
        F3=F3+CONJG(DX(M, N))*DX(M, N)+CONJG(DY(M, N))*DY(M, N)
350     CONTINUE
360     CONTINUE
C**** THE ITERATIVE PROCESS STARTS NOW !!!!! ***
365     CALL FFT3D(TX, IX, IX, IX, IX, 1, 69, IWK, RWK, CWK)
        CALL FFT3D(TY, IX, IX, IX, IX, 1, 69, IWK, RWK, CWK)
        DO 400 M=1, IX
        DO 370 N=1, IX
        CXMN=TX(M, N)
        TX(M, N)=((G(M, N)-V(M, N)**2/G(M, N))*TX(M, N)-(U(M)*V(M, N)/G(M, N))
       . *TY(M, N))/(J*W*EP)/2.
        TY(M, N)=(-U(M)*V(M, N)/G(M, N)*CXMN+(G(M, N)-U(M)**2/G(M, N))
       . *TY(M, N))/(J*W*EP)/2.
370     CONTINUE
400     CONTINUE
        CALL FFT3D(TX, IX, IX, IX, IX, 1, -69, IWK, RWK, CWK)
        CALL FFT3D(TY, IX, IX, IX, IX, 1, -69, IWK, RWK, CWK)
        F1=0. 0
        DO 410 M=1, IX
        DO 410 N=1, IX
        TX(M, N)=TX(M, N)-DX(M, N)*ZINT
        TY(M, N)=TY(M, N)-DY(M, N)*ZINT
        IF(M. GE. NX1. AND. M. LE. NX2. AND. N. GE. NY1. AND. N. LE. NY2)
       . TX(M, N)=CZERO
        IF(M. GE. NX1. AND. M. LE. NX2. AND. N. GE. NY1. AND. N. LE. NY2)
       . TY(M, N)=CZERO
410     F1=F1+CONJG(TX(M, N))*TX(M, N)+CONJG(TY(M, N))*TY(M, N)
C *** CALCULATE THE FACTOR AN  ***
        ITER=ITER+1
        AN=F3/F1
        CH(ITER)=SQRT(abs(error))/SQRT(F5)
C *** CALCULATE THE ERROR ***
        ERROR=ERROR-(F3**2/F1)
C *** UPDATE THE VALUES FOR X AND Y   ***
        DO 560 M=1, IX
        DO 550 N=1, IX
        X(M, N)=X(M, N)+AN*DX(M, N)
        Y(M, N)=Y(M, N)+AN*DY(M, N)
550     CONTINUE
560     CONTINUE
C **** FIND A NEW ESTIMATE FOR THE RESIDUAL VECTORS RX  AND RY ***
        DO 580 M=1, IX
        DO 570 N=1, IX
        RX(M, N)=RX(M, N)-AN*TX(M, N)
        RY(M, N)=RY(M, N)-AN*TY(M, N)
        TX(M, N)=RX(M, N)
        TY(M, N)=RY(M, N)
```

```
570     CONTINUE
580     CONTINUE
        RR(ITER)=FLOAT(ITER)
        WRITE(*,*) CH(ITER),RR(ITER)
C*****MULTIPLY TX AND TY BY THE CONJG. TRANS. OF THE MATRIX  Z **
        CALL FFT3D(TX,IX,IX,IX,IX,1,69,IWK,RWK,CWK)
        CALL FFT3D(TY,IX,IX,IX,IX,1,69,IWK,RWK,CWK)
        DO 600 M=1,IX
        DO 590 N=1,IX
        CXMN=TX(M,N)
        TX(M,N)=(CONJG(G(M,N)-V(M,N)**2/G(M,N))*TX(M,N)-
     .  CONJG(V(M,N)*U(M)/G(M,N))*TY(M,N))/CONJG(J*W*EP)/2.
        TY(M,N)=(CONJG(-V(M,N)*U(M)/G(M,N))*CXMN+
     .  CONJG(G(M,N)-U(M)**2/G(M,N))*TY(M,N))/CONJG(J*W*EP)/2.
590     CONTINUE
600     CONTINUE
        CALL FFT3D(TX,IX,IX,IX,IX,1,-69,IWK,RWK,CWK)
        CALL FFT3D(TY,IX,IX,IX,IX,1,-69,IWK,RWK,CWK)
        F2=F3
C       F3=F3/400.
C       IF(CH(ITER).LT.0.30) F3=0.0
        F3=0.0
        DO 644 M=1,IX
        DO 644 N=1,IX
        TX(M,N)=TX(M,N)-RX(M,N)*CONJG(ZINT)
        TY(M,N)=TY(M,N)-RY(M,N)*CONJG(ZINT)
        IF(M.GE.NX1.AND.M.LE.NX2.AND.N.GE.NY1.AND.N.LE.NY2)
     .  TX(M,N)=CZERO
        IF(M.GE.NX1.AND.M.LE.NX2.AND.N.GE.NY1.AND.N.LE.NY2)
     .  TY(M,N)=CZERO
        F3=F3+CONJG(TX(M,N))*TX(M,N)+CONJG(TY(M,N))*TY(M,N)
644     CONTINUE
C **** CALCULATE THE FACTOR BN ****
        BN=(F3/F2)
C ***** UPDATE THE DIRECTION VECTORS  DX  AND  DY  *****
C
        DO 664 M=1,IX
        DO 654 N=1,IX
        DX(M,N)=TX(M,N)+BN*DX(M,N)
        DY(M,N)=TY(M,N)+BN*DY(M,N)
        TX(M,N)=DX(M,N)
        TY(M,N)=DY(M,N)
654     CONTINUE
664     CONTINUE
C **** GO FOR ANOTHER ITERATION IF YOU WANT ****
        IF(ITER.GT.NOI) GO TO 800
        GO TO 365
800     DO 820 I=1,IX
        AMP(I)=CABS(Y(I,16))
        RINDEX(I)=(FLOAT(I-IX/2)-.5)/IX*AA*1.045
        WRITE(*,*) AMP(I),RINDEX(I)
820     CONTINUE
        WRITE(11,*) ITER
        CALL FFT3D(X,IX,IX,IX,IX,1,69,IWK,RWK,CWK)
        CALL FFT3D(Y,IX,IX,IX,IX,1,69,IWK,RWK,CWK)
        DO 840 M=1,IX
        DO 830 N=1,IX
        CXMN=X(M,N)
        X(M,N)=((G(M,N)-V(M,N)**2/G(M,N))*X(M,N)-(U(M)*V(M,N)/G(M,N))
     .  *Y(M,N))/(J*W*EP)/2.
```

```
        Y(M,N)=(-U(M)*V(M,N)/G(M,N)*CXMN+(G(M,N)-U(M)**2/G(M,N))
     .*Y(M,N))/(J*W*EP)/2.
830     CONTINUE
840     CONTINUE
C **** CALCULATE REFLECTION COEFFICIENTS
        CREFX=X(1,1)/FLOAT(IX)**2
        CREFY=Y(1,1)/FLOAT(IX)**2
        CREF=CREFX*SIN(-PHI/RTD)+CREFY*COS(PHI/RTD)
        CRET=CREFX*COS(PHI/RTD)+CREFY*SIN(PHI/RTD)
        IF(ITM.GT.0) GO TO 850
C
C ****  TE POLARIZATION ****
C**     THIS IS THE CO-POLARIZED COMPONENT  ****
        REFF=CABS(CREF/EF)
        CTF=1-CREF
        TFF=CABS(CTF)
C ***   THIS IS THE CROSS-POLARIZED COMPONENT ***
        REFT=CABS(CRET/EF)
        WRITE(11,*) 'CREF,CRET,REFF,REFT,TFF'
        WRITE(11,*)  CREF,CRET,REFF,REFT,TFF
850     CONTINUE
C *** TM POLARIZATION ***
C *** THE CO-POLARIZED COMPONENT **
        RETT=CABS(CRET/ET)
        CTT=1-CRET
        TTT=CABS(CTT)
C **** THE CROSS-POLARIZED COMPONENT***
        RETF=CABS(CREF/ET)
        WRITE(11,*) 'CRET,CREF,RETT,RETF,TTT'
        WRITE(11,*)  CRET,CREF,RETT,RETF,TTT
900     STOP
        END
C
C
        COMPLEX FUNCTION SINHH(X)
        COMPLEX X
        SINHH=0.5*(CEXP(X)-CEXP(-X))
        END
C
C
        COMPLEX FUNCTION COSHH(X)
        COMPLEX X
        COSHH=0.5*(CEXP(X)+CEXP(-X))
        END
```

PART II

THE ONE DIMENSIONAL PROBLEM (GRATING)USING

THE SECANT-CORRECTOR SPECTRAL ITERATION APPROACH

(MASTER's THESIS BY ROBERT MIDDELVEEN)

ABSTRACT

The secant method is applied to an iterative algorithm of electromagnetic scattering from planar surfaces with periodic structure. The theory of convergent solutions for iterative techniques is discussed and examined. The Secant method is applied to the spectral iteration approach to accelerate and assure convergence of the basic iterative scheme. The derivation of the method as applied to surfaces containing parallel thin wire gratings is presented, and the conditions for achieving convergence are explored. This new method is also applied to gratings made of coated wires. The reflection characteristics of the grating as a function of wire spacing, wire conductivity, and polarization of the incident field are computed, and the results are compared with those of previous works. Suggestions and recommendations for applying the method to more complicated structures are also included.

TABLE OF CONTENTS

LIST OF TABLES

LIST OF FIGURES

I. INTRODUCTION

Scattering from periodic structures such as grids or gratings has been of particular interest in the field of electromagnetics for many years. The field distribution about the structure caused by a plane incident wave, the induced current densities in the wires, and the reflection coefficient are the most important parameters used in designing grids and gratings.

The objective of this thesis is to model the problem of electromagnetic wave scattering from a grating and compute the current density and reflection coefficient. Grids are important because they can be used as reflecting surfaces instead of solid metal surfaces, especially for modeling light-weight antennas for space applications. Moreover, by making use of the frequency dependence of these structures, they can be applied to filtering from the microwave to the optical wave regions.

Many different methods have evolved for solving the problem of electromagnetic scattering from such structures. The most popular approach, the method of moments, usually requires large amounts of computer memory when applied to periodic structures. Another technique, the spectral-iteration technique (S.I.T.) developed by Tsao and Mitra [1]

circumvents this memory requirement, but suffers from convergence problems. For example, if the separation of adjacent wires, or strips is less than two wavelengths, then the S.I.T method will not converge.

Brand [2] applied a corrective scheme that assured the convergence of the basic iterative equation for any wire spacing. This method, however, depends on the evaluation of numerical derivatives to generate a series of convergent iterations. In some cases the computation of the derivative can be so critical that the new corrective scheme fails to converge. This thesis presents an alternative, derivative-free technique which always converges for any spacing of adjacent wires, polarization of incident wave, and angle of incidence of the incoming wave.

Another alternative method for solving scattering problems is the Fast Fourier transform-conjugate gradient method (FFT-C.G.) developed by Chistodoulou [3]. This technique can be used to solve for either the strip currents or the electric field separately. Results obtained using this method are compared with those obtained using the new algorithm.

Also included in this thesis is a study of electro-magnetic scattering from gratings made of coated wires. An internal impedance is used which takes into consideration

the effects of the substrate on the induced currents and reflection coefficient. This approach is particularly useful for space applications where a highly conductive coating is used in conjunction with a light substrate. Usually the electrical characteristics of the substrate are unimportant. For certain frequency ranges, however, the electrical fields and currents penetrate both coating and substrate so that the properties of both materials become important in the calculation of fields and currents.

II. DERIVATION OF THE ORIGINAL ITERATIVE SCHEME

A model is presented here that can determine the electric field and current density along the surface of a unit cell illustrated in Figure 1.

First, the electric field arising from a magnetic current is given by:

$$\overline{E} = -(1/\epsilon) \ \nabla \times \overline{F} \hspace{3cm} [1]$$

where $\overline{F}$ is the vector magnetic potential caused by the ficticious magnetic current source $\overline{K}$, and ϵ is the permittivity of the medium. The sources here will all be considered as harmonic, so that $\overline{E}$ and $\overline{H}$ fields will be phasor quantities. The vector potential $\overline{F}$, can be derived from $\overline{K}$ by making use of the free-space Greens function $\overline{\overline{G}}$. The vector potential is a convolution of $\overline{K}$ and $\overline{\overline{G}}$, given by

$$\overline{F} = \int \overline{\overline{G}}(\overline{r}, \overline{r}') \ \overline{K}(\overline{r}) \ d\overline{r}' \hspace{2cm} [2]$$

where the free-space Greens function is defined by:

$$G = (1/4\pi \ |\overline{r}|) \ \overline{\overline{I}} \ Exp(-j \ \overline{k} \cdot \overline{r}) \hspace{2cm} [3]$$

The dyadic is denoted by $\overline{\overline{I}}$. The two vectors $\overline{r}$ and $\overline{k}$ are illustrated in Figure 1. Returning to equation 1, the magnetic field intensity as a function of magnetic vector
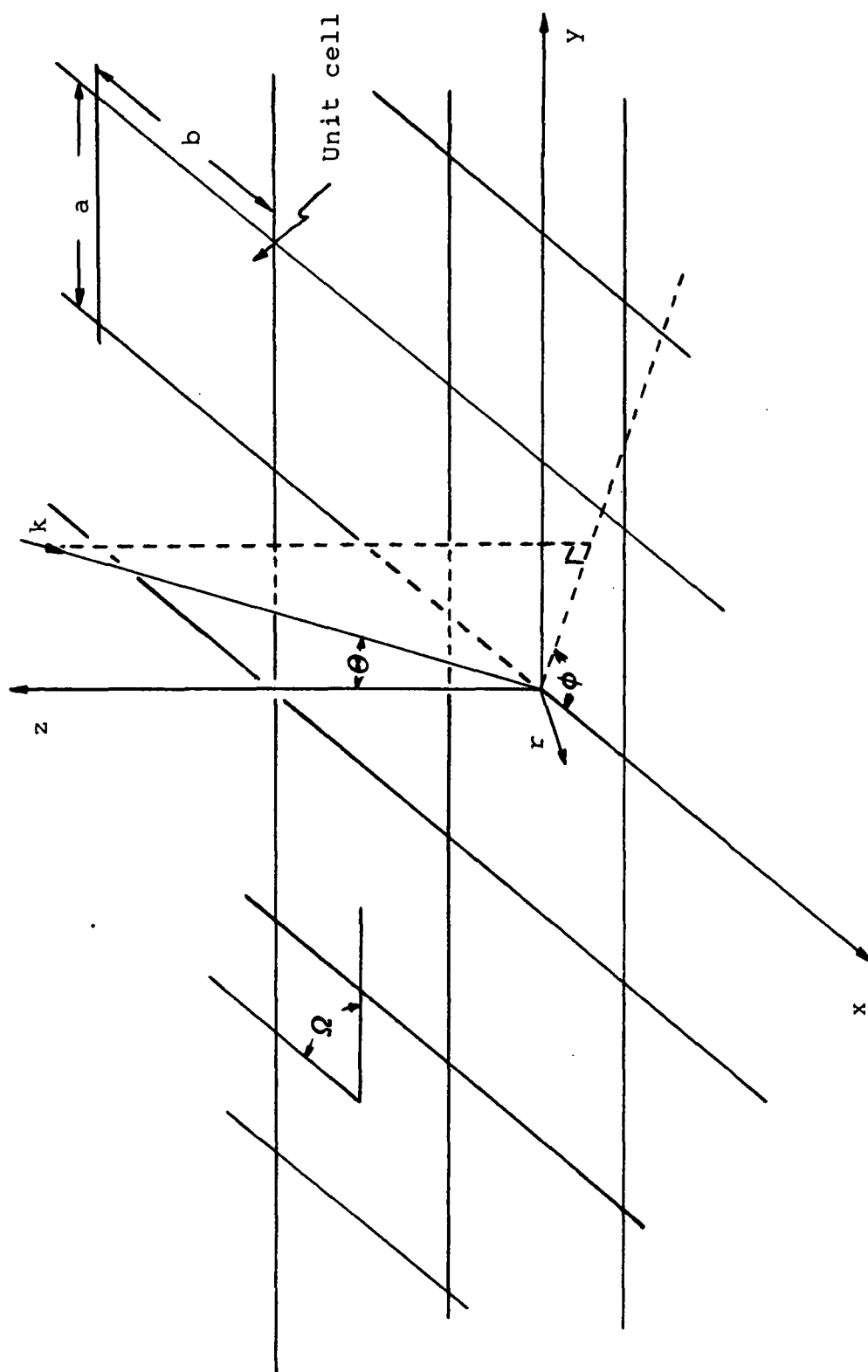
4

Figure 1. The Geometry of the Plane.

potential can be derived from Maxwell's equations and applying the Lorentz gauge condition (see Appendix B).

$$\overline{H} = -j\omega\epsilon \ \overline{F} + (1/j\omega\mu) \ \nabla \ (\ \nabla \cdot \overline{F}) \qquad [4]$$

Where μ is the permeability of the medium, and ω is the angular frequency. Referring to Figure 1, there can be no magnetic current in the z direction because the planar structure is limited to the x-y plane. Therefore no component of the magnetic vector potential can exist in the z direction. Also because the stucture is located in the plane z = 0, $\overline{\overline{G}}$ will be a function of x and y only. If the medium is allowed to be that of free space, then the permeability and permittivity will remain constant and are given by μ_o and ϵ_o respectively. The propagation constant for this medium is defined by:

$$k = \omega \ \sqrt{\mu_o\epsilon_o} \qquad [5]$$

Equation 4 can now be expanded in the Cartesian coordinate system as follows:

$$\overline{H}_s = \quad 1/j\omega\mu_o\left[\left(k_o^2 F_x + \frac{\partial^2 F_x}{\partial x \, \partial y} + \frac{\partial^2 F_y}{\partial x^2}\right) \ \overline{a}_x \qquad [6]\right.$$
$$\left. + \left(k_o^2 F_y + \frac{\partial^2 F_x}{\partial x \, \partial y} + \frac{\partial^2 F_y}{\partial y^2} \right) \ \overline{a}_y\right]$$

The subscript s in this equation signifies that this is the scattered field. The scattered field is caused by the incident field generating the magnetic currents in equation 6. These currents in turn produce the scattered fields. The total $\overline{H}$ field can be found by adding the incident and

scattered fields. In vector notation equation 6 is expressed as:

$$\bar{H}_s = \begin{bmatrix} H_x \\ H_y \end{bmatrix}_s = 1/j\omega\mu_o \begin{bmatrix} k_o^2 + \partial^2/\partial x^2 & \partial^2/\partial x \partial y \\ \partial^2/\partial x \partial y & k_o^2 + \partial^2/\partial y \end{bmatrix} \begin{bmatrix} F_x \\ F_y \end{bmatrix} \qquad [7]$$

Equation 2 is now substituted into equation 7. Taking the Fourier Transform of equation 7, the convolution of $\bar{\bar{G}}$ and $\bar{K}$ in the space domain becomes a multiplication in the Fourier domain. The transformed scattered magnetic intensity is given by:

$$\tilde{\bar{H}}_s = 1/j\omega\mu_o \begin{bmatrix} k_o^2 - \alpha_{mn}^2 & \alpha_{mn}\beta_{mn} \\ -\alpha_{mn}\beta_{mn} & k_o^2 - \beta_{mn}^2 \end{bmatrix} \tilde{\bar{\bar{G}}} \; \tilde{\bar{K}} \qquad [8]$$

The tilde symbol is used to denote the transform of the variable in the Fourier domain. The parameters α_{mn} and β_{mn} are referred to as the Floquet modes and they are defined as follows, reference [2]:

$$\alpha_{mn} = 2\pi m/a \qquad - k_o \sin\theta \cos\phi \qquad [9]$$

$$\beta_{mn} = 2\pi n/c \; - \; (2\pi m/a) \cot\Omega \; - \; k_o \sin\theta \sin\phi \qquad [10]$$

Their values depend upon the cell geometry of the planar surface being studied. The angles θ, ϕ, and Ω are shown in Figure 1. The number of sampling points across the unit cell in the x and y direction are given by m and n respectively. The Floquet modes allow for the effects of coupling between the conducting regions of the planar surface. The Fourier Transform of Green's function is given by:

$$\tilde{\bar{\bar{G}}} = -(j/2)(k_o^2 - \alpha_{mn}^2 - \beta_{mn}^2)^{-1/2} \bar{\bar{I}} \qquad [11]$$

If the Inverse Fourier Transform is applied again to equation 8, the scattered field in the space domain will be given by:

$$\overline{H}_s = 1/j\omega\mu_o \sum_{mn} \begin{bmatrix} k_o - \alpha_{mn} & \alpha_{mn}\beta_{mn} \\ -\alpha_{mn}\beta_{mn} & k_o - \beta_{mn} \end{bmatrix} \overset{\approx}{G}\ \tilde{K}\ Exp(j[\alpha_{mn}x + \beta_{mn}y]) \quad [12]$$

By using the equivalence theorem and applying the appropriate boundary conditions to the scattered H field at z = 0, the total tangential H field can be solved in terms of the transformed electric field in the aperture as:

$$\overline{H}_{tinc} = -2/j\omega\mu_o \sum_{mn} \begin{bmatrix} \alpha_{mn}\beta_{mn} & k_o - \alpha_{mn} \\ -k_o + \beta_{mn} & -\alpha_{mn}\beta_{mn} \end{bmatrix} \overset{\approx}{G}\ \tilde{E}\ Exp(j[\alpha_{mn}x + \beta_{mn}y]) \quad [13]$$

To include the contribution of the $\overline{H}$ field along the conducting strip, the current densities have to be added to equation 12 to yield, reference [2]:

$$Trc'(\overline{J}) = \overline{H}_{tinc} + 2/j\omega\mu_o \sum_{mn} \begin{bmatrix} \alpha_{mn}\beta_{mn} & k_o - \alpha_{mn} \\ -k_o + \beta_{mn} & -\alpha_{mn}\beta_{mn} \end{bmatrix} \overset{\approx}{G}\ \tilde{E} \quad [14]$$

$$Exp(j[\alpha_{mn}x + \beta_{mn}y])$$

Because the current density can only be present on the conducting strips, the truncation operator Trc and its complement are introduced. These are defined by:

$$Tcr\ [\ X(\overline{r})\ ] = \begin{cases} X(\overline{r}) & \text{for } \overline{r} \text{ in the aperture} \\ 0 & \text{for } \overline{r} \text{ in the conducting region} \end{cases} \quad [15]$$

$$Tcr'[\ X(\overline{r})\ ] = \begin{cases} 0 & \text{for } \overline{r} \text{ in the aperture} \\ X(\overline{r}) & \text{for } \overline{r} \text{ in the conducting region} \end{cases} \quad [16]$$

In equation 14, direct solution for the electric field is not possible since both the strip current and electric field are unknown. For this reason Tsao and Mittra [4] developed an iterative equation to solve for both the electric field and the strip current. Returning to equation 14, the following simplification is made:

$$\widetilde{\widetilde{G}}_2 = \begin{bmatrix} \alpha_{mn}\beta_{mn} & k_o - \alpha_{mn} \\ -k_o + \beta_{mn} & \alpha_{mn}\beta_{mn} \end{bmatrix} \widetilde{\widetilde{G}} \qquad [17]$$

With this substitution, and the fact that the tangential field is present only in the aperture and the current density exists only along the conductor, equation 14 can be written as:

$$Trc'(\overline{J}) = Trc'(\overline{H}_{tinc} + 2/j\omega\mu_o \ F^{-1}[\widetilde{\widetilde{G}}_2 \ F \ (Trc \ [\overline{E}_t])]) \qquad [18]$$

Similarly the tangential electric field can be derived from equation 14:

$$\overline{E}_t = F^{-1}[\widetilde{\widetilde{G}}_2^{-1}F \ (j\omega\mu_o \ /2 \ [Trc'[\overline{J}] - \overline{H}_{tinc}])] \qquad [19]$$

This electric field represents the field across the entire cell. The field is also valid on the conducting strip because the truncation operation is performed on this field in equation 18. Equation 18 is substituted into equation 19 yielding the basic form of the iterative equation in terms of the electric field.

$$\overline{E}_{ti} = F^{-1}[\widetilde{\widetilde{G}}_2^{-1} \ F \ (j\omega\mu_o \ /2 \ [Trc' \ (\overline{H}_{tinc} + 2/j\omega\mu_o \ F^{-1}$$
$$[\widetilde{\widetilde{G}}_2 \ F \ (Trc \ [\overline{E}_{ti-1}])]) - \overline{H}_{tinc}])] \qquad [20]$$

Brand [2] imposed his corrective technique on this equation. As an alternative to Brand's correction, the secant technique can also be applied to equation 20. This technique will eliminate the convergence problems caused by the unavailability of an analytic derivative.

III. THE SOLUTION OF FIXED POINT PROBLEMS VIA ITERATION FUNCTIONS

General Theory of Iterative Functions

Iterative functions are often constructed to solve equations of the following form:

$$f(x) = 0 \qquad [21]$$

$$\text{and} \quad F(\overline{X}) = 0 \qquad [22]$$

Equation 21 represents a single variable complex function. In equation 22, both the function and argument are vector quantities whose elements can be complex. If these functions are of a very complex nature, a direct solution may not be available. However, a solution of arbitrary precision may be obtained using iterative techniques. These techniques make use of equations 21 or 22 to construct iterative functions of the form:

$$x_{i+1} = g(x_i) \qquad [23]$$

$$\overline{X}_{i+1} = G(\overline{X}_i) \qquad [24]$$

Equation 23 is a single variable function and equation 24 is the vector equivalent.

Solutions of f(x)=0

The iterative process consists of starting with an initial guess x_o, and inserting this value in equation 23 to

obtain a new iterate x_1. The process is repeated until $x_{i+1} = x_i + e$ where e is an allowable error. If $x^* = x_{i+1} = x_i$, then x^* is called the fixed point or the best numerical solution of equation 23. The fixed point of g(x) is a root of f(x). There are two conditions required to assure a convergent solution:

1) On a closed region containing the solution x, g(x) should be continuous.

2) For any arbitrary points s and t in this region the following condition must be met:

$$|g(s) - g(t)| < p |s - t| \qquad [25]$$

$$0 \leq p < 1$$

These conditions imply that g(x) must be differentiable over the interval of interest and that the magnitude of its derivative must be less than unity. Froberg [4] has an in-depth proof of this statement. If the above conditions hold then g(x) is said to be a contraction, and the iterative process will eventually produce a fixed point x^*. The graphical description of the iteration process is illustrated in Figure 2. The fixed point x^* is obtained by finding the intersection of y = x and y = g(x). The first four iterations are included beginning with the initial guess denoted x_0 .
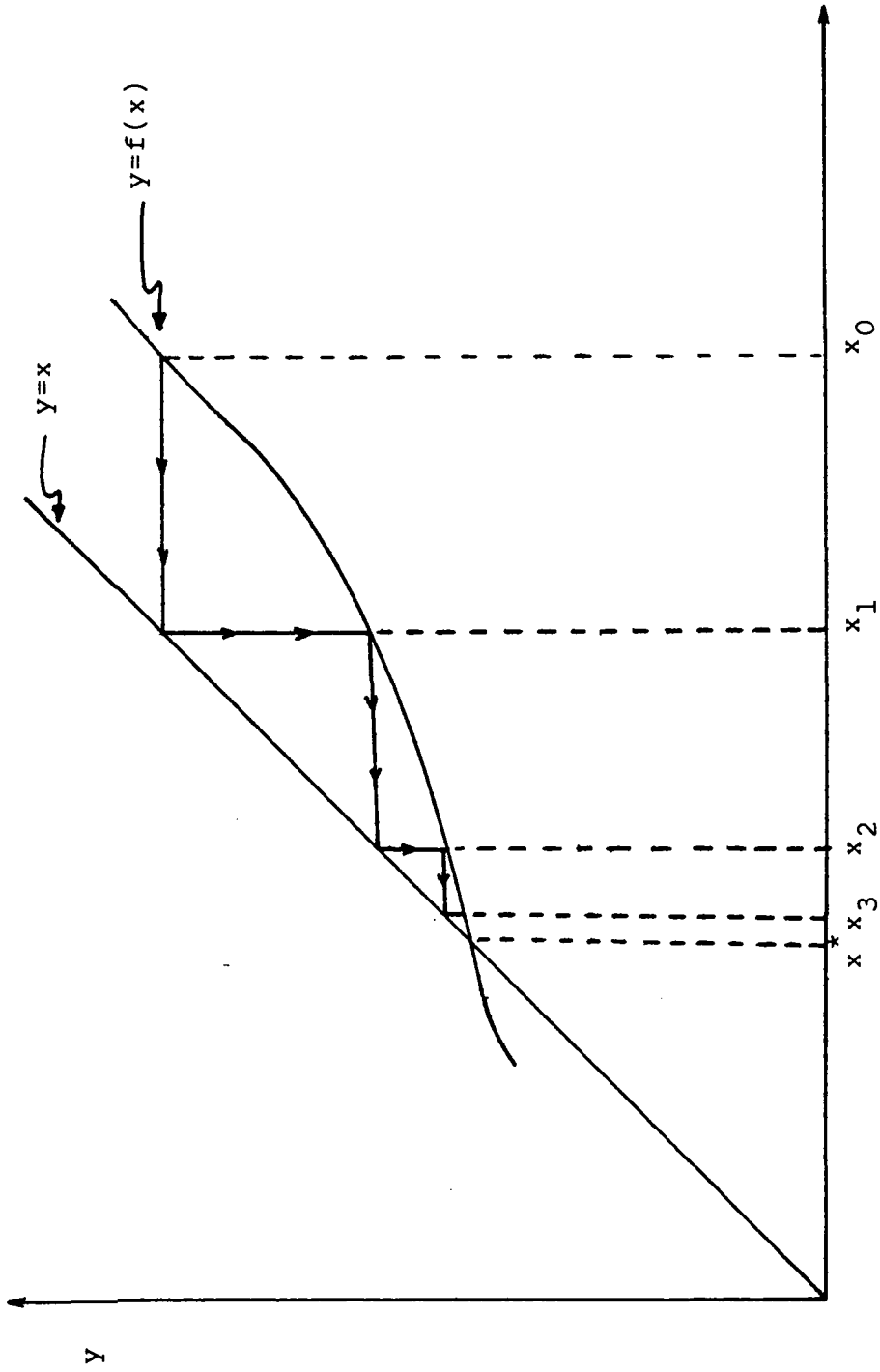
Figure 2. Graphical Illustration of the Iterative Process.

To illustrate the iterative process, consider the following equation:

$$0 = f(x) = x^4 + 11x^3 + 35.5x^2 + 57x^1 + 31.5 \qquad [26]$$

This equation contains roots at -1, -7, -1.5-j1.5 and -1.5+j1.5. It is desired to find these roots using an iterative process. An obvious choice for g(x) is obtained by solving equation 26 for x^1.

$$g(x) = (-1/57)(x^4 + 11x^3 + 35.5x^2 + 31.5) \qquad [27]$$

The derivative of this function is:

$$g'(x) = (-1/57)(4x^3 + 33x^2 + 71x) \qquad [28]$$

The values of this derivative at the different roots are:

$$g'(-1) = 0.7368 \qquad [29]$$

$$g'(-7) = 4.4211 \qquad [30]$$

$$g'(-1.5-j1.5) = 1.4193 \, Exp(-j0.1865) \qquad [31]$$

$$g'(-1.5+j1.5) = 1.4193 \, Exp(j0.1865) \qquad [32]$$

Note that f(x) and g(x) are both continuous over the entire complex plane but that the derivative of g(x) is less than unity only in the interval about the root at x = -1. With an appropriate initial guess g(x) should therefore converge to the fixed point $x^* = -1$. The first 20 iterations, generated by equation 27, when $x_o = 2$ are tabulated in Table 1. It should be mentioned that this choice of g(x) cannot be used to find the other roots, and for an inappropriate initial guess the iterative process may diverge altogether. Fortunately, there are other techniques which can be applied

TABLE 1

EXAMPLE OF ITERATIVE EQUATION DERIVED FROM f(x).
CONVERGENT ABOUT THE REGION x = -1.0

Iteration	$g(x_i)$
0	-4.868421
1	-2.901527
2	-2.325328
3	-2.006732
4	-1.785657
5	-1.618081
6	-1.485960
7	-1.380177
8	-1.295302
9	-1.227566
10	-1.174003
11	-1.132097
12	-1.099659
13	-1.074794
14	-1.055895
15	-1.041630
16	-1.030925
17	-1.022926
18	-1.016970
19	-1.012546

$$f(x) = x^4 + 11x^3 + 35.5x^2 + 57x + 31.5$$

$$g(x) = \frac{-1}{57} \left(x^4 + 11x^3 + 35.5x^2 + 31.5 \right)$$

to this problem to assure convergence and increase the convergence rate.

Techniques to Accelerate and Assure Convergence

The techniques used to resolve these problems involve the synthesis of a better iterative function than the example illustrated in equation 27. These methods involve the use of derivatives of the function f(x) and the knowledge of previous iterates stored in memory.

One of the techniques that can be used to find all the roots of equation 26 is the Newton-Raphsom method. The new iterative function synthesized with this technique involves the use of derivatives of f(x) and is written in the following form:

$$g(x_i) = x_i - f(x_i)/f'(x_i) \qquad [33]$$

This new iterative function has a derivative with a magnitude that is always less than unity over the complex plane if f(x) and f'(x) are well-behaved functions. The problem encountered with the previous sample iteration function is no longer present and equation 33 can now be used to solve for the missing roots. Table 2 lists the first 10 iterations of the solutions to the real roots of equation 26. From this table it can be seen that the rate of convergence has also been increased. This acceleration is to

TABLE 2

EXAMPLE OF THE NEWTON-RAPHSON I.F. APPLIED TO $f(x)$ TO
ACCELERATE CONVERGENCE AND FIND ADDITIONAL ROOTS

Iteration (i)	$x_o = 2.0$ $g(x_i)$	$x_o = -10.0$ $g(x_i)$
0	0.921488	-8.513304
1	0.117348	-7.575745
2	-0.470798	-7.121042
3	-0.846059	-7.006845
4	-0.985979	-7.000025
5	-0.999888	-7.000000
6	-1.000000	-7.000003
7	-1.000000	-7.000003
8	-1.000000	-7.000002
9	-1.000000	-7.000000

$$f(x) = x^4 + 11x^3 + 35.5x^2 + 57x + 31.5$$

$$g(x_i) = x_i - f(x_i)/f'(x_i)$$

be expected as more information about f(x) is used in the formulation of new iterations. The technique is also valid for complex valued functions. The first 10 iterations solving for the complex root are shown in Table 3. A graphical illustration of this technique is depicted in Figure 3. The first three iterations are shown beginning with the initial guess x_0. The fixed point is denoted by x^*. Note that the true tangent is used to calculate the next iterate.

The Newton-Raphson method is universally known and is the most popular and useful iterative function. Occasionally, when an analytic derivative is not available, one can be approximated by perturbing the original function by a small increment, denoted by del (Δ). However, the error introduced using this method may be critical. If del is too large, the approximation will not be valid at the desired point. Figure 4 shows how the numeric derivative will contain a large error if the function is changing too rapidly with x. If del is too small the approximation is limited by the precision of the numerical operation.

The secant method does not depend on the evaluation of any numerical derivative. The secant iterative function is defined by:

$$g(x_i, x_{i-1}) = x_i - f(x_i)[(x_i - x_{i-1})/(f(x_i) - f(x_{i-1}))] \qquad [34]$$

TABLE 3

EXAMPLE OF COMPLEX VALUED NEWTON-RAPHSON I.F. APPLIED TO
f(x) TO ACCELERATE CONVERGENCE AND FIND COMPLEX ROOTS

	x_o =	-4.000000 -	j4.000000
Iteration (i)		$g(x_i)$ real	$g(x_i)$ imaginary
0		-3.485554	-2.714932
1		-2.896810	-1.753410
2		-2.228628	-1.196201
3		-1.583420	-1.059435
4		-1.152799	-1.751122
5		-1.370047	-1.506637
6		-1.495772	-1.483877
7		-1.500129	-1.500248
8		-1.500000	-1.500001
9		-1.499999	-1.500000

$$f(x) = x^4 + 11x^3 + 35.5x^2 + 57x + 31.5$$
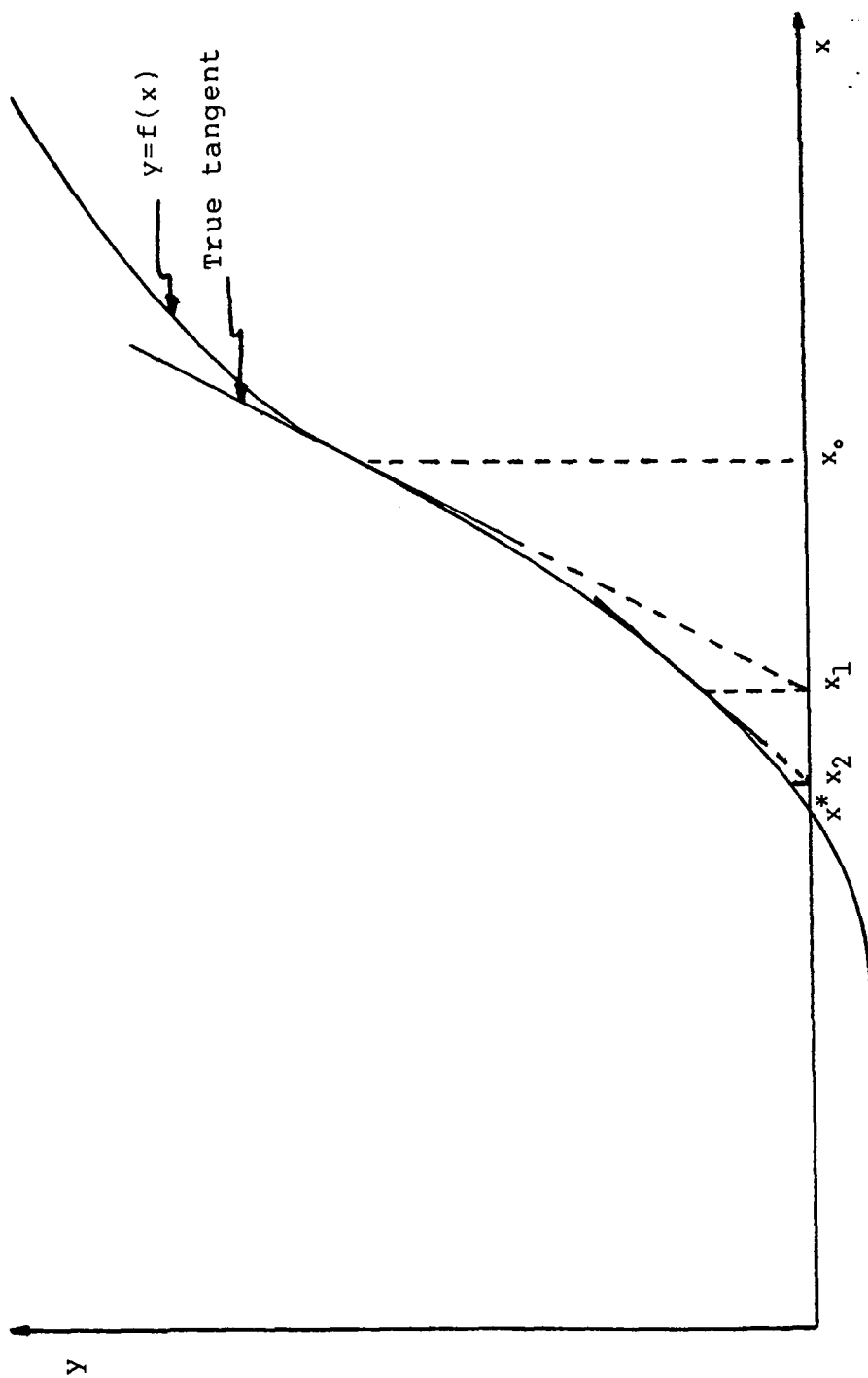
$$g(x_i) = x - f(x_i)/f'(x_i)$$

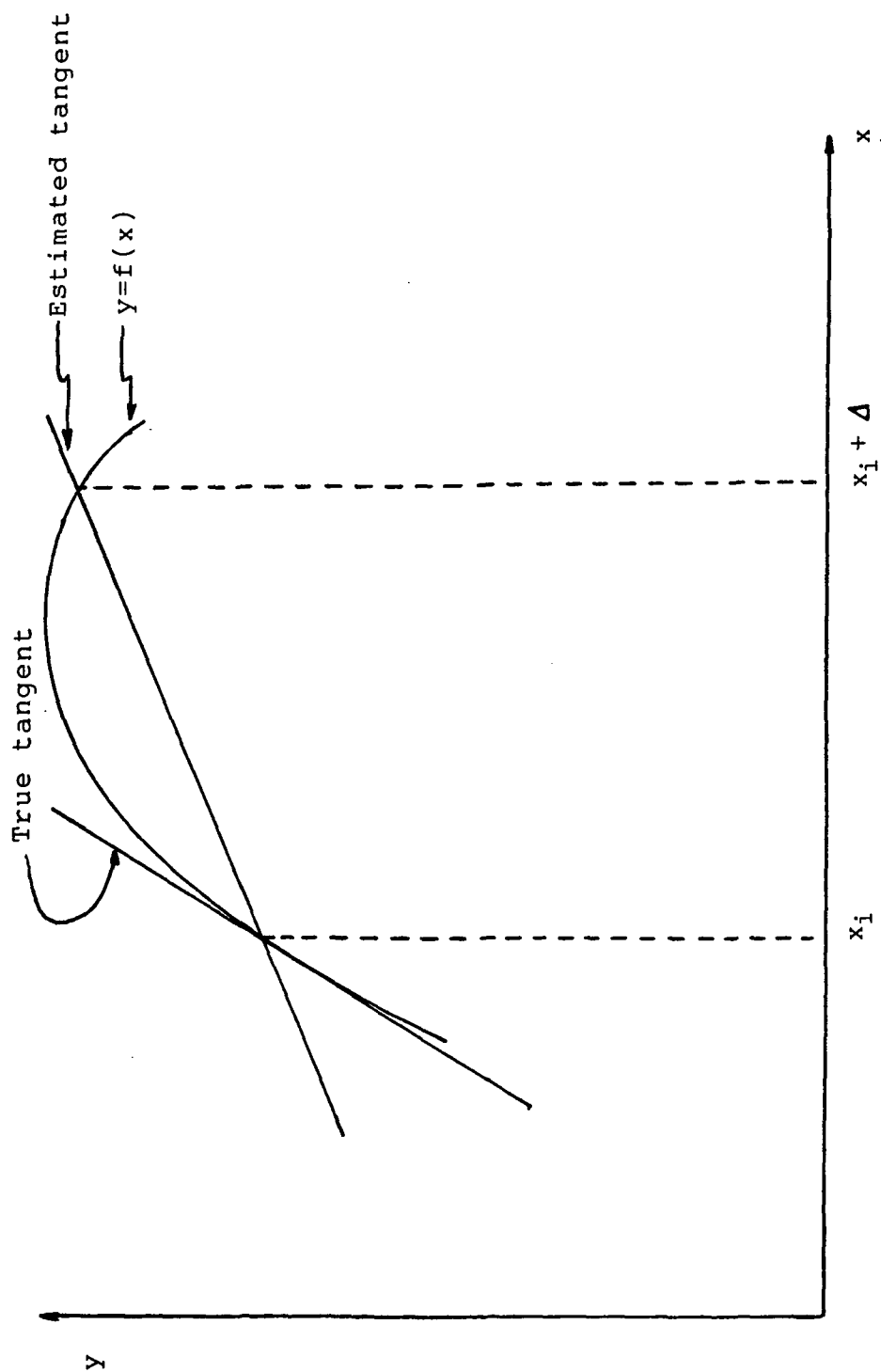Figure 3. Illustration of the Newton-Raphson Technique.

Figure 4. Numerical Approximation of the Derivative.

This method is based on a similar geometry as that of the Newton-Raphson method. Figure 5 shows that sequential iterates are used to estimate the tangent. This method tends to converge more slowly but always locks in to the fixed point. The previous method, when the derivative was approximated numerically, occasionally oscillated about a point in the vicinity of the solution. The first 10 iterations of the solutions for the real roots of the sample function are shown in Table 4. The first 10 iterations solving for the complex root are shown in Table 5. As with the Newton-Raphson method, the secant method converges much more rapidly than the original iterative function given by equation 27 because more information is being used. In addition, convergence is assured for all roots.

Formulation of the Problem

The preceeding example was concerned with single valued complex functions, such as those described by equation 1. In some useful applications, however, the domain and range of the function are vector quantities such as those described by equation 22. Such is the case with the original iterative function derived by Tsao and Mittra [1]. This function (see chapter II) is repeated below for convenience:

$$\overline{E}_{ti} = F^{-1}[\ \widetilde{\overline{G}}_2^{-1}F \ (\ .j\omega\mu_o/2 \ [\ Trc'(\ \overline{H}_{tin}\not{t} \ 2/j\omega\mu_o \ F^{-1} \qquad [20]$$
$$[\ \widetilde{\overline{G}}_2F \ (Trc[\overline{E}_{ti-1}]) \ - \ \overline{H}_{tinc}])]$$
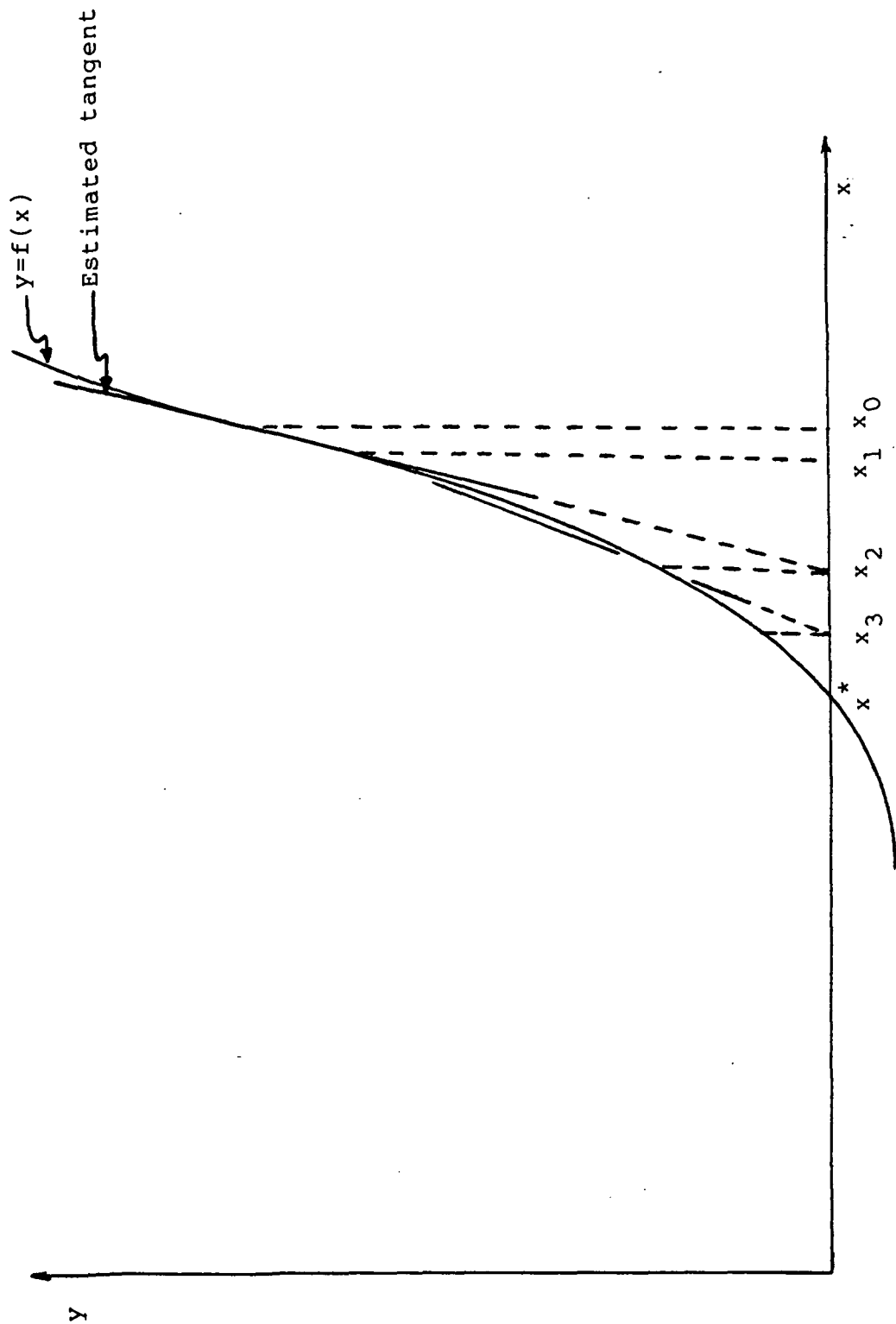
Figure 5. Illustration of the Secant Technique.

TABLE 4

EXAMPLE OF THE SECANT I.F. APPLIED TO f(x) TO ACCELERATE
CONVERGENCE AND FIND ADDITIONAL ROOTS

Iteration (i)	$x_{-1} = 3.0$ $x_0 = 2.0$ $g(x_i)$	$x_{-1} = -11.0$ $x_0 = -10.0$ $g(x_i)$
0	1.230089	-8.808706
1	0.587572	-8.044291
2	0.068331	-7.486720
3	-0.351034	-7.169444
4	-0.671497	-7.034141
5	-0.881845	-7.002733
6	-0.977097	-7.000047
7	-0.998424	-7.000005
8	-0.999980	-6.999999
9	-1.000000	-7.000000

$$f(x) = x^4 + 11x^3 + 35.5x^2 + 57x + 31.5$$

$$g(x_i, x_{i-1}) = x_i - f(x_i)[(x_i - x_{i-1})/(f(x_i) - f(x_{i-1}))]$$

25

TABLE 5

EXAMPLE OF COMPLEX VALUED SECANT I.F. APPLIED TO
f(x) TO ACCELERATE CONVERGENCE AND FIND COMPLEX ROOTS

$$x_{-1} = \quad 5.000000 + \quad j5.000000$$
$$x_0 = \quad 4.000000 + \quad j4.000000$$

Iteration (i)	$g(x_i)$ real	$g(x_i)$ imaginary
0	-3.827079	-3.051936
1	-3.365816	-2.280450
2	-2.940393	-1.648176
3	-2.441053	-1.230939
4	-1.956624	-1.021398
5	-1.482012	-1.010186
6	-0.944583	-1.453021
7	-1.845381	-1.300908
8	-1.660885	-1.734051
9	-1.567421	-1.431206

$$f(x) = x^4 + 11x^3 + 35.5x^2 + 57x + 31.5$$

$$g(x_i, x_{i-1}) = x_i - f(x_i)[(x_i - x_{i-1})/(f(x_i) - f(x_{i-1}))]$$

To simplify the above expression, the left side of the
equation 20 is defined as an operator of the electric field
vector.

$$\overline{E}_i = L_1(\overline{E}_{i-1})$$ [35]

The iterative equation described by equation 20 does not
always converge to a solution for the electric field. This
is analogous to the convergence problems encountered with
the sample iterative function, equation 27. Specifically,
equation 20 was found only to converge for very large wire
spacings. There are two equivalent techniques to alleviate
this problem. Brand [2] chose to relax equation 20 using the
following equation:

$$e_i = l_2(\overline{E}_{i-1}) = R\, e_{i-1} + (1 - R)\, l_1(\overline{E}_{i-1})$$ [36]

where l_2 and e are the individual elements of the $\overline{L}_2$ and $\overline{E}$
vectors resectivly and

$$R = l_1{}'(\overline{E}) / (l_1{}'(\overline{E}) - 1)$$ [37]

It is in equation 36 that problems with convergence emerge.
This equation requires the derivative of $\overline{L}_1$. Because an
analytic derivative is not available, an approximate
derivative is defined by:

$$l\,'(\overline{E}) = \frac{l(\overline{E}+\Delta) - l(\overline{E})}{\Delta}$$ [38]

It was this approximation that was often found to be
inadequate. Because of intrinsic differences between the IBM
and VAX computers and their compilers, Brand's results could
not be duplicated on the VAX due to the limitations in
precision when approximating the derivative.

An alternative approach was taken here, by defining a new equivalent vector function, which has as its root the solution of the electric field. This new function is defined by:

$$F\ (\overline{E}) = L_1\ (\overline{E})\ -\ \overline{E} \qquad [39]$$

The Newton-Raphson and Secant techniques can be applied directly to equation 39. The vector $\overline{F}$ is called the residue vector and has a value proportional to the remaining error in the electric field. Table 6 compares the value of this vector after 10 iterations for the S.I.T. with the contraction and secant correctors applied. It can be seen that the secant method produces a much smaller residue. The Newton-Raphson method can be applied to equation 39 as shown below:

$$l_2(E) = e\ -\ f\ (\overline{E})\ /\ f'(\overline{E}) \qquad [40]$$

where f represents an individual element of $\overline{F}$. Equations 36 and 40 are mathematically identical. Brand [2] included a formal proof repeated in Appendix C showing this equivalence. The Newton-Raphson iterative function produced results virtually identical to Brand's original model. Convergence problems persisted for certain input parameters such as low angles of incidence and small wire spacings.

The secant method can be applied to equation 14 in the following fashion:

TABLE 6

COMPARISON OF RESIDUE VECTORS

Array Element	S.I.T. (Real)	(Imaginary)	S.C.S.I. (Real)	(Imaginary)
1	0.003697	0.004007	-.00000054	0.00000182
2	0.003874	0.002393	-.00000024	-.00000909
3	0.003956	0.001639	0.00000703	-.00001219
4	0.004024	0.001026	-.00000775	-.00000885
5	0.004069	0.000608	-.00000519	-.00000742
6	0.004109	0.000244	-.00000465	-.00000682
7	0.004139	-.000029	-.00000477	-.00000659
8	0.004166	-.000273	-.00000471	-.00000641
9	0.004168	-.000459	-.00000477	-.00000635
10	0.004204	-.000625	-.00000477	-.00000632
11	0.004218	-.000749	-.00000477	-.00000626
12	0.004230	-.000857	-.00000483	-.00000626
13	0.004238	-.000930	-.00000471	-.00000626
14	0.004244	-.000989	-.00000477	-.00000620
15	0.004247	-.001018	-.00000477	-.00000626
16	0.004249	-.001033	-.00000471	-.00000626
17	0.004247	-.001018	-.00000471	-.00000626
18	0.004244	-.000989	-.00000471	-.00000626
19	0.004238	-.000930	-.00000483	-.00000620
20	0.004230	-.000857	-.00000477	-.00000608
21	0.004218	-.000749	-.00000477	-.00000620
22	0.004204	-.000625	-.00000471	-.00000620
23	0.004186	-.000459	-.00000471	-.00000629
24	0.004166	-.000273	-.00000471	-.00000641
25	0.004139	-.000029	-.00000471	-.00000656
26	0.004109	0.000244	-.00000477	-.00000679
27	0.004069	0.000608	-.00000519	-.00000739
28	0.004024	0.001026	-.00000781	-.00000888
29	0.003956	0.001639	0.00000703	-.00001213
30	0.003874	0.002393	-.00000024	-.00000909
31	0.003697	0.004007	-.00000060	0.00000188
32	0.003328	0.007377	0.00000649	-.00001098

$$l_3(\overline{E}_i, \overline{E}_{i-1}) = e_i - f(\overline{E}_i)(e_i - e_{i-1}) / f(\overline{E}_i) - f(\overline{E}_{i-1}) \quad [41]$$

where l_3 is an individual element of the vector produced by operator $\overline{L}_3$.

Although the vector and single valued iterative functions appear to be constructed in identical fashion, there are important differences regarding the number of solutions and the conditions necessary to assure convergence. The vector operator L is called a contraction operator in a particular domain if it satisfies the following condition:

$$d_2[L(\overline{U}), L(\overline{V})] \quad p \ d_2[\overline{U}, \overline{V}] \quad [42]$$

The magnitude of p is always less than unity and $\overline{U}$ and $\overline{V}$ are any two vectors in the domain. The operator d_2 referred to in equation 42 is the distance function and is defined by:

$$d_2(\overline{U}, \overline{V}) = \left[\sum_{i=1}^{n} |u_i - v_i|^2 \right]^{1/2} \quad [43]$$

If L is a contraction throughout a given domain, then from any starting point within that domain, there will be one and only one fixed point defined by:

$$\overline{U}^* = L(\overline{U}^*) \quad [44]$$

The formal proof and a discussion of vector spaces is provided by Stakgold [5].

Brand [2] proves with mathematical rigor that the Newton-Raphson iterative equation, given infinite numerical precision, will always converge to the fixed point.

Restrictions are imposed that are even more stringent than those of equation 42. It is shown that the Newton-Raphson method complies with these new conditions. Given that the Secant method is an approximation of the Newton-Raphson method, it is intuitive that this method should also force convergence upon the original iterative scheme devised by Tsao and Mitra. In fact Traub [6] shows that the order of the iterative function for the secant method is 1.62 as compared with 2 for the Newton-Raphson method. Any two vectors in the domain of L can be chosen as the $\bar{U}$ and $\bar{V}$ of equation 42. Brand [2] chose as his two vectors $\bar{E}$ and $\bar{E} + \Delta$. To monitor the performance of the contraction of the secant iterative function, E_i and E_{i+1} proved to be convenient vectors. A contraction factor is defined below for the secant method:

$$\text{Con} = \frac{d(L(\bar{E_i}), L(\bar{E_{i-1}}))}{d(\bar{E_i}, \bar{E_{i-1}})} \qquad [45]$$

This factor was verified to comply with equation 17 when the contraction process was taking place. Applying the secant method, it was found that convergence was obtained for any wire spacings, any polarization of the incident wave, and a wide range of wire conductivity.

IV. THE INTERNAL IMPEDANCE OF THE WIRES IN THE GRATING

To account for the finite conductivity in coated wires, the following boundary condition must be met:

$$E_{tinc} + E_s = Z I \qquad [46]$$

where Z is the internal impedance of the conductor and I is the current present in the conductor. It is now necessary to derive an expression for the impeadance.

At very high frequencies the impedance of a solid wire can be obtained using the impedance formulas for a semi-infinite plane solid. At a sufficiently high frequency the curvature of the wire becomes unimportant. This occurs when the skin depth for the conductor becomes small compared with the radius. The wire may then be considered a plane solid with infinite depth and a width equal to its circumference. The internal impedance of the wire for this case is given by:

$$Z = Z_s / 2\pi r \qquad [47]$$

where Z_s is the impedance of the plane solid, and $2\pi r$ is the circumference of the wire. Z is then measured in Ohms per unit length. Z_s for a good conductor is given by

$$Z_S = \frac{(1 + j)}{\sigma \delta} = R_S(1 + j) \qquad [48]$$

where σ is the conductivity of the conductor in Siemens, δ is the skin depth in meters and R_S is the surface resistivity in ohms per square. The skin depth, δ, is:

$$d = \frac{1}{\sqrt{\pi f \mu \sigma}} \qquad [49]$$

where f is the frequency, and μ is the permeability of the conductor. The surface resistivity therefore becomes:

$$R_S = \frac{1}{\sigma \delta} = \sqrt{\pi f \mu / \sigma} \qquad [50]$$

Although the actual mesh structures of interest are made of small round wires, the algorithm used to estimate the characteristics of this mesh apply only to a planar structure of negligible thickness. Therefore the conductors have to be modeled as conducting strips. For scattering problems this modeling is done using the concept of equivalent radius. The wire of radius r can be replaced by a strip of width w, where r is given by:

$$r = 0.25w \qquad [51]$$

The final expression for the impedance of the wire using equations 47, 48, and 51 is given by:

$$Z = \frac{2R_S(1 + j)}{\pi w} \qquad [52]$$

Finally the mesh is usually not made of solid wire but a coated material. In this way full advantage can be taken of both the mechanical characteristics of the substrate and the electrical characteristics of the coating. If currents and

fields are able to penetrate both materials, then the wire impedance will no longer be predicted by equation 51. A more accurate measure of impedance, [7] derived in Appendix C, is given by:

$$Z = \frac{2 R_s}{\pi w} (1 + j) \frac{[\ \sinh(T_1 d) + (R_{s2}/R_{s1})\cosh(T_1 d)\ ]}{[\ \cosh(T_1 d) + (R_{s2}/R_{s1})\sinh(T_1 d)\ ]} \qquad [53]$$

where, $\quad T_1 = \dfrac{(1 + j)}{\delta_1} = (1 + j)\sqrt{\pi f \mu_1 \sigma_1} \qquad [54]$

d is the thickness of the coating in meters, and R_{s1} and R_{s2} are the surface resistivities of the surface and the substrate respectively. For very small values of coating thickness, equation 53 reduces to the impedance of a wire made of only the substrate. For large values of thickness the wire appears as if it is made entirely of the coated material. For intermediate values of thickness the resistive and reactive parts of the impedance are no longer equal in magnitude. Figures 6 and 7 show the wire impedance, normalized with respect to that of the coating material, for varying ratios of thickness to the skin depth of the coating. Figure 6 corresponds to a solder coating on a copper substrate, with $R_{s2}/R_{s1} = 0.34$. Figure 7 corresponds to a silver coating on a brass substrate, with $R_{s2}/R_{s1} = 1.6$.
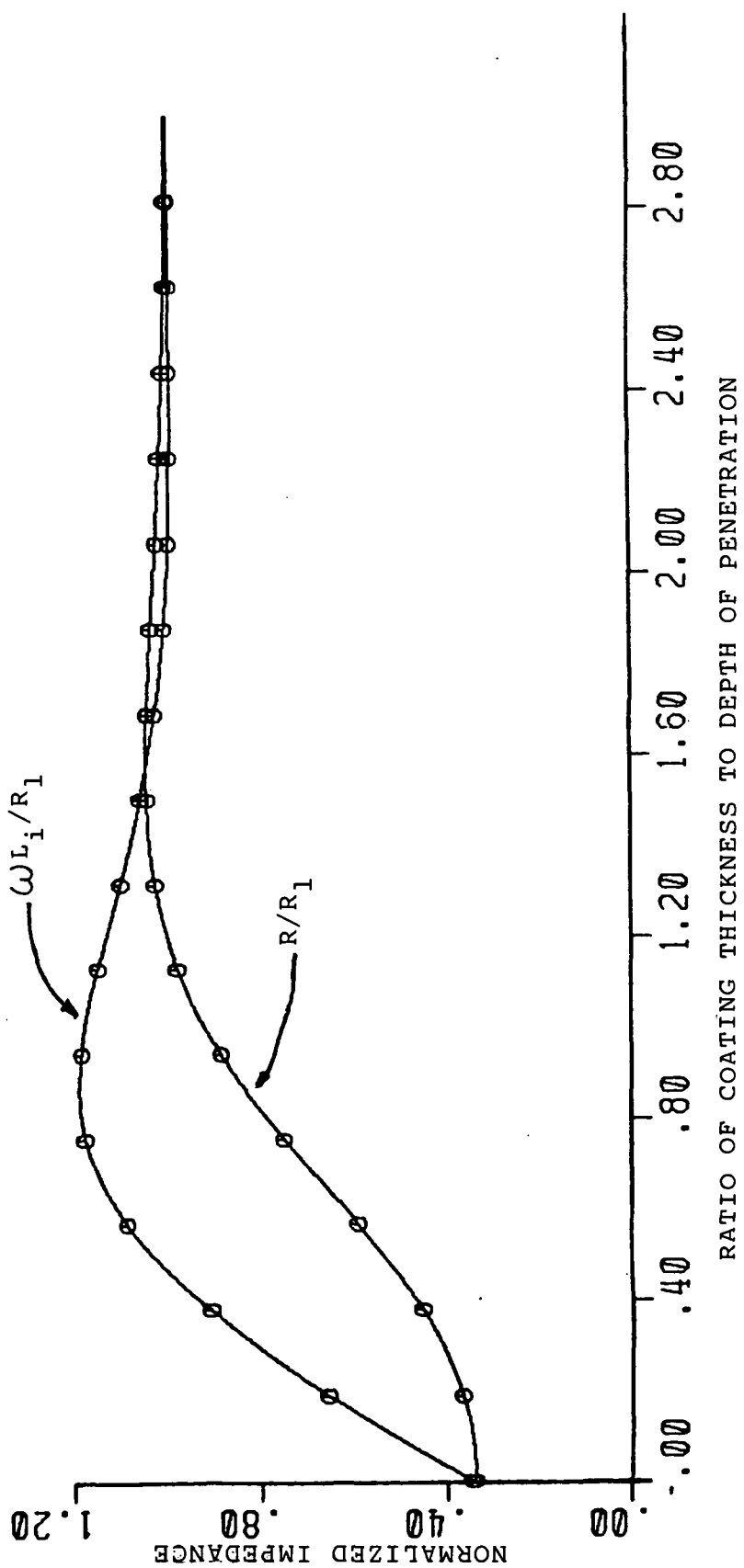
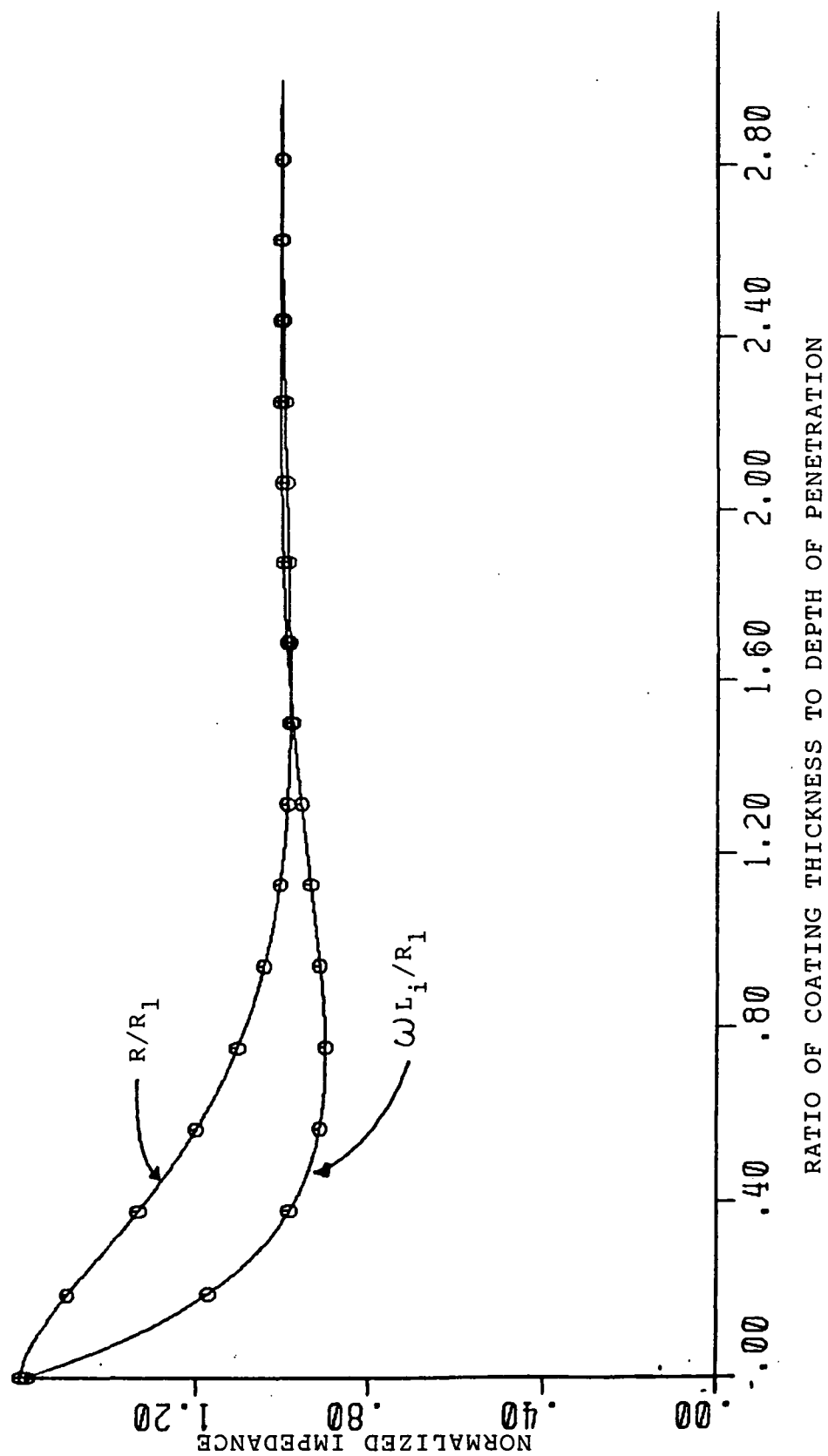Figure 6. Normalized Impedance. Solder coating on a copper substrate.
Rs2/Rsl = 0.34

Figure 7. Normalized Impedance. Silver Coating on a Brass Substrate.
Rs2/Rsl = 1.6

V. RESULTS

First the fields and currents, as calculated by the secant method, will be examined and compared with other published results. There are two sources of published results with which the new algorithim is compared. Brand [2] used the spectral domain approach with the contraction factor denoted by S.I.T, and Chistodoulou [3] used the the fast Fourier transform-conjugate gradient method denoted by FFT-C.G.

An important parameter that needs to be mentioned at this point is the number of sampling points required to represent the physical situation. For very thin wires a greater number of sampling points will produce more accurate results because there will be less quantitization error of the strip width. The position in the cell at which each sample is taken can effect the results. In addition, the greater the number of sampling points the slower the contraction process will be.

Table 7 shows a comparison of the three methods for a grating of very thin wires. For each case the current density of the wire was computed. All cases were examined

36

TABLE 7

COMPARISON OF CURRENT DENSITIES

S	W	FFT-C.G.	S.I.T.	S.C.S.I.
0.55	0.005	0.02664928	0.02770429	0.020257652
0.25	0.005	0.05155611	0.05183827	0.040708277
0.125	0.005	0.07172995	0.07114100	0.061060846
0.100	0.002	0.07545375	0.07521373	0.066166893

with the incident field normal to the plane and the E field
parallel to the wires. There were 32 sampling points for
each unit cell with one point laying on the strip. The
results of these methods are in good agreement. Any of these
methods can be used to predict the current density on a
strip for different wire spacing and wire thickness.

Figure 8 illustrates the current density across a wide
strip. Sixteen sampling points lie on both the strip and
the aperature. The incident field generating this current is
again normal and copolar. The current density is seen to be
very large at the edges of the strip. This result shows that
the new algorithim can predict edge effects.

Table 8 shows a comparison of the electric fields
across the entire cell as predicted by the three methods. It
should be mentioned that the FFT-C.G. method does not
actually compute the field across the strip region, it is
assumed zero because the conductivity of the strips is very
large. There are again 32 sampling points with two points
lying on the strip. Note that the electric field located on
the strip is predicted to be much lower for the S.C.S.I.
method than for the S.I.T. For perfectly conducting strips,
low field values on the strip indicate that the boundary
condition $\overline{E}_{tinc} + \overline{E}_s = 0$ is satisfied. This condition
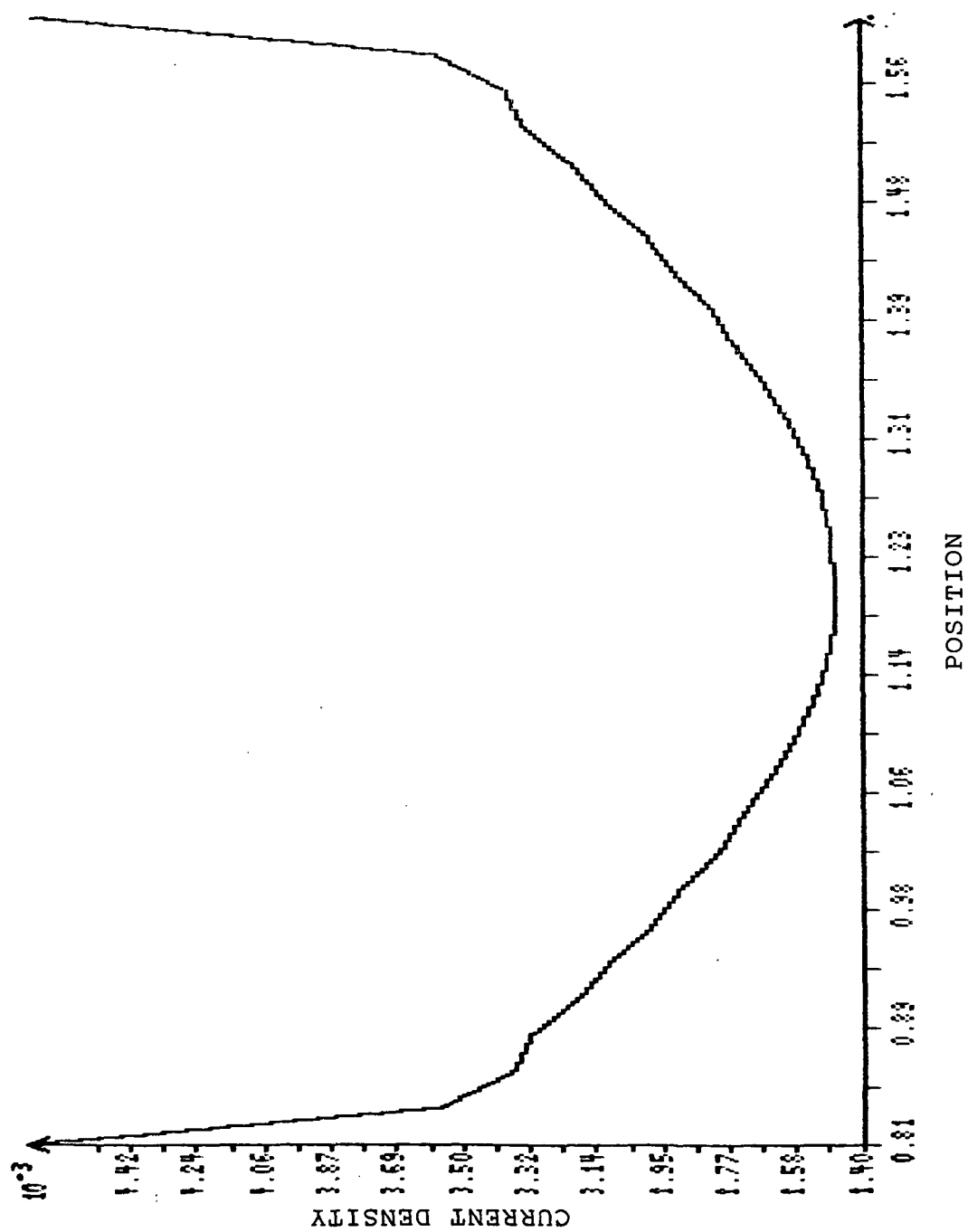could always be used as an accuracy-check.

Figure 8. Strip Current

TABLE 8

COMPARISON OF THE ELECTRIC FIELD IN A UNIT CELL

CELL POINT	S.I.T.	FFT-C.G.	S.C.S.I.
-0.129126310	0.182258561E-1	0.000000000	4.8894606E-5
-0.120795548	0.384013295	0.377430677	0.3747891
-0.112464786	0.560089946	0.556849957	0.5529166
-0.104134083	0.661797166	0.660458642	0.6556744
-0.095803320	0.738476992	0.738587141	0.7332161
-0.087472617	0.796682596	0.797879934	0.7919211
-0.079141915	0.844159245	0.846264482	0.8399065
-0.070811152	0.882627010	0.885471702	0.8787327
-0.062480479	0.914659142	0.918128848	0.9110555
-0.054149747	0.940926552	0.944895148	0.9375529
-0.045819018	0.962553382	0.966925740	0.9593651
-0.037488285	0.979851842	0.984547973	0.9768083
-0.029157557	0.993371725	0.998328090	0.9904386
-0.020826824	1.00326443	1.00839138	1.000410
-0.012496091	1.00979042	1.01503468	1.006989
-0.004165362	1.01301479	1.01830196	1.010238
0.004165362	1.01301575	1.01831055	1.010238
0.012496091	1.00979042	1.01503181	1.006989
0.020826824	1.00326347	1.00839233	1.000410
0.029157557	0.993371725	0.998323321	0.9904386
0.037488285	0.979854842	0.984559417	0.9768084
0.045819018	0.962553859	0.966914829	0.9593652
0.054149747	0.940926552	0.944902539	0.9375528
0.062480479	0.914659023	0.918127894	0.9110555
0.070811152	0.882627010	0.885474324	0.8787327
0.079141915	0.844159365	0.846258521	0.8399065
0.087472618	0.796682477	0.797884822	0.7919205
0.095803320	0.738476753	0.738585949	0.7332161
0.104174083	0.661787643	0.660460711	0.6556743
0.112464786	0.560090780	0.556844115	0.5529164
0.120795548	0.384014010	0.377436161	0.3747890
0.129126310	0.182278380E-1	0.000000000	4.8571634E-5

Figure 9 shows the electric field across a unit cell with a large strip size. The electric field magnitude along the strip is seen to be very small. The shape of the electric field is in good agreement with results published by Brand [2].

Next, the reflection coefficent predicted using the secant method is compared with FFT-C.G and S.I.T. methods. In addition, comparisons are made with results published by Wait [8]. The reflection coefficient for cell widths less than one-half wavelength is equal to the first element in the transformed electric field vector, i.e., the first mode.

$$\Gamma = \tilde{E}_{00}^- = \tilde{E}_{00}^+ - E_{tinc} \qquad [55]$$

For these cell widths only one propogating mode will be present so that only one array element is needed. These narrow cell widths are important because when the wire spacings become 0.5 wavelengths or smaller, the planar surface begins to resemble a solid reflector.

In Table 9 the magnitude of the reflection coefficient for different values of wire spacing for normal incidence and wire radius of 1/600 wavelengths is compared with other methods. As expected, the grating begins to appear as a solid reflecting surface as the wire spacing becomes small. All three methods are in very good agreement.

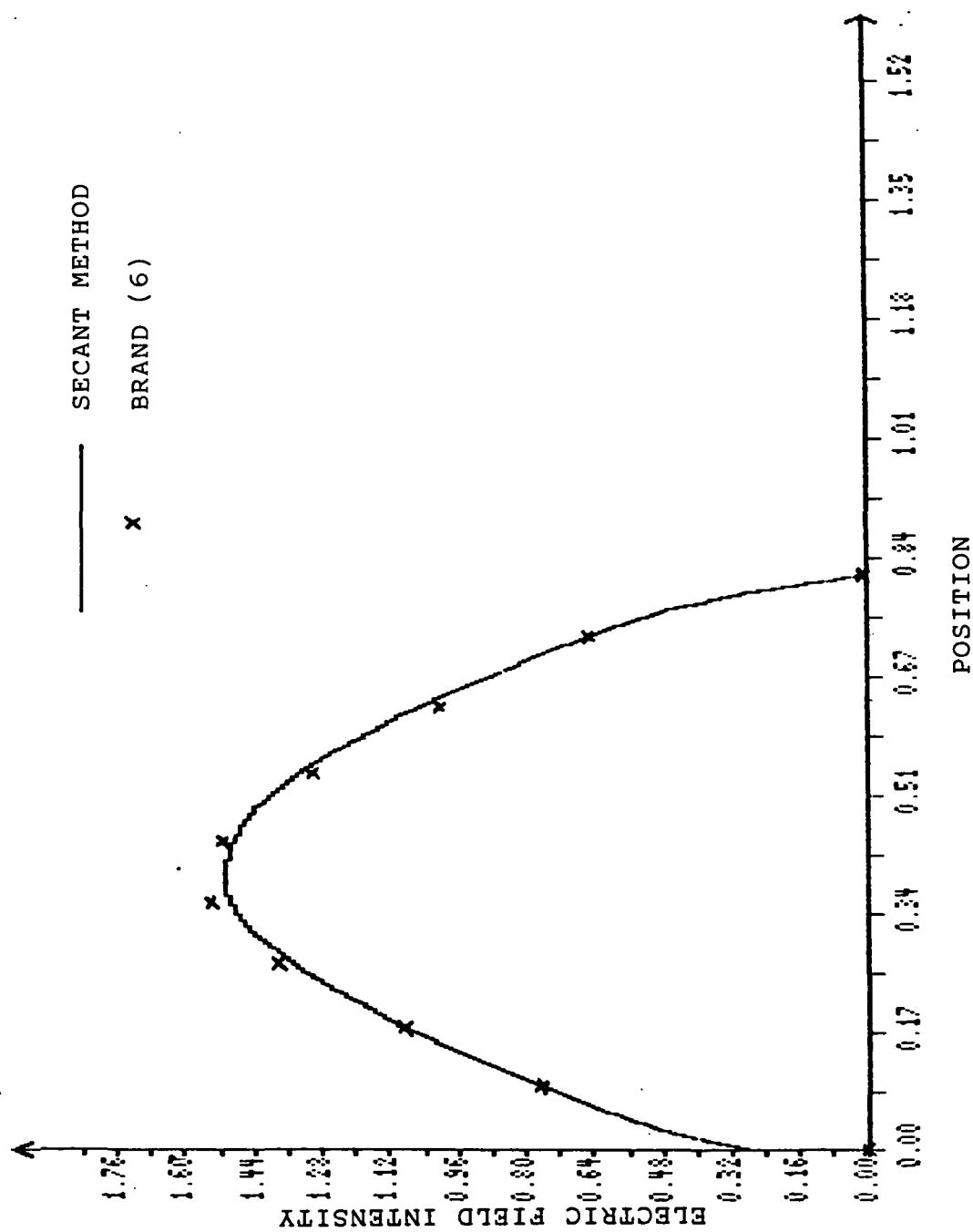Figure 9. Electric Field Across Unit Cell.

TABLE 9

COMPARISON OF REFLECTION COEFFICIENTS
FOR DIFFERENT WIRE SPACINGS

SPACING	FFT-C.G.	S.C.S.I.	S.I.T
0.125	0.844	0.844	0.843
0.10	0.888	0.892	0.885
0.06	0.954	0.971	0.960
0.05	0.967	0.985	0.969
0.02	0.994	0.999	0.994
0.01	0.999	1.000	0.999

Figure 10 depicts the changes in the reflection coefficient for cell widths of 1/2, 1/4, and 1/8 wavelengths as θ is varied from 0 to 90 degrees. The wire radius remains constant at 1/600 wavelength. The angle ϕ remains constant at zero degrees corresponding to TE polarization of the electric field. These results are in good agreement with results published by Wait [8] and Brand [2].

Figure 11 illustrates the behavior of the reflection coefficient when the angle ϕ is held constant at 90 degrees. The cell width is held constant at 1/4 wavelength while θ is varied from 0 to 90 degrees. The wire radius is again 1/600 wavelength. For this angle of ϕ it is observed that there exists a region of maximum transmission at θ equal to approximately 67 degrees. This is analogous to the Brewster angle associated with dialectric materials.

The effects of the substrate conductivity of coated wires on the reflection coefficient were studied next. In Figure 12 the conductivity of the coating was held constant at $5(10^8)$ Siemens while the substrate remained constant at 50 Siemens. The top curve corresponds to a very thick coating so that the conductivity of the strips is equal to the conductivity of the coating alone. The lower curve corresponds to a very thin coating so that the conductivity of the strip is greatly reduced. The complete set of curves illustrate the effects of varying the coating thickness. It
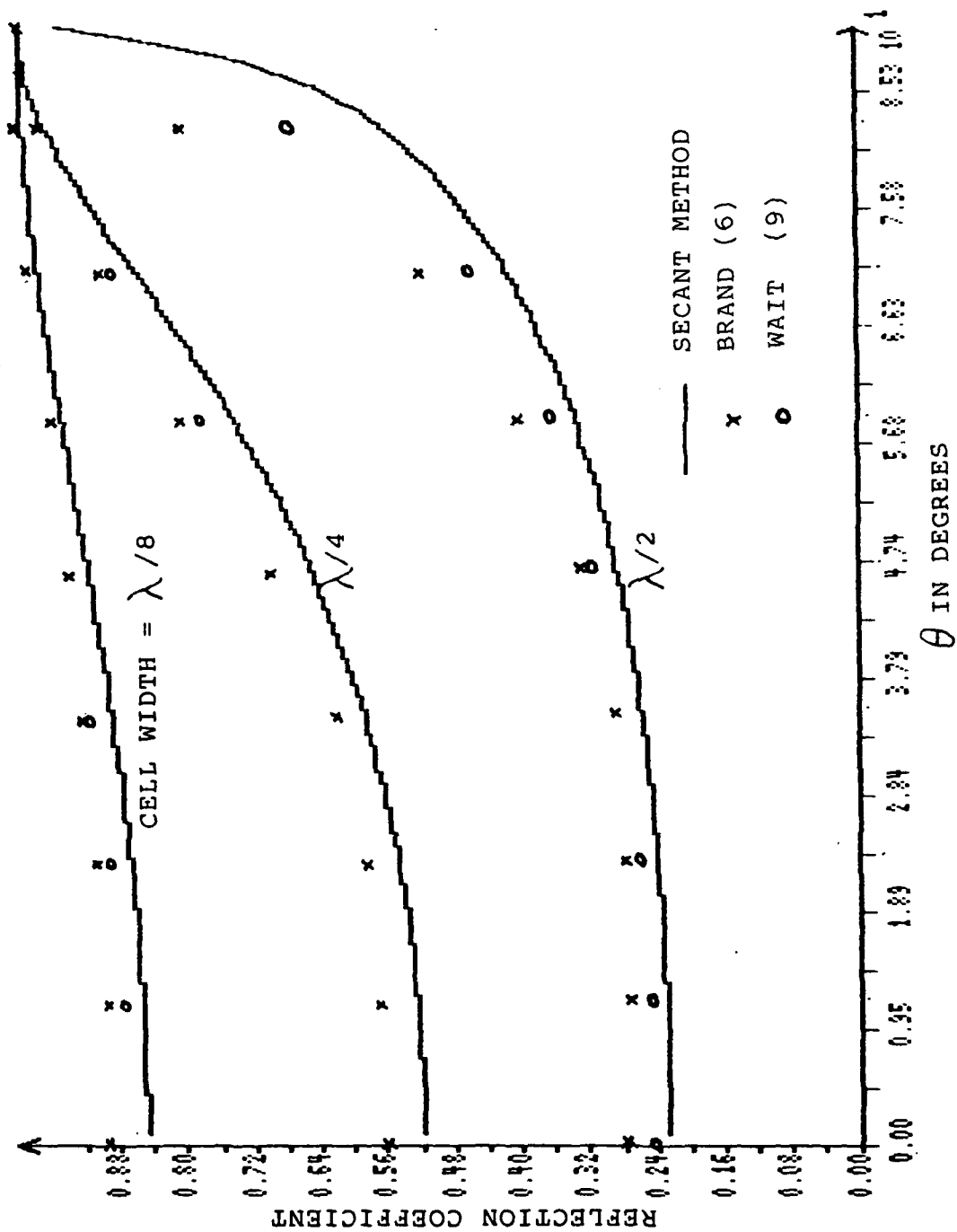
45

Figure 10. Reflection Coefficient
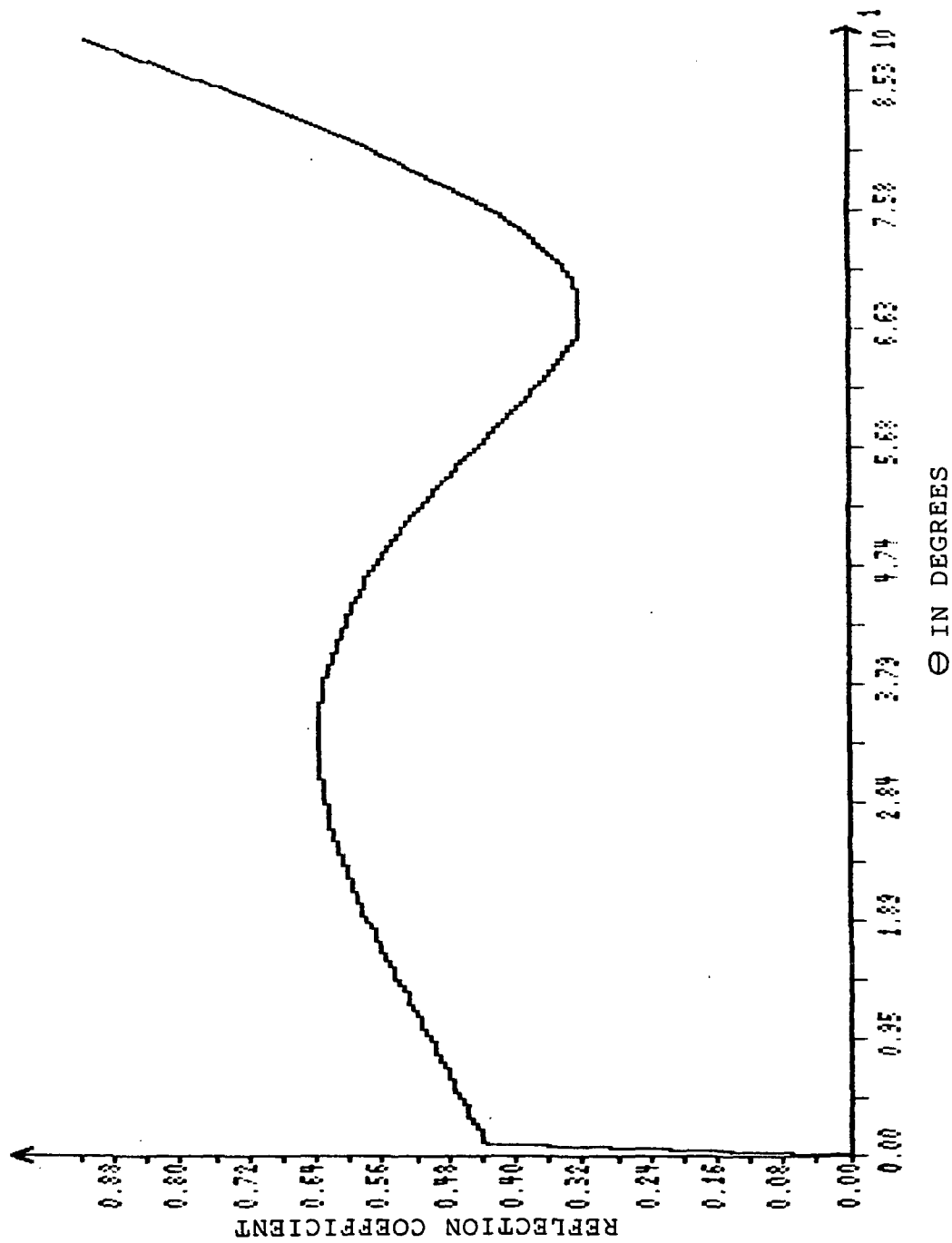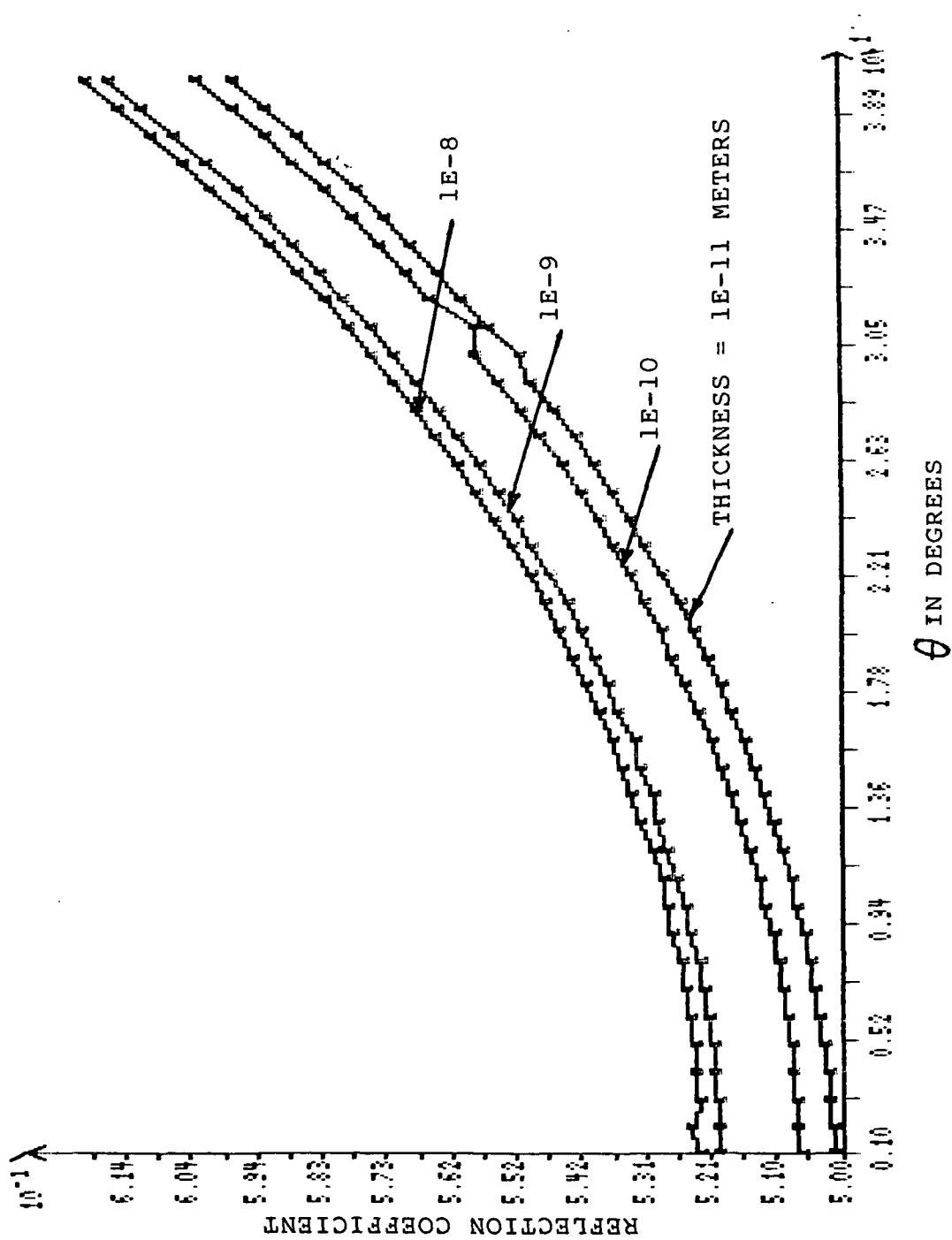for Varying Values of Cell Width and ϕ =0.

Figure 11. Reflection Coefficient. Pseudo-Brewster Angle.

Figure 12. Effects of Finite Surface Conductivity and Coating Thickness.

can be seen that as the thickness of the coating becomes smaller, the incident field penetrates deeper into the substrate. Since the substrate is of lower conductivity than the coating, it is expected to have more current losses in the wire and hence a lower reflection coefficient is obtained.

Figures 13, 14, 15 and 16 depict the effects of the substrate alone. The conductivity of the coating is held constant at 10 Siemens while the substrate is allowed to vary from 10 to 10^9 Siemens. Note that the x axis corresponding to the substrate conductivity has a log scale for each case. When the angle of incidence is perpendicular to the plane, the substrate is seen to have the most pronounced effect as shown in figures 13 and 14. The reflection coefficient increases as expected with an increase in strip conductivity. As the angle of the incident wave becomes much lower in relation to the plane, the reflection coefficient remains more constant as the substrate conductivity changes as shown in figures 15 and 16. An interesting phenomenon appeared when ϕ and θ were set equal to 90 and 70 respectively. These particular values of ϕ and θ are analogous to the Brewster angle of dialectrics. At this angle, the grating no longer behaves entirely as predicted for a reflecting surface. As the overall strip conductivity increases, the reflection coefficient drops slightly. At
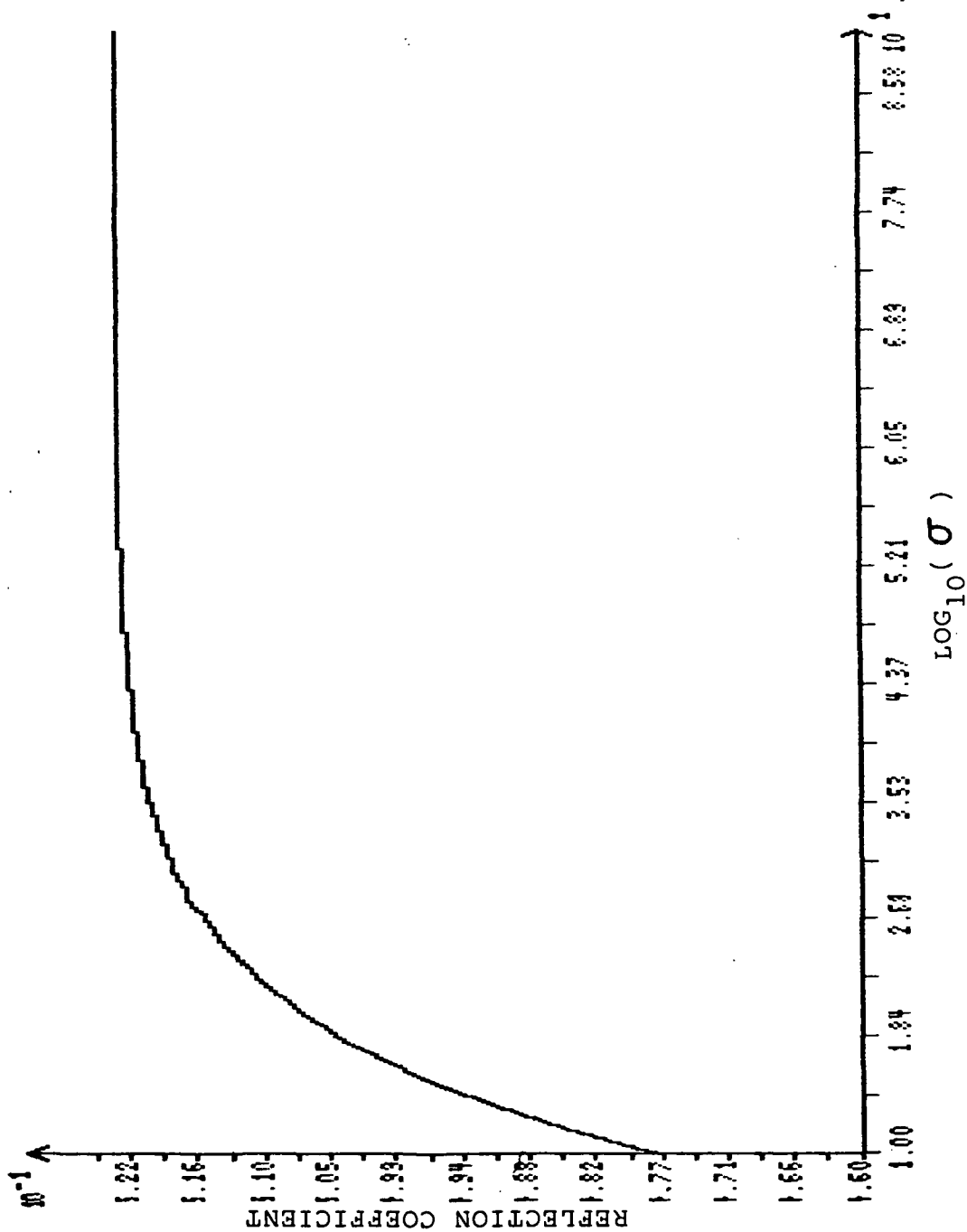
Figure 13. Effects of the Substrate Conductivity
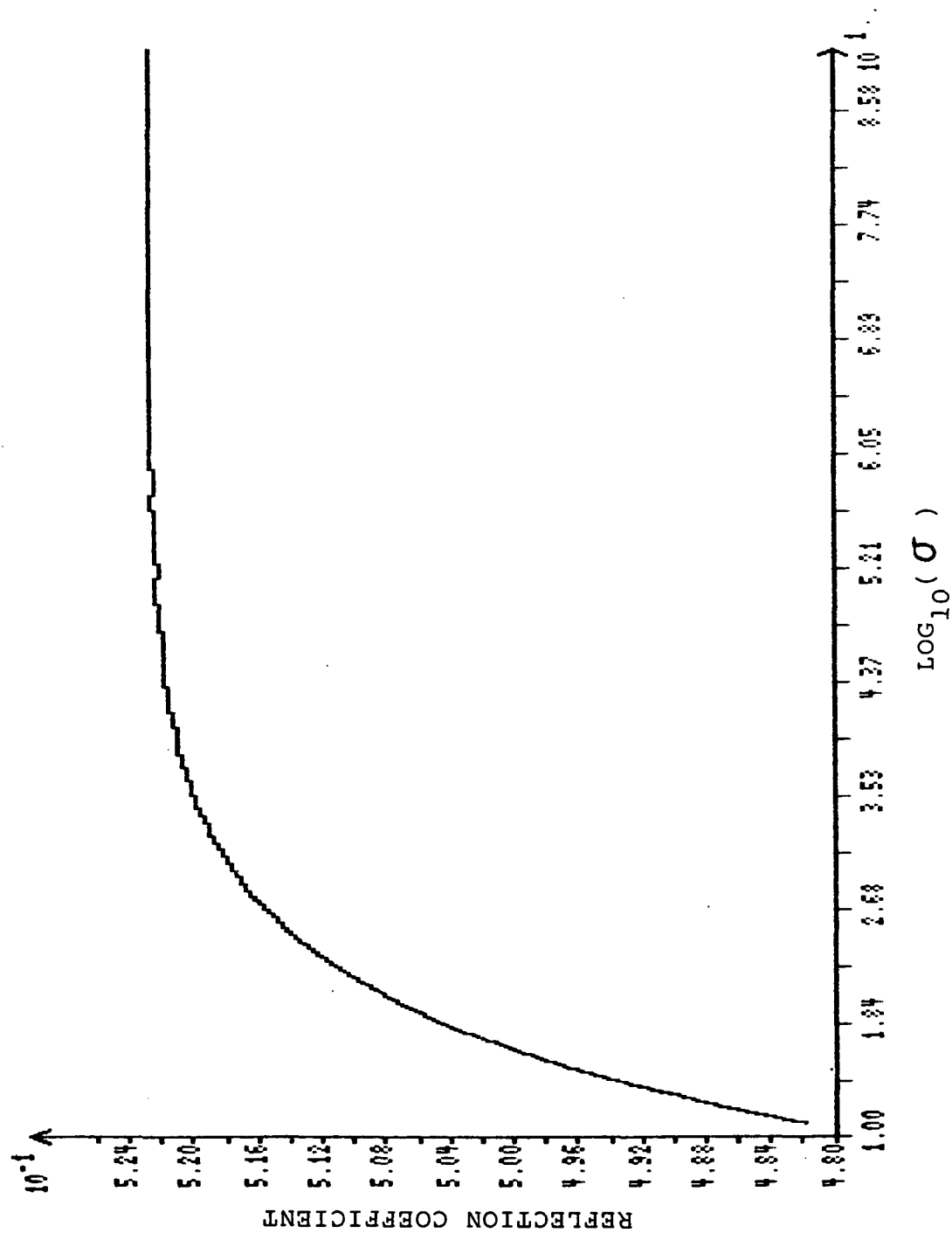
Figure 14. Effects of the Substrate Conductivity
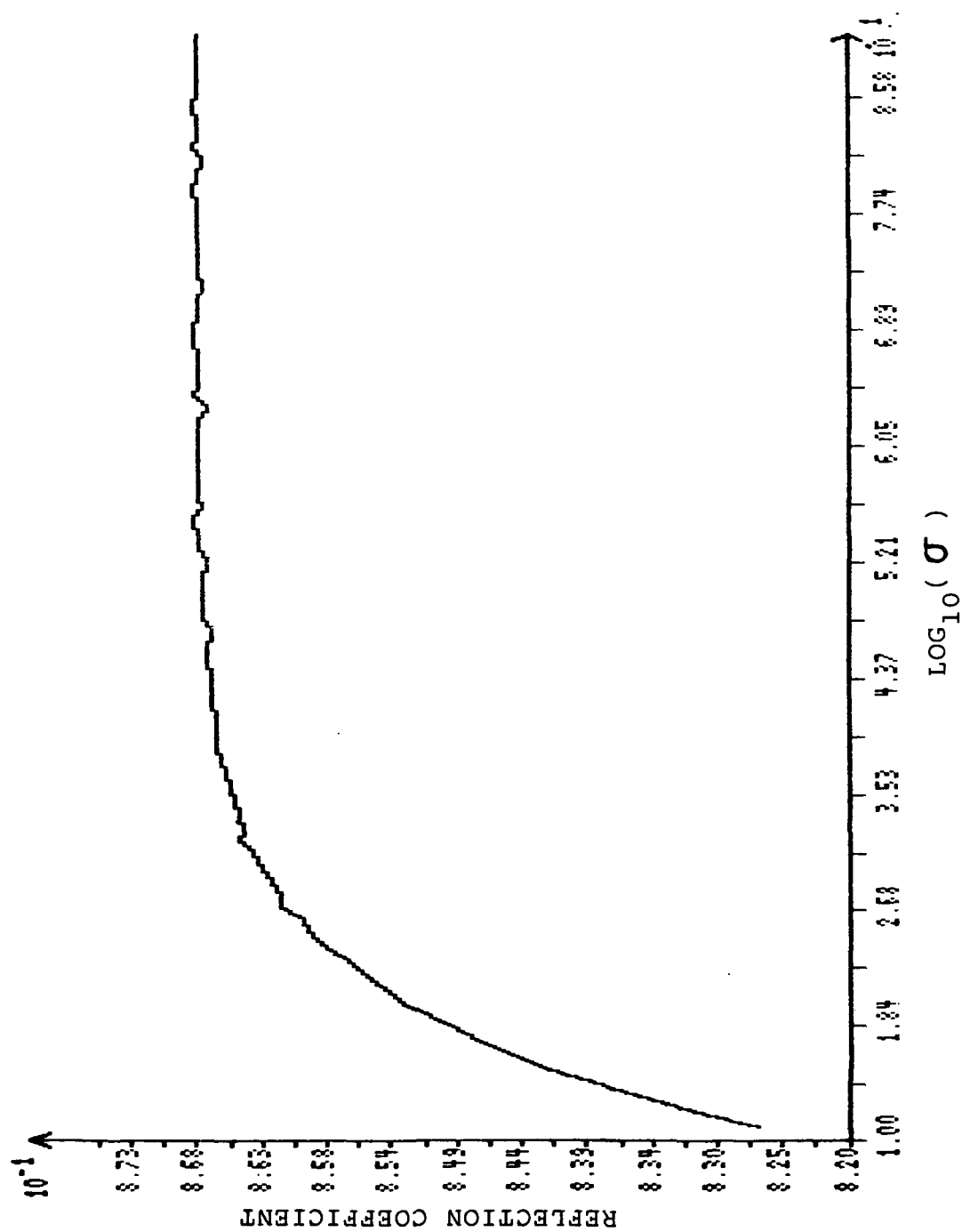
Figure 15. Effects of the Substrate Conductivity
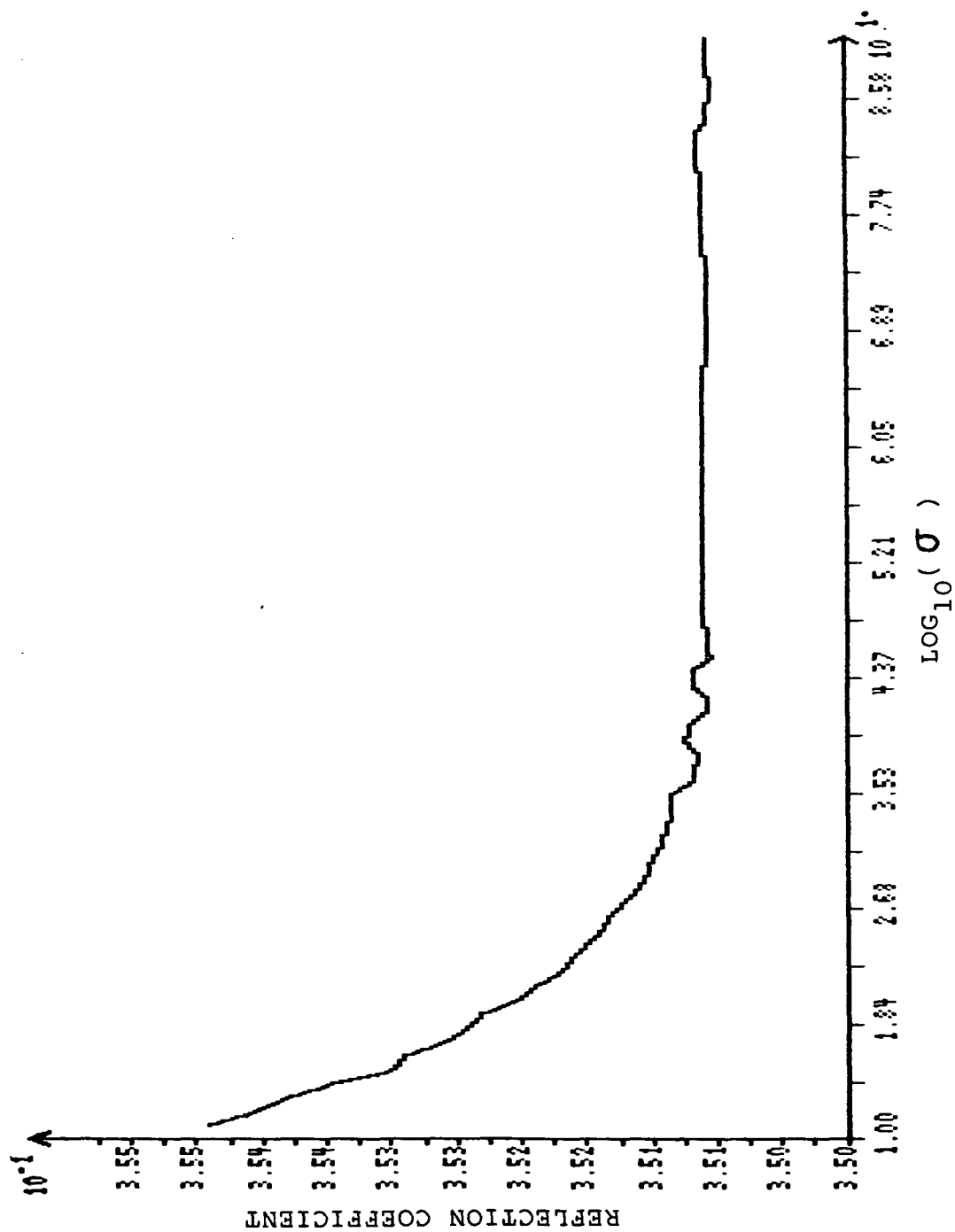
Figure 16. Effects of the Substrate Conductivity

this angle the surface appears more as a dialectric material with its permeability changing.

These results were all run on the VAX 11/750. For 32 sampling points with ϕ equal to 0 degees and θ varying, the secant method converged to the third decimal of the reflection coefficient within 8 to 12 iterations. For very low angles, θ being greater than 88, more iterations are needed. Convergence took 290 iterations when θ was equal 89. There is also a correlation between the number of iterations and the number of sampling points. Table 10 shows that convergence is more difficult to obtain with a greater number of sampling points.

TABLE 10

SAMPLING POINTS VS. ITERATIONS REQUIRED

Sampling points	Iterations
32	8
64	8
128	16
256	14
512	20

The 32 sample points with 8 iterations require 5.25 seconds of CPU time while 512 sampling points with 20 iterations requires 38.58 seconds.

VI. SUMMARY, CONCLUSIONS, AND RECOMMENDATIONS

Brand's contractor corrector method failed to converge on occasion for various input parameters when running on the VAX computer. The reason for this failure was found to be the error introduced by using a numeric estimate of the derivative.

An alternative derivative-free method was developed to insure the convergence of the spectral iteration approach as applied to the electromagnetic scattering from gratings. This method was derived by beginning first with the original spectral-iterative equation to which no correction was made. The general theory of iterative techniques was then covered. Basic examples were presented illustrating how the secant technique could be applied to solve single-valued complex functions. Finally, the secant method was applied to the vector space used by the spectral-iteration equation. Alternative methods for solving electromagnetic scattering are always of interest because the criteria for obtaining solutions become more stringent as the geometry of the problem becomes more complex.

This new method was used to solve for the currents and fields lying in the plane of the grating. The reflection

coefficient was computed for cell widths under 1/2 wavelength. These results were compared with previously published data and found to be in good agreement.

The solution of scattering from a grating is a one-dimensional application of the spectral iterative technique. The cell geometry only changes along one axis of the plane containing the grating. A grid would require a two-dimensional application of the basic technique because the geometry changes along both the x and y axis. The contractor corrector has been applied to this two dimensional configuration and failed to yield a convergent scheme. Because the conditions necessary to assure convergence are more stringent, the error introduced by using a numeric derivative could be the critical factor causing this failure. The secant method has yet to be applied to this type of problem and could possibly provide a method of solution leading to convergence.

No spectral iterative method has as yet been applied to geometries more complex than grids or gratings. For the one-dimensional problem the cell could contain various strips of varying size. The two-dimensional problem can be that of virtually any repeating planar structure. This case is important because surfaces approximating reflectors are not usually a grid, but a mesh structure which can have a very complex geometry. The spectral iterative techniques are

particularly well suited for these types of studies because only the truncation operators are geometry dependent. It is recommended that wire mesh geometries be studied to verify that convergence will still take place and that the results remain acceptable.

APPENDIX A

MAIN PROGRAM AND ASSOCIATED SUBROUTINES

The following program is written in FORTRAN 77 source code. It should run on most FORTRAN compilers and has run successfully on the VAX and IBM PC computers. This program will solve for the electric field across the aperature of a unit cell consisting of parallel wires. This unit cell is the repeating section of an infinite grating. The program will also solve for the current densities on the wires and the reflection coefficient of the grating. The program is presented in its interactive version, with appropriate prompts to request input data. This appendix consists of a summary of variables, subroutines and a program listing.

Program Variables

Some variables and constants are self explanatory and are not defined.

E(I)   Electric field in the aperture

GUESS(I)   Previous estimate of the electric field

FI(I)   Current value of the residue function

FIM1(I)   Previous value of the residue function

JC(I)   Current density across the aperature

G(I)   Transformed Green's function

EINC   Incident electric field

HI   Incident magnetic field

Z   Internal impedance of the wires

CREF   Reflection coefficient

CONVERGED   Boolean indicator of convergence

K   Propagation constant

CK_   Constants used in the original iterative eq.

RS1,RS2   Surface resistivities of coating and substrate

RATIO   Ratio of coating thickness and skin depth

MAX   Number of sampling points

ITER   Running count of the number of iterations

CYCLES   Maximum number of iterations allowed

Subroutines and Functions

SINHH,COSHH	Complex hyperbolic sin and cosine for a complex argument
FNCTZ	The residual vector
XFORM	Original transformation for the electric field
TRCOPR_	Subroutines dependent upon cell geometry
FFT	Fast fourier transform

START

Initialize:

Declare variables
Input data
Initialize constants

Calculate incident electric
and magnetic fields

Calculate the internal impedance
of the coated wires

Calculate the sampling point
locations on the strips
and aperature

Calculate the Green's function
transform

Constuct the first 2 guesses of
the electric field

Calculate F   CALL FNCTZ

Has covergence occured ?   Yes

No

Calculate F   CALL FNCTZ

Has convergence occured ?   Yes

No

Perform next iterate of the
electric field

Save the previous E field

STOP

FNCTZ

$F = E - L(E)$
CALL XFORM

RETURN

XFORM

Perform initial transformation

Perform inverse transformation
of GE

Truncation operation T(GE)

Perform inverse transformation
on T(GE)

Perform T(GE)/G and add B

Calculate the reflection
coefficient

Perform the inverse
transformation to obtain
the first iterated E field

RETURN

Print the reflection
coefficient
Print the E field and current
values

Figure 17. Flow Chart.

```
C *************** SECANT32.FOR ***************************
C
C SECANT METHOD APPLIED TO ASSURE CONVERGENCE
C
C OCTOBER 23,1983 BY ROBERT MIDDELVEEN
C
C DIMENSION ALL ARRAYS
      COMPLEX E(32),PI(32),FIM1(32),JC(32),G(32)
      COMPLEX RI,CREF,HI,EHOLD(32)
      COMPLEX GUESS(32)
      COMPLEX J,CK1(32),CK2(32),CK(32),Z,T1,SINHH,COSHH
      REAL K,K2,RS1,RS2,SKIND1,RATIO
      INTEGER ITER,CYCLES
      LOGICAL CONVERGED
      COMMON RI,CREF,HI,EINC
      COMMON JC,G,J,Z,CK
      COMMON N,N1,IW,MAX,W,UU,STH,DR,REF,B,ITER
C A = FLOQUET CELL DIMENSION
C B = STRIP SIZE
      WRITE(*,*) ' ** ENTERING MAIN PROGRAM **'
      WRITE(*,*) ' HOW MANY ITERATIONS DO YOU WISH TO PERFORM?'
      READ (*,*) CYCLES
      WRITE(*,*) ' INPUT FLOQUET CELL SIZE, STRIP SIZE '
      WRITE(*,*) ' NORMALIZED IN WAVELENGTHS '
      READ(*,*) A,B
C FREQ = FREQUENCY IN HZ
      WRITE(*,*) ' INPUT FREQUENCY IN HZ'
      READ(*,*) FREQ
C MAX = FFT SIZE = NUMBER OF SAMPLES PER CELL
C IW = LOG2(MAX) ; i.e. MAX = 2**IW
      MAX=32
      IW=5
C CIG = CONDUCTANCE OF THE STRIP
      WRITE(*,*) ' INPUT CONDUCTANCE OF COATING IN SIEMANS'
      READ(*,*) SIG1
      WRITE(*,*) ' INPUT CONDUCTANCE OF SUBSTRATE IN SIEMANS'
      READ(*,*) SIG2
      WRITE(*,*) ' INPUT THE THICKNESS OF THE COATING IN METERS'
      READ(*,*) THICKNESS
C TH = THETA ANGLE OF INCIDENCE
C PH = PHI ANGLE OF INCIDENCE
      WRITE(*,*) ' INPUT THETA ANGLE, PHI ANGLE'
487   READ(*,*) TH,PH
C INITIALIZE ROUTINE CONSTANTS
      PI=3.141593
      TPI=2*PI
      C=2.997956E8
      UU=4.0E-7*PI
      EP=8.854E-12
      ETA=SQRT(UU/EP)
      ITER=0
      J=(0.0,1.0)
      ALAMB=C/FREQ
      RD=180.0/PI
      DR=1.0/RD
```

```
          CONVERGED=.FALSE.
C CALCULATE THE INCIDENT ELECTRIC AND MAGNETIC FIELD COMPONENTS
C FOR THE ELECTRIC FIELD PARALLEL TO THE WIRES, i.e. NO CROSS-
C POLARIZATION INCLUDED
          IF (PH.LT.45.0) EINC =1.0
          IF (PH.GE.45.0) EINC=COS(TH*DR)
          IF (PH.LT.45.0) STH=0.0
          IF (PH.GT.45.0) STH=TH
          HI=1.0/ETA*(COS(TH*DR)+J*SIN(TH*DR))
          IF(PH.LT.45.0) HI=1.0/ETA*COS(TH*DR)
C
C         THIS SECTION COMPUTES THE INTERNAL IMPEDANCE FOR A COATED WIRE
C
          T1=(1.0,1.0)*SQRT(PI*FREQ*UU*SIG1)
          RS1=SQRT(PI*FREQ*UU/SIG1)
          RS2=SQRT(PI*FREQ*UU/SIG2)
          SKIND1=1/SQRT(PI*FREQ*UU*SIG1)
          RATIO=THICKNESS/SKIND1
          IF(RATIO.GT.4.00)THEN
            Z=SQRT(TPI*FREQ*UU/2.0/SIG1)*(1.0,1.0)/TPI/B
          ELSE
            Z=(1.0,1.0)*(SINHH(T1*THICKNESS)+(RS2/RS1)*COSHH(T1*THICKNESS))
            Z=Z/(COSHH(T1*THICKNESS)+(RS2/RS1)*SINHH(T1*THICKNESS))
            Z=Z*RS1/TPI/B
          END IF
          WRITE(*,15) RATIO,Z
15        FORMAT('-',' RATIO = ',F10.5,' Z = ( ',E10.2,' , ',E10.2,' )')
C
C
C
C CALCULATE THE NUMBER OF SAMPLES ON THE STRIP AND IN THE APERTURE
          TAU=A-B
          N=IFIX(TAU/A*FLOAT(MAX))
          WRITE (*,*) 'N= ',N
          N1=N+1
          WRITE(*,30) A,B,TAU,FREQ,TH,N,MAX
30        FORMAT('-',1E10.5,' ',1E10.5,' ',1E10.5, ' ',E10.3,1E10.4,2I10)
          IF(N1.GT.MAX) GOTO 998
          K=TPI/ALAMB
          K2=K*K
          SK=K*SIN(TH*DR)*COS(PH*DR)
          SSK=K*SIN(TH*DR)*SIN(PH*DR)
          W=TPI*FREQ
C CALCULATE GREEN FUNCTION TRANSFORM
          DO 40 I=1,MAX
          IF(I.GT.MAX/2+1) GOTO 50
          U=TPI*(I-1)/A-SK
          GOTO 60
50        U=TPI*(I-MAX-1)/A-SK
60        U=U*U+SSK*SSK
          IF(U.GE.K2) GOTO 70
          G(I)=-J*SQRT(K2-U)
          GOTO 44
70        G(I)=-SQRT(U-K2)
44        G(I)=G(I)-SSK*SSK/G(I)
```

```
40      CONTINUE
C INITIAL E FIELD ESIMATE
        DO 320 I=1,MAX
320     E(I)=(1.0,0.0)
        CALL TRCOPR(E,N1)
        DO 321 I=1,MAX
321     GUESS(I)=E(I)+(0.1,0.0)
C NOTE....ITERATIVE FORM USED IN THIS PROGRAM IS X=AX+B
C CALCULATE B PORTION OF ITERATIVE EQUATION
        DO 110 I=1,MAX
110     CK1(I)=HI*J*W*UU
        CALL FFT(CK1,IW)
        DO 120 I=N1,MAX
120     CK2(I)=HI*W*UU/J
        DO 140 I=1,N
140     CK2(I)=(0.0,0.0)
        CALL FFT(CK2,IW)
        DO 130 I=1,MAX
130     CK(I)=(CK1(I)+CK2(I))/G(I)
C
C       THE FOLLOWING SECTION IMPLEMENTS THE SECANT METHOD
C
        WRITE(*,*)'SECANT ALGORITHM APPLIED'
81      CONTINUE
        ITER=ITER+1
        DO 357 I=1,MAX
        FI(I)=E(I)
        FIM1(I)=GUESS(I)
        EHOLD(I)=E(I)
357     CONTINUE
        CALL FNCTZ(FI,MAX,CONVERGED)
        IF (CONVERGED) GOTO 259
        CALL FNCTZ(FIM1,MAX,CONVERGED)
        IF (ITER.GT.CYCLES.OR.CONVERGED) GOTO 259
        DO 358 I=1,MAX
        E(I)=E(I)-FI(I)*((E(I)-GUESS(I))/(FI(I)-FIM1(I)))
358     CONTINUE
        DO 359 I=1,MAX
        GUESS(I)=EHOLD(I)
359     CONTINUE
        GOTO 81
C
C
C
C       THE SECANT METHOD ENDS HERE
C
C
C
259     CONTINUE
C
C
        WRITE(*,*)' HIT `RETURN" TO CONTINUE'
        READ(*,*)
        OPEN(10,FILE='SEC32OUT',STATUS='NEW')
        WRITE(*,*) ' ELECTRIC FIELD MAGNITUDE'
```

```
        WRITE(10,*) ' ELECTRIC FIELD MAGNITUDE'
        DO 261 I=1,MAX
        BINDEX=FLOAT(I-1)/FLOAT(MAX-1)*A
        WRITE(10,*) ' ',BINDEX,' ',CABS(E(I))
        WRITE(*,*) ' ','BINDEX = ',BINDEX,' !E! = ',CABS(E(I))
261     CONTINUE
        WRITE(*,*)' HIT `RETURN" TO CONTINUE'
        READ (*,*)
        WRITE(*,*) ' STRIP CURRENT'
        WRITE(10,*) ' STRIP CURRENT'
        DO 262 I=N1,MAX
        BINDEX=FLOAT(I-1)/FLOAT(MAX-1)*A
        WRITE(10,*)' ',BINDEX,' ',CABS(JC(I))
        WRITE(*,*)' ','BINDEX = ',BINDEX,' !JC! = ',CABS(JC(I))
262     CONTINUE
C
C
        WRITE(*,260)
260     FORMAT('-',10X,' T I M E L Y    E X I T')
        GOTO 9999
998     WRITE(*,99)
99      FORMAT('-',' E R R O R    I N    N')
9999    STOP
        END
C
C
C
C       THIS SUBROUTINE PRODUCES THE VECTOR WE WANT TO ZERO
C
C
C
C
        SUBROUTINE FNCTZ(E,MAX,CONVERGED)
        COMPLEX E(32),HOLD(32)
        LOGICAL CONVERGED
        DO 1234 I=1,MAX
        HOLD(I)=-E(I)
1234    CONTINUE
        CALL XFORM(E,CONVERGED)
        DO 1235 I=1,MAX
        E(I)=E(I)+HOLD(I)
1235    CONTINUE
        RETURN
        END
C
C
C
C       THIS SUBROUTINE IMPLEMENTS THE TRANSFORMATION ON THE E FIELD
C
C
C
        SUBROUTINE XFORM(E,CONVERGED)
        COMPLEX E(32),G(32),JC(32),CK(32)
        COMPLEX RI,CREF,HI,J,Z
        REAL REF,REFM1,REFM2
        LOGICAL CONVERGED
```

```fortran
      COMMON RI,CREF,HI,EINC
      COMMON JC,G,J,Z,CK
      COMMON N,N1,IW,MAX,W,UU,STH,DR,REF,B,ITER
C     CALCULATE FIELD ON STRIP DUE TO FINITE CONDUCTIVITY
      CALL TRCOPR3(E,JC,N1,MAX,Z,B)
C     START BY PERFORMING THE INITIAL TRANSFORMATION
      CALL FFT(E,IW)
      DO 100 I=1,MAX
100   E(I)=CONJG(E(I)*G(I))
C PERFORM INVERSE TRANSFORM OF (G*E)
      CALL FFT(E,IW)
C PERFORM THE TRUNCATION OPERATION T(G*E)
      CALL TRCOPRC(E,N)
      CALL TRCOPR4(E,JC,N1,MAX,J,W,UU,HI)
C PERFORM INVERSE TRANSFORMATION ON T(G*E)
      CALL FFT(E,IW)
C PERFORM T(G*E)/G AND ADD CONSTANT "B"
      DO 170 I=1,MAX
      E(I)=E(I)/G(I)+CK(I)
170   CONTINUE
C
C
C
C CALCULATE REFLECTION COEFFICIENT
      TOL=0.0001
      REFM2=REFM1
      REFM1=REF
      RI=J*SIN(STH*DR)/COS(STH*DR)
      CREF=(E(1)/MAX+EINC)+J*SIN(STH*DR)*ABS(1.0-ABS(E(1)/MAX+EINC))
      CREF=CREF/(COS(STH*DR)+J*SIN(STH*DR))
      REF=CABS(CREF)
      IF (ABS(REF-REFM1).LT.TOL.AND.ABS(REF-REFM2).LT.TOL) THEN
        WRITE(*,*)' ITER= ',ITER,'  REF= ',REF,'  CREF= ',CREF
        CONVERGED=.TRUE.
      END IF
C
C
      DO 171 I=1,MAX
      E(I)=CONJG(E(I))/MAX
171   CONTINUE
C PERFORM INVERSE TRANSFORMATION TO OBTAIN FIRST ITERATED
C ELECTRIC FIELD
      CALL FFT(E,IW)
      DO 200 I=1,MAX
200   E(I)=CONJG(E(I))
      RETURN
      END
C
C
C
      SUBROUTINE TRCOPR(E,N)
      COMPLEX E(32)
      DO 400 I=N,32
      E(I)=(0.0,0.0)
400   CONTINUE
```

```
        RETURN
        END
C
C
C
        SUBROUTINE TRCOPRC(E,N)
        COMPLEX E(32)
        DO 401 I=1,N
        E(I)=(0.0,0.0)
401     CONTINUE
        RETURN
        END
C
C
C
        SUBROUTINE TRCOPR3(E,JC,N1,MAX,Z,B)
        COMPLEX E(32),JC(32),Z
        DO 402 I=N1,MAX
        E(I)=-JC(I)*Z*B
402     CONTINUE
        RETURN
        END
C
C
C
        SUBROUTINE TRCOPR4(E,JC,N1,MAX,J,W,UU,HI)
        COMPLEX E(32),JC(32),J,HI
        DO 403 I=N1,MAX
        E(I)=CONJG(E(I))/MAX
C CALCULATE THE CURRENT DENSITY ON THE STRIP
        JC(I)=E(I)*J/W/UU-HI
403     CONTINUE
        RETURN
        END
C
C
C
        SUBROUTINE FFT(A,M)
C THIS IS THE FFT SUBROUTINE CALLED FOR FROM THE MAIN PROGRAM
        COMPLEX A(32),U,W,T
        N=2**M
        NV2=N/2
        NM1=N-1
        J=1
        DO 7 I=1,NM1
        IF(I.GE.J) GOTO 5
        T=A(J)
        A(J)=A(I)
        A(I)=T
5       K=NV2
6       IF(K.GE.J) GOTO 7
        J=J-K
        K=K/2
        GOTO 6
7       J=J+K
```

```
      PI=3.141592653589793
      DO 20 L=1,M
      LE=2**L
      LE1=LE/2
      U=(1.0,0.0)
      W=CMPLX(COS(PI/LE1),SIN(PI/LE1))
      DO 20 J=1,LE1
      DO 10 I=J,N,LE
      IP=I+LE1
      T=A(IP)*U
      A(IP)=A(I)-T
   10 A(I)=A(I)+T
   20 U=U*W
      RETURN
      END
C
C
C
      COMPLEX FUNCTION SINHH(X)
      COMPLEX X
      SINHH=0.5*(CEXP(X)-CEXP(-X))
      END
C
C
C
      COMPLEX FUNCTION COSHH(X)
      COMPLEX X
      COSHH=0.5*(CEXP(X)+CEXP(-X))
      END
```

APPENDIX B

The purpose of this appendix is to solve for the magnetic field intensity as a function of magnetic vector potential, this derivation is included in reference 7. Given equation 1, it is desired to derive equation 4. For this derivation all sources will be considered sinusoidal, $\overline{E}$ and $\overline{H}$ will be phasor quantities and the sinusoidal steady state versions of Maxwell's equations will be used along with three vector identities. Considering $\overline{A}$ and $\overline{B}$ as arbitrary vectors and C as an arbitrary scalar:

$$\nabla \times (\overline{A} + \overline{B}) = \nabla \times \overline{A} + \nabla \times \overline{B} \qquad [56]$$

$$\nabla \times \nabla C = 0 \qquad [57]$$

$$\nabla \times \nabla \times \overline{A} = \nabla (\nabla \cdot \overline{A}) - \nabla^2 \overline{A} \qquad [58]$$

Starting with the relation of electric and magnetic fields given by maxwell's equation:

$$\nabla \times \overline{H} = j\omega\epsilon \overline{E} \qquad [59]$$

Equation 1, repeated below,

$$\overline{E} = -1/\epsilon (\nabla \times \overline{F}) \qquad [1]$$

is substituted in equation 59 becoming:

$$\nabla \times \overline{H} + j\omega(\nabla \times \overline{F}) = 0 \qquad [60]$$

Making use of identity 56 this can be written as:

$$\nabla \times (\overline{H} + j\omega\overline{F}) = 0 \qquad [61]$$

Making use of identity 57 this can be written again as:

$$\nabla \times (\overline{H} + j\omega \overline{F}) = \nabla \times (-\nabla\phi_m) \qquad [62]$$

The magnetic scalar potential is denoted by ϕ_m in this equation. From 62 the following implication can be made:

$$\overline{H} + j\omega\overline{F} = -\nabla\phi_m \qquad [63]$$

To specify $\overline{H}$ completely from $\overline{F}$ it is necessary to find the relation between ϕ_m and $\overline{F}$. Taking the curl of equation 1 results in:

$$\nabla \times \overline{E} = -1/\epsilon \; \nabla \times \nabla \times \overline{F} \qquad [64]$$

Making use of identity 58 this can be written as:

$$\nabla \times \overline{E} = -1/\epsilon \left[\nabla (\nabla\cdot\overline{F}) - \nabla^2\overline{F} \right] \qquad [65]$$

To specify any vector both its curl and divergence must be known. The curl of $\overline{F}$ is already defined in equation 1. To specify the divergence of $\overline{F}$, the Lorentz gauge condition is applied so that equation 65 is simplified. The divergence of $\overline{F}$ is defined by:

$$\nabla\cdot\overline{F} = -j\omega\epsilon\mu\phi_m \qquad [66]$$

The scalar magnetic potential is now given in terms of vector magnetic potential by:

$$\phi_m = -1/j\omega\mu\epsilon (\nabla\cdot\overline{F}) \qquad [67]$$

This value can be substituted back into equation 62 resulting in eqation 4:

$$\overline{H} = -j\omega\overline{F} + 1/j\omega\mu\epsilon \; \nabla(\nabla\cdot\overline{F}) \qquad [4]$$

APPENDIX C

The following proof is also found in the reference of Brand [6]. It is a proof that the Newton-Raphson method is identical to the contraction corrector method. The starting point is the definition of the Newton-Raphson method.

$$x_{i+1} = x_i - f(x_i)/f'(x_i) \qquad [68]$$

where it is desired that

$$f(x_i) = 0 \qquad [69]$$

and that equivalently

$$g(x_i) - x_i = 0 \qquad [70]$$

equation 68 can now be manipulated as follows:

$$x_{i+1} = x_i - \frac{g(x_i) - x_i}{g'(x_i) - 1} \qquad [71]$$

$$x_{i+1} = \frac{[g'(x_i) - 1] x_i - [g(x_i) - x_i]}{g'(x_i) - 1} \qquad [72]$$

$$x_{i+1} = \frac{g'(x_i) x_i - g(x_i)}{g'(x_i) - 1} \qquad [73]$$

$$x_{i+1} = \left[\frac{g'(x_i)}{g'(x_i) - 1} \right] x_i - \left[\frac{1}{g'(x_i) - 1} \right] g(x_i) \qquad [74]$$

$$x_{i+1} = \left[\frac{g'(x_i)}{g'(x_i) - 1} \right] x_i + \left[\frac{g'(x_i) - 1 - g'(x_i)}{g'(x_i) - 1} \right] g(x_i) \qquad [75]$$

$$x_{i+1} = \left[\frac{g'(x_i)}{g'(x_i) - 1} \right] x_i + \left[1 - \frac{g'(x_i)}{g'(x_i) - 1} \right] g(x_i) \qquad [76]$$

The optimum correction factor is defined by:

$$R = g'(x_i) / [g'(x_i) - 1] \qquad [77]$$

70

So that equation 75 becomes the definition of the optimum contraction corrector when the substitution stated in equation 77 is made as follows:

$$x_{i+1} = R \, x_i + (1 - R) \, g(x_i) \tag{78}$$

The solution for the internal impedance of the coated conductor (refer to reference 2) is found by solving for the distribution equations in both media and then matching at the boundary between the two (see Figure 19). The solution for either material, assuming an electric field with only a z component, is of the following form:

$$i_z = i_0 \; EXP(-x/\delta) \; EXP(-jx/\delta) \tag{79}$$

Figure 19 Coated Conductor
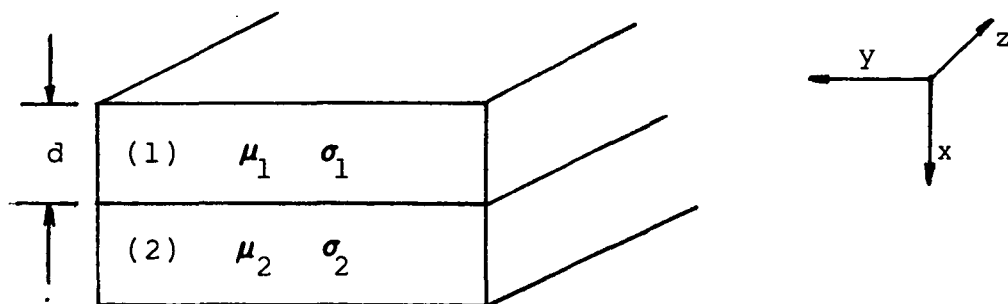
There can be no positive exponential for the substrate, however, because the current becomes zero for large values of x. The current density for the substrate then becomes:

$$i_{z2} = C \; EXP(-T_2 \; x) \tag{80}$$

$$\text{where } T_2 = \frac{(1 + j)}{\delta_2} = (1 + j)\sqrt{\pi f \mu_2 \sigma_2}$$

The current density for the coating has both the positive and negative exponetial:

$$i_{z1} = D \ EXP(-T_1 \ x) + E \ EXP(+T_1 \ x) \qquad [81]$$

where $\qquad T_1 = \dfrac{(1 + j)}{\delta} = (1 + j)\sqrt{\pi f \mu \ \sigma}$

It is more convenient to express this expression in terms of the equivalent hyperbolic functions. Then i_{z1} becomes:

$$i_{z1} = A \ SINH(T_1 \ x) + B \ COSH(T_1 \ x) \qquad [82]$$

The electric and magnetic fields now need to be matched at the boundary. These fields can be found using the following relations:

$$E_z = i_z/\sigma \qquad [83]$$

$$H_y = \dfrac{1}{j\omega\mu} \dfrac{d(E_z)}{dx} = \dfrac{\sigma \ d(E_z)}{T_2 \ dx} \qquad [84]$$

Solving for the electric and magnetic fields yields:

$$E_{z2} = \dfrac{C}{\sigma_2} \ EXP(-T_2 \ x) \qquad [85]$$

$$E_{z1} = \dfrac{1}{\sigma_1}(\ A \ SINH(T_1 \ x) + B \ COSH(T_1 \ x)) \qquad [86]$$

$$H_{y2} = \dfrac{-C}{T_2} \ EXP(-T_2 \ x) \qquad [87]$$

$$H_{y1} = \dfrac{1}{T_1}(\ A \ COSH(T_1 \ x) + B \ SINH(T_1 \ X)) \qquad [88]$$

The tangential electric and magnetic fields are continuous across the boundaries, yielding two equations and three unknowns. Combining equations will obtain the ratio, B/A:

$$E_{z1} = E_{z2}, \quad H_{y1} = H_{y2} \quad @ \ x = d \qquad [89]$$

$$\frac{B}{A} = \frac{-[SINH(T_1 \ d) + (T_2 \sigma_1/T_1 \sigma_2)COSH(T_1 \ d)]}{[COSH(T_1 \ d) + (T_2 \sigma_1/T_1 \sigma_2)SINH(T_1 \ d)]} \qquad [90]$$

The total current is obtained from the relationship:

$$\overline{J} = \overline{n} \ X \ \overline{H} \qquad [91]$$

Solving fo J :

$$J_z = -H_y \qquad [92]$$

The impedance per square can be obtained from observing the ratio of the electric field and the current density at x=0:

$$Z = \frac{E_z}{J_z} = \frac{-E}{H_y} = \frac{-B \ T_1}{A \ \sigma_1} \ at \ x = 0 \qquad [93]$$

Using equation 90 and substituting for T1 and T2 yields the ratio of the internal impedance to the surface resistivity of the coating.

$$\frac{Z}{R_{s1}} = (1 + j)\frac{[SINH(T_1 \ d) + (R_{s2}/R_{s1})COSH(T_1 \ d)]}{[COSH(T_1 \ d) + (R_{s2}/R_{s1})SINH(T_1 \ d)]} \qquad [94]$$

REFERENCES

[1] Tsao, C. M. and Mittra, R., " A spectral-iteration approach for analyzing scattering from frequency selective surfaces. " IEEE Trans. Ant. and Prop., vol. AP-30, No. 2, pp. 303-308, January 1982.

[2] Brand, J. C., " On the convergence of an iterative formulation of the electromagnetic scattering from an infinite grating of thin wires. " Ph.D. Disertation, Dept. of Electrical and Computer Engineering North Carolina State University, Raleigh, North Carolina. May 1985

[3] Christodoulou, C. G. and Kauffman, J. F., " On the Electromagnetic Scattering from Infinite Rectangular Grids with Finite Conductivity. " IEEE Trans. Ant. and Prop., vol. AP-34 pp. 144-154, Febuary 1986

[4] Froberg, C. E., Introduction to Numerical Anaysis. (Addison-Wesley Publishing Company, Inc., Reading, Mass. 1965)

[5] Stakgold, I., Green's Functions and Boundary Value Problems (John Wiley, New York, 1979)

[6] Traub, J.F., Iterative Methods for the Solution of Equations (Chelsea Publishing Company, New York, N.Y., 1982)

[7] Ramo, S., Whinnery, J. R. and Van Duzer, T., Fields and Waves in Communication Electronics (John Wiley & Sons, New York, 1965)

[8] Wait, J. R., " Theories of Scattering from Wire and Mesh Structures. " in Electromagnetic Scattering.P.LE. Uslenghi, Ed., New York: Academic, pp 253-287, 1978

[9] Butler, C. M., " The Equivalent Radius of a Narrow Conducting Strip. " IEEE Trans. Ant. and Prop., vol. AP-30, No. 4, pp. 775-758, July 1982

[10] Balanis, C. A., Antenna Theory Analysis and Design. (Harper and Row, Publishers, New York, 1982)